Eigenvalue Optimization in C^2 Subdivision and Boundary Subdivision

by

Sara M Grundel

A dissertation submitted in partial fulfillment

of the requirements for the degree of

Doctor of Philosophy

Department of Mathematics

New York University

May 2011

Michael Overton—Advisor

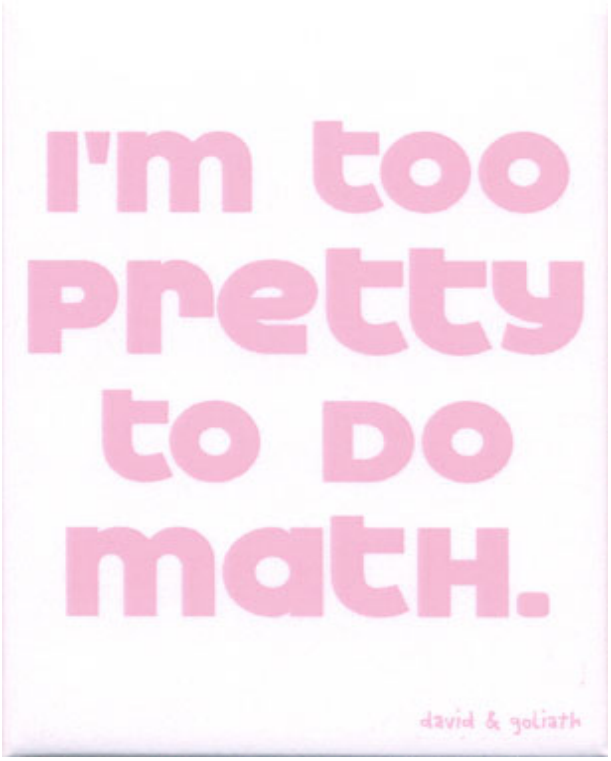

Figure 1: I wish.

An meine Eltern

ohne die weder diese Arbeit noch ich je entstanden waere.

An meinen Mann und meine Kinder

die mir täglich die nötige Freude und Energie gegeben haben.

Acknowledgments

I thank my husband Douglas Kawano for supporting me through the last years of my PhD in every possible way. I would also like to thank everybody at the Courant Institute for making the last 6 years a fabulous experience even though it wasn't always easy. I would like to especially say thank you to Michael Overton my Advisor for leading and guiding me through the process of becoming an independent researcher. I would furthermore like to thank Denis Zorin for offering me an interesting research problem and helping me solve it in the final stages of my PhD thesis. And last but not least I would like to thank Thomas Yu for his inspiration and endless patience through the years as a mentor and research partner.

Abstract

Subdivision is a method to construct smooth surfaces from polygonal meshes used in computer graphics and geometric modeling applications. In order to obtain subdivision surfaces that are C^2 smooth we have to use a rather cumbersome scheme. The main difficulty is caused by the so-called extraordinary vertices, which are vertices that do not have 6 neighbors in the triangular case (4 neighbors in the quadrilateral case). The extraordinary vertex with half the number of vertices as the regular vertex turns out to be a special case. We use this fact to create a subdivision scheme that is C^2 flexible for this vertex. The scheme's characteristic map is equal to Bers' chart.

For both types of meshes, in the final step of creating the subdivision scheme, we solve an eigenvalue optimization problem. In the triangular case we find the exact global optimum. In the quadrilateral case we solve the optimization problem numerically. In both cases the function that is minimized is the reduced spectral radius of the subdivision matrix depending on parameters, that is the largest modulus of the eigenvalues excluding certain known, fixed, eigenvalues.

We are able to approximate a round sphere very well with a very coarse mesh and explore several other applications of the scheme in the triangular setting.

We furthermore develop theory to handle boundary subdivision. The starting point for our theory is a precise description of the class of surfaces that we would like to be able to model using subdivision. We demonstrate how the standard constructions of subdivision theory generalize to the case of surfaces with piecewise-smooth boundary and extend the techniques for analysis of C^1-continuity. Since the extraordinary vertex is a boundary point we have to change some aspects of the theory. We analyze several specific boundary subdivision rules for Loop and Catmull-Clark subdivision schemes.

Finally, we give an analysis of the subdifferential of the spectral abscissa (maximum of the real part of the eigenvalue), a nonsmooth, nonconvex function, for a matrix with a specific Jordan structure.

Contents

List of Figures

List of Tables

Chapter 1

Introduction

This thesis is concerned with subdivision schemes and eigenvalue optimization. Chapter 2 develops a refinement scheme to represent C^2 smooth subdivision surfaces. The refinement scheme only works on meshes with valence 3 and 6 vertices. This is however good enough since genus 0 surfaces can be approximated by such meshes. There are several interesting phenomena that can be modeled on the round sphere alone and several more on arbitrary genus 0 surfaces. The advantage of a subdivision surface as modeling tool is the fact that it is multi-scale in nature. It is for example well-known that, because of its dimples, a golf ball flies further than a ball which is perfectly round. This seems counter-intuitive and complex fluid dynamics play a role in this type of phenomena. Given a C^2 subdivision scheme we are able to simulate such phenomena on as subdivision surface. Thomas Yu proposed the idea of finding such a C^2 subdivision scheme to me since it involved

an eigenvalue optimization problem. He had previously invented a similar scheme which is however very complicated to analyze and implement [42]. By exploiting eigenvalue optimization we found a simpler scheme. We emphasize the importance of the valence 3 vertex and explain how subdivision rules for such a vertex can be developed. We can apply the same idea to the valence 2 vertex for a refinement scheme on quadrilateral meshes, which we discuss in Chapter 4. In both cases, we have several degrees of freedom left after we enforce the conditions for C^2 smoothness. In order to find the optimal scheme we solve an eigenvalue optimization problem. We found that we can reduce all the non-fixed eigenvalues to zero (exactly in the triangular case and approximately in the quadrilateral case). In the former case the zero eigenvalue has one Jordan block of order 2 and two of order 1. In the latter case it apparently has one Jordan block of order 5, one of order 3 and two of order 2.

We implemented a simulation of the curvature flow on genus zero surfaces modeled over triangular meshes with only valence 3 and 6 vertices, as presented in Chapter 3. The algorithm is local and therefore easy parallelizable. We also use a simple Finite Element Method to approximate functions on a surface by using our subdivision scheme to generate basis functions. It compares well with Wahba's smoothing spline on the round sphere. We can furthermore approximate the round sphere very well by using a rather coarse mesh. Having such an approximation of the round sphere can be very useful in simulation phenomena on the sphere or phenomena involving a sphere.

Chapter 5 gives a theoretical analysis on how to handle boundary subdivision in general. Most of the theory for interior extraordinary vertices can easily be generalized to the boundary. However, we need to find a new measure to check global injectivity of the characteristic map. We also found a way to easily check that the boundary of a specific scheme has the correct behavior. We then used this theory to check the boundary rules for Loop and Catmull-Clark proposed in [2]. My work builds on work by Henning Biermann, Adi Levin and Denis Zorin, which has not yet been published and appears as the first part of Chapter 5. My main contributions were in Theorems 5.4 and 5.5 and Propositions 5.2, 5.3 and 5.4. Important features of subdivision schemes include creases which can be handled with boundary rules.

Finally. in Chapter 6 we derive the subgradient of the spectral abscissa (maximum of the real parts of the eigenvalues) for the simplest derogatory and defective matrix. This analysis is motivated by the fact that subgradients provide necessary conditions for eigenvalue optimization. We originally started with the goal of finding a description for arbitrary matrices but the result we obtained for a special case suggests that this is a hard problem.

Most of Chapters 2,3 and 4 was done in collaboration with Thomas Yu, with the eigenvalue optimization part done with Michael Overton. Chapter 5 was done in collaboration with Denis Zorin and Chapter 6 with Michael Overton.

Chapter 2

A C^2 smooth MRA on the topological sphere

2.1 Introduction

In this chapter we develop a subdivision scheme for triangular meshes that is C^2 over the valence 3 vertex. We will furthermore explain why the valence 3 vertex is special and how we use that to construct our subdivision scheme. The characteristic map is given by Bers' chart and the curvature is flexible which means that depending on the input mesh we can generate all different type of curvatures. We also find that the scheme we pick has very desirable curvature properties and discuss that in detail. The applications of this work will be explained in Chapter 3. In Chapter 4 we will discuss the valence 2 case for quadrilateral meshes and the resulting eigenvalue optimization. This

chapter will focus on the theory of subdivision smoothness and how we used it to create our scheme.

It is known that generating a subdivision scheme that is C^2 smooth for valences that are not equal to 3 requires a polynomial degree of at least 8. And the construction using this minimal polynomial degree leads to a very cumbersome subdivision scheme. The theory doesn't talk about the case of the valence 3 vertex.

Recall that a standard subdivision surface scheme is constructed based on a subdivision scheme in the regular grid setting followed by construction of special extraordinary vertex rules. The standard Loop scheme is based on the three directional box spline with directions $[1,0]$, $[0,1]$, $[1,1]$ each repeated twice. Recall the following definition of box-spline [32, 10]: Let $\Xi = \{v_1, v_2, \ldots, v_k\}$ be a set of k vectors in $\mathbb{R}^2$ with the first 2 vectors being linearly independent. The box-spline function B_Ξ is defined as follows. Let B_2 be the indicator function on the parallelogram $[v_1, v_2][0,1)^2$, scaled by the constant $1/\det[v_1, v_2]$, i.e. $B_2 := 1_{[v_1,v_2][0,1)^2}/\det[v_1, v_2]$. Then define $B_3, \ldots,$ $B_k =: B_\Xi$ recursively by

$$B_\kappa(x) = \int_0^1 B_{\kappa-1}(x - tv_\kappa)\, dt, \quad \kappa > 2. \tag{2.1}$$

When the direction vectors have integral entries, the box spline $B_\Xi(x)$ can be generated by a dyadic subdivision scheme, which also means that it satisfies a refinement equation of the form $B_\Xi(x) = \sum_{\alpha\in\mathbb{Z}^2} a_\alpha B_\Xi(2x - \alpha)$.

We consider the three directional box spline with directions $[1,0]$, $[0,1]$, $[1,1]$ each repeated thrice. This box spline can be generated by a subdivision scheme whose mask $(a_\alpha)_\alpha$ has the following symbol (z-transform):

$$\sum_{\alpha\in\mathbb{Z}^2} a_\alpha z_1^{\alpha_1} z_2^{\alpha_2} =: \widehat{a}(z_1,z_2) = \frac{z_1^{-3}z_2^{-3}}{128}(1+z_1)^3(1+z_2)^3(1+z_1z_2)^3. \qquad (2.2)$$

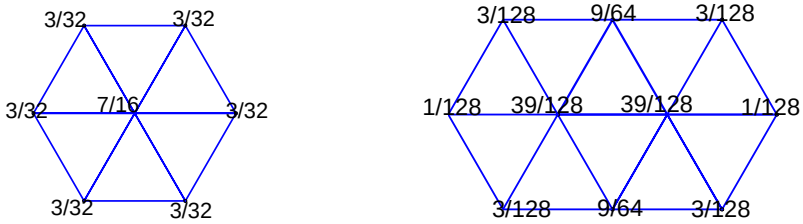

(a) vertex rule (b) edge rule, with a marquise-shaped stencil

Figure 2.1: Subdivision rules for the box spline with directions $[1,0]$,$[0,1]$,$[1,1]$ each repeated thrice.

Since this scheme has the usual hexagonal symmetry of the regular triangular grid, it can be used to construct subdivision surfaces in the arbitrary topology setting; the vertex and edge rules associated with the mask (2.2) are shown in Figure 2.1. Notice that the vertex rule has the same stencil as that of the Loop scheme; the edge rule, however, has a bigger stencil compared to Loop's, but is still dependent only on the data in the 1-rings of the two end vertices of the edge.

Using standard sum rule conditions from subdivision theory, one can show that this subdivision scheme is the one and only one, among all the schemes with the same support, that reproduces all polynomials of total degree 4. In

fact, this scheme also reproduces all polynomials of total degree 5. On the other hand, the box-spline function associated with (2.2) consists of degree 7 polynomial pieces (easy to see from (2.1), as each integration increases the degree by 1), and it is C^4 smooth. We will furthermore see why this subdivision scheme is the optimal one in the regular setting to achieve the C^2 smoothness over the valence 3 vertex.

2.2 Valence 3 Extraordinary Vertex Rules

In this section, we develop a valence 3 extraordinary vertex rule based on the regular rules in Figure 2.1. For this purpose, it suffices to work on the 3-regular complex, see Figure 2.3. Recall that the 3-regular complex has a central valence 3 extraordinary vertex with all other vertices being ordinary (valence 6). Away from the extraordinary vertex, our subdivision scheme uses the rules in Figure 2.1. In the vicinity of the valence 3 vertex, our proposed subdivision rules have the stencils, together with the weights labeled and to be determined, specified in Figure 2.2, where

$$z = 1 - 3(s + t + u) \quad a = 1 - b - 2(c + d) - e \tag{2.3}$$

The goal of this section is to determine a set of weights that give rise to a flexible C^2 scheme. Note that, according to Prautzsch-Reif's degree estimate [33], such a C^2 scheme is impossible for any valence greater than 3 other than

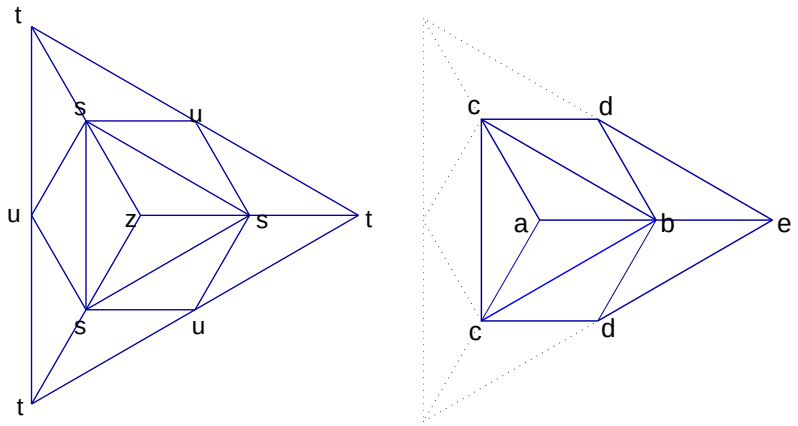

(a) extraordinary vertex rule (b) extraordinary edge rule

Figure 2.2: Valence 3 extraordinary vertex rules.

6.

2.2.1 Linear algebra

Like any other standard subdivision scheme, our scheme is **stationary**, meaning that the same set of rules is used at *all* levels. Together with the fact that these subdivision rules are linear, it is hardly surprising that eigen-decomposition plays a key role in the analysis of subdivision schemes. The study of subdivision matrix and the relevance of their Jordan decomposition is well-studied [34, 30, 31, 43, 45, 46].

Given the support size of our proposed scheme, we need to use 3 rings of data around the extraordinary vertex in order to determine the subdivision limit function on the 1-disc (colored region in Figure 2.3(a)) around the extraordinary vertex. On the other hand, it is enough to use just 2 rings of

data around the extraordinary vertex in order to determine the value of the limit function at the extraordinary vertex. Thus, the **subdivision matrix** of our scheme has the following block form

$$S = \begin{bmatrix} M & 0 \\ A & B \end{bmatrix} \tag{2.4}$$

if we order the vertices in the 3-regular complex as shown in Figure 2.3(a). Here,

$$M = \begin{bmatrix}
z & s & s & s & t & u & t & u & t & u \\
a & b & c & c & e & d & 0 & 0 & 0 & d \\
a & c & b & c & 0 & d & e & d & 0 & 0 \\
a & c & c & b & 0 & 0 & 0 & d & e & d \\
\frac{3}{32} & \frac{7}{16} & \frac{3}{32} & \frac{3}{32} & \frac{3}{32} & \frac{3}{32} & 0 & 0 & 0 & \frac{3}{32} \\
\frac{9}{64} & \frac{39}{128} & \frac{39}{128} & \frac{3}{64} & \frac{3}{128} & \frac{9}{64} & \frac{3}{128} & \frac{1}{128} & 0 & \frac{1}{128} \\
\frac{3}{32} & \frac{3}{32} & \frac{7}{16} & \frac{3}{32} & 0 & \frac{3}{32} & \frac{3}{32} & \frac{3}{32} & 0 & 0 \\
\frac{9}{64} & \frac{3}{64} & \frac{39}{128} & \frac{39}{128} & 0 & \frac{1}{128} & \frac{3}{128} & \frac{9}{64} & \frac{3}{128} & \frac{1}{128} \\
\frac{3}{32} & \frac{3}{32} & \frac{3}{32} & \frac{7}{16} & 0 & 0 & 0 & \frac{3}{32} & \frac{3}{32} & \frac{3}{32} \\
\frac{9}{64} & \frac{39}{128} & \frac{3}{64} & \frac{39}{128} & \frac{3}{128} & \frac{1}{128} & 0 & \frac{1}{128} & \frac{3}{128} & \frac{9}{64}
\end{bmatrix} \tag{2.5}$$

using Equation 2.3 is the 10×10 matrix that maps the 2-ring data from one scale to the 2-ring data in the next finer scale, whereas the whole 19×19 matrix S maps the 3-ring data from one scale to the 3-ring data in the next scale. The entries in the blocks A and B come solely from the regular rules

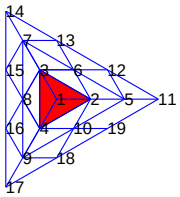

(a) Ordering of vertices
In red: the 1-disc around
the e.v. (denoted by D)

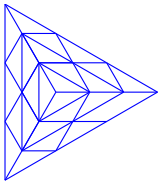

(b) Level 0 complex

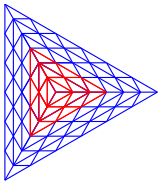

(c) Level 1 complex
(once subdivided)

Figure 2.3: Ordering and subdivision of the 3-regular complex

in Figure 2.1:

$$A = \frac{1}{128}\begin{bmatrix} 1 & 39 & 3 & 3 & 39 & 18 & 0 & 0 & 0 & 18 \\ 3 & 39 & 18 & 1 & 18 & 39 & 3 & 0 & 0 & 3 \\ 3 & 18 & 39 & 1 & 3 & 39 & 18 & 3 & 0 & 0 \\ 1 & 3 & 39 & 3 & 0 & 18 & 39 & 18 & 0 & 0 \\ 3 & 1 & 39 & 18 & 0 & 3 & 18 & 39 & 3 & 0 \\ 3 & 1 & 18 & 39 & 0 & 0 & 3 & 39 & 18 & 3 \\ 1 & 3 & 3 & 39 & 0 & 0 & 0 & 18 & 39 & 18 \\ 3 & 18 & 1 & 39 & 3 & 0 & 0 & 3 & 18 & 39 \\ 3 & 39 & 1 & 18 & 18 & 3 & 0 & 0 & 3 & 39 \end{bmatrix}$$

$$B = \frac{1}{128}\begin{bmatrix} 1 & 3 & 0 & 0 & 0 & 0 & 0 & 0 & 3 \\ 0 & 3 & 1 & 0 & 0 & 0 & 0 & 0 & 0 \\ 0 & 1 & 3 & 0 & 0 & 0 & 0 & 0 & 0 \\ 0 & 0 & 3 & 1 & 3 & 0 & 0 & 0 & 0 \\ 0 & 0 & 0 & 0 & 3 & 1 & 0 & 0 & 0 \\ 0 & 0 & 0 & 0 & 1 & 3 & 0 & 0 & 0 \\ 0 & 0 & 0 & 0 & 0 & 3 & 1 & 3 & 0 \\ 0 & 0 & 0 & 0 & 0 & 0 & 0 & 3 & 1 \\ 0 & 0 & 0 & 0 & 0 & 0 & 0 & 1 & 3 \end{bmatrix}.$$

The spectrum of S is the union of the spectra of M and B. The eigenvalues of the 9×9 matrix B are $1/32$, $1/64$, $1/128$ each repeated thrice. As we will see, the six dominant eigenvalues of S should be $1, 1/4, 1/4, 1/16, 1/16, 1/16$, so these eigenvalues must come from the spectrum of M.

2.2.2 Characteristic map and C^2 condition

Note that if $v \in \mathbb{R}^{19}$ is a set of scalar values assigned to the first 3 rings of the level 0 3-regular complex (as shown in Figure 2.3(a)), then according to our subdivision rules, the subdivision data on the first $2^j + 2$ rings of the level j 3-regular complex can be determined. Therefore, we obtain in the limit a subdivision function

$$f_v : D \to \mathbb{R}. \tag{2.6}$$

Here D is the 1-disc around the extraordinary vertex.

It is easy to see that every subdivision function satisfies the scaling relation

$$f_v(u) = f_{Sv}(2u), \quad \forall\, u \in \frac{1}{2}D. \tag{2.7}$$

In particular, if v is an eigenvector of S associated with an eigenvalue μ, then

$$f_v(u) = f_{\mu v}(2u) = \mu f_v(2u).$$

Despite the (rather artificial) way we embed D and the 3-regular complex into the plane as shown in Figure 2.3(a), one should not think of D as a subset of $\mathbb{R}^2$. That said, it is senseless to talk about the smoothness of f_v before we put a suitable differentiable structure on D (in differential geometry terms) or, equivalently, before we suitably parametrize f_v. On the other hand, since our subdivision scheme is based on a C^4 smooth box-spline, any subdivision function f_v is C^4 in the interior of each sector of D (assuming f_v is parametrized by the affine coordinates within each of the triangular sectors of D.)

The standard way to parametrize subdivision functions is based on *characteristic maps*, due to Reif [34]. Assume that we have a subdivision scheme. Let u_1 and u_2 be two linearly independent eigenvectors associated with the

sub-dominant eigenvalue λ. The characteristic map is given by

$$\chi = (f_{u_1}, f_{u_2}) : D \to \mathbb{R}^2. \tag{2.8}$$

If χ is **injective**, we can think of $\chi^{-1} : \chi(D) \to D$ as a parametrization of D. If χ is also **regular**, i.e. χ has a non-singular Jacobian in the interior of each sector of D, then $f_v \circ \chi^{-1} : \chi(D) \to \mathbb{R}$ is C^1 smooth for any v. This follows for example from [43] where the following is proved.

Theorem 2.1. *Given a subdivision matrix with largest eigenvalue 1 with multiplicity 1 and second largest eigenvalue $\lambda \in \mathbb{R}$ with geometric and algebraic multiplicity 2 we have two independent eigenvectors for λ. They define the characteristic map. If the characteristic map is injective and the Jacobian has the same sign everywhere on the domain $D\backslash\{0\}$ then the scheme is C^1. Furthermore the scheme is C^k if any nonzero complex eigenbasis function f_w corresponding to an eigenvalue $\mu = \lambda^2$ is a homogeneous polynomial of degree 2 in characteristic coordinates and all other eigenvalues of the matrix are smaller than λ^2 in modulus.*

If we have a subdivision schemes that satisfies all the conditions above that gives us C^1 and all the eigenvalues smaller than λ are *strictly smaller* than λ^2 in modulus, then Theorem 2.1 tells us that the subdivision scheme is C^2 smooth. Such schemes are also easy to construct; the only problem is that they are not so useful since they produce limit functions with vanishing second derivatives *regardless of the initial data*, and hence are not so interest-

ing from an approximation or modeling point of view. A **flexible** C^2 scheme is one that is both C^2 and capable of producing all quadratic polynomials.

If we assume that the sub-subdominant eigenvalue is exactly λ^2 with geometric multiplicity 3, let w_i, $i = 1, 2, 3$, be three linearly independent eigenvectors associated with λ^2. Then we have the following well-known result:

Theorem 2.2. Such a subdivision scheme is a flexible C^2 one if

$$\text{span}\{f_{w_i} \circ \chi^{-1}(x_1, x_2) : i = 1, 2, 3\} = \text{span}\{x_1^2, x_1 x_2, x_2^2\}. \tag{2.9}$$

This result is not specific to the valence 3 case. In fact, everything we have said so far is either directly applicable to or has a generalization to any valence $k \geqslant 3$.

The condition in Theorem 2.2 seems hard to satisfy and, as illustrated by Reif-Prautzsch's degree estimates [33, 36], is indeed hard to satisfy when $k > 3$. In the rest of this section, we show:

Proposition 2.1. The weights in Figure 2.2 can be chosen such that:

(I) The resulted characteristic map χ is the valence 3 Bers' chart [1, 15] (called "fractional power embedding" in the quadrilateral case [31, Page 50], in which $z \mapsto z^{6/k}$ (see below) is replaced by $z \mapsto z^{4/k}$.)

(II) The eigenfunctions corresponding to sub-sub-dominant eigenvalues satisfy the flexible C^2 condition (2.9).

2.2.3 Valence 3 Bers' chart

The valence k Bers' chart is a piecewise fractional power function: on the first sector of a k-gon it is given by the analytic map $z \mapsto z^{6/k}$, assuming that the first sector is affine transformed into the equilateral triangle bounded by $[0, 0]$, $[1, 0]$ and $[\cos(2\pi/3), \sin(2\pi/3)]$, followed by identifying this equilateral triangle with part of the complex plane. In the other $k-1$ sectors, the chart is defined by rotational symmetry. It is not hard to check that these charts endow a triangle mesh with a conformal structure.

There is something special about the $k = 3$ case. First of all, the only $k \neq 6$ (and $\geqslant 3$) that makes $6/k$ an integer is $k = 3$. Moreover, we can identify the 3-gon D with the 'projective regular hexagon', i.e. the regular hexagon with antipodal points identified, as shown in Figure 2.4(a)-(b). Then under this identification, the valence 3 Bers' chart is the **single** map $z \mapsto z^2$. This representation of the valence 3 Bers' chart will be very useful in Section 2.2.6.

2.2.4 Connection to Prautzsch-Reif's degree estimate

The valence 3 Bers' chart also gives a concrete illustration of how a key argument in Prautzsch-Reif's degree estimate breaks down in the valence 3 case. It is observed in [33] that if a valence k characteristic map consists of polynomial patches stitched together in a C^r fashion, and the polynomial pieces are only of degree r, then the characteristic map must be 6-periodic

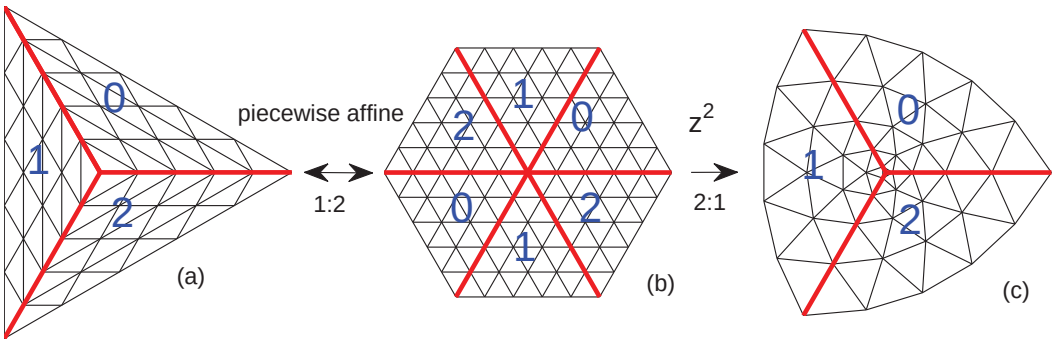

Figure 2.4: A general valence k Bers' chart is defined piecewisely. The valence 3 Bers' chart, however, can be expressed by the **single** polynomial $z \mapsto z^2$ if we identify the 3-gon D with the 'projective regular hexagon'.

(see Lemma 5.1 and Theorem 5.1 of [33]), which is, in general, impossible as the characteristic map must also be k-periodic. (As a result, the polynomial degree must, in general, be $\geqslant r+1$; this lower bound is further improved to $\geqslant 3r/2+1$ by a finer argument.) The only exception is when $k=3$, as illustrated by the valence 3 Bers' chart: it is both 3- and 6-periodic, and consists only of polynomial patches of degree 2 stitched together in a C^∞ fashion away from the extraordinary point.

2.2.5 Relating valence 3 to regular scheme

Let N_r be the number of vertices in the first r rings of the 3-regular complex, so $2N_r-1$ is the corresponding number for the 6-regular complex. Corresponding to (2.4), we have a size $2N_3-1=37$ subdivision matrix S_6 that

acts on the 3 ring in the case of valence $k = 6$ in the following block form:

$$S_6 = \begin{bmatrix} M_6 & 0 \\ A_6 & B_6 \end{bmatrix}, \tag{2.10}$$

where all three blocks are determined by the regular rules in (2.1); M_6 is of size $2N_2 - 1 = 19$. (We order the vertices on the 6-regular complex in a way similar to Figure 2.3(a).) Corresponding to (2.6), we have $F_{\widetilde{v}} : H \to \mathbb{R}$ where $\widetilde{v} \in \mathbb{R}^{2N_3-1}$ is any set of data on the first three rings of the 6-regular complex, H is the 1-disc (a regular hexagon) around the central vertex, and $F_{\widetilde{v}}$ is the corresponding subdivision function.

Figure 2.4(a)-(b) suggests a 'doubling-up' operator from the 3-regular complex to the 6-regular complex; restricting this operator to the first r rings, we denote it by

$$\mathcal{D}_r : \mathbb{R}^{N_r} \to \mathbb{R}^{2N_r-1}.$$

The observation we need for proving Proposition 2.1 is the following:

Lemma 2.1. If $\widetilde{u} \in \mathbb{R}^{2N_3-1}$ is such that $F_{\widetilde{u}}$ is a homogeneous polynomial p of degree 2ℓ and the subdivision scheme is such that $F_v = 0 \Leftrightarrow v = 0$, then

1. $\widetilde{u}$ is an eigenvector of S_6 associated with eigenvalue $2^{-2\ell}$,
2. $\widetilde{u} \in \text{range}(\mathcal{D}_3)$, so $u := \mathcal{D}_3^{-1}\widetilde{u}$ is well-defined, and
3. $F_{\widetilde{u}}$, being an even function, can be viewed as a function on the projective regular hexagon $H/\!\sim$. (Here, $\mathbf{x} \sim \mathbf{y} \Leftrightarrow \mathbf{x} = \pm\mathbf{y}$.)

Furthermore, if (the parameters in M are chosen such that) $Su = 2^{-2\ell}u$, then

$$\mathbb{R} \leftarrow D : f_u = F_{\widetilde{u}} : H/\!\sim \to \mathbb{R} \tag{2.11}$$

if we identify D with $H/\!\sim$ (as in Figure 2.4.)

Proof. If $F_{\widetilde{u}} = p$ a homogeneous polynomial of degree 2ℓ then we get that

$$F_{S_6\widetilde{u}}(x) = F_{\widetilde{u}}(1/2x) = 2^{-2\ell}F_{\widetilde{u}}(x) = F_{2^{-2\ell}\widetilde{u}}(x).$$

This means that $F_{S_6\widetilde{u}-2^{-2\ell}\widetilde{u}} = 0$ and therefore it follows that $\widetilde{u}$ is an eigenvector of S_6 to the eigenvalue $2^{-2\ell}$. Since the limit function is an even polynomial is follows that it has the symmetry $F_{\widetilde{u}}(x) = F_{\widetilde{u}}(-x)$. This lets us conclude that $\widetilde{u} \in \text{range}(\mathcal{D}_3)$ since otherwise there would be a vector with that symmetry giving rise to the same limit function contradicting the assumption that only the zero vector produces a zero function. Since we have the symmetry we can now interpret $F_{\widetilde{u}}$ as a function on the projective regular hexagon $H/\!\sim$. Let $u := \mathcal{D}_3^{-1}\widetilde{u}$ and find parameters in the subdivision matrix S for the 3-regular complex such that $Su = 2^{-2\ell}u$ then

$$f_u(2^{-1}x) = f_{Su}(x) = f_{2^{-2\ell}u}(x) = 2^{-2\ell}f_u(x).$$

This means that $f_u = F_{\widetilde{u}}$ since away from the extraordinary vertex the subdivision rules are the same and the behavior of f_u is the same as the

behavior of $F_{\widetilde{u}}$ in the neighborhood of the center vertex. $\square$

Due to the block forms (2.4) and (2.10), to specify the vector $\widetilde{u}$ (resp. u) in the lemma above, it is enough to specify its first $2N_2 - 1$ (resp. N_2) entries. Call this shorter vector $\widetilde{u}^s$, if $\widetilde{u}^s \neq 0$, then $\widetilde{u}$ is uniquely determined by

$$\widetilde{u} = \begin{bmatrix} \widetilde{u}^s \\ (2^{-2\ell} I - B_6)^{-1} A_6 \widetilde{u}^s \end{bmatrix}.$$

Notice that $\widetilde{u}^s \in \text{range}(\mathcal{D}_2)$. In the second half of the lemma above, we can actually weaken the assumption $Su = 2^{-2\ell} u$ to $M\mathcal{D}_2^{-1}\widetilde{u}^s = 2^{-2\ell}\mathcal{D}_2^{-1}\widetilde{u}^s$.

2.2.6 Proof of Proposition 2.1 and choice of parameters

The 6-regular grid, with coordinates denoted here by (x, y), can be identified with $\mathbb{Z}^2$, with coordinates denoted by (x_1, x_2), via a linear isomorphism:

$$\begin{bmatrix} x \\ y \end{bmatrix} = \begin{bmatrix} 1 & -1/2 \\ 0 & \sqrt{3}/2 \end{bmatrix} \begin{bmatrix} x_1 \\ x_2 \end{bmatrix},$$

so we are now back to the shift-invariant setting, and checking the polynomial reproduction condition above becomes a classical Strang-Fix-type calculation (a well-studied subject by itself.)

Using standard results in subdivision theory, any monomial of total degree $\leqslant 5$ can be written as a linear combination of the integer shifts of the three-

directional box spline B_Ξ with subdivision mask (2.2). More precisely, if $\mu = (\mu_1, \mu_2)$, $|\mu| = \mu_1 + \mu_2 \leqslant 5$, then

$$x^\mu = \sum_{\alpha \in \mathbb{Z}^2} c_\alpha^\mu \, B_\Xi(x - \alpha), \tag{2.12}$$

where

$$c_\alpha^\mu = \sum_{\nu \leqslant \mu} \binom{\mu}{\nu} \alpha^\nu b_{\mu-\nu}, \tag{2.13}$$

and the b_μ, $|\mu| \leqslant 5$, are given by the following table[1]: The real and imaginary

Table 2.1: values of b_{mu}

$\mu_1 \backslash \mu_2$	0	1	2	3	4	5
0	1	0	$-1/2$	0	$4/5$	0
1	0	$-1/4$	0	$2/5$	0	
2	$-1/2$	0	$2/5$	0		
3	0	$2/5$	0			
4	$4/5$	0				
5	0					

parts of $z \mapsto z^2$ are

$$x^2 - y^2 = x_1^2 - x_1 x_2 - x_2^2/2, \quad 2xy = \sqrt{3}(x_1 x_2 - x_2^2/2). \tag{2.14}$$

Computing c_α^μ for a given μ computes the control mesh to reproduce x^μ

[1]These b_μ are computed recursively by the formula: $b_{(0,0)} = 1$, $b_\mu = \sum_{0 \neq \nu \leqslant \mu} \binom{\mu}{\nu} 2^{|\mu-\nu|} b_{\mu-\nu} [(-iD)^\nu \widehat{\mathbf{a}}](0)(1 - 2^{|\mu|}\widehat{\mathbf{a}}(0))^{-1}$, where $\widehat{\mathbf{a}}(\omega) = \sum_\alpha a(\alpha) e^{-i\alpha\cdot\omega}/4$. One can verify the values of b_μ in the table using this formula and (2.2).

Using (2.12)-(2.14),[2] we compute the control data u_1, u_2 on the first two rings needed to reproduce the function z^2. This means that that M in (2.5) needs to have eigenvectors u_1 and u_2 associated to the eigenvalue $1/4$

$$\begin{aligned} u_1 &= \frac{1}{2}\Big[0,\ 2,\ -1,\ -1,\ 8,\ 3,\ -4,\ -6,\ -4,\ 3\Big]^T, \\ u_2 &= \frac{\sqrt{3}}{2}\Big[0,\ 0,\ 1,\ -1,\ 0,\ 3,\ 4,\ 0,\ -4,\ -3\Big]^T. \end{aligned} \tag{2.15}$$

For (II) (the C^2 conditions), we need to force the sub-sub-dominant eigenvectors of M, w_i, $i = 1, 2, 3$, after 'doubling-up', to be the unique initial data that generate, under the regular subdivision rule, the following homogeneous degree 4 polynomials:

$$\begin{aligned} (x^2 - y^2)^2 &= x_1^4 - 2x_1^3x_2 + x_1x_2^3 + x_2^4/4, \\ (x^2 - y^2)(2xy) &= \sqrt{3}(x_1^3x_2 - 3x_1^2x_2^2/2 + x_2^4/4), \\ (2xy)^2 &= 3x_1^2x_2^2 - 3x_1x_2^3 + 3x_2^4/4. \end{aligned} \tag{2.16}$$

By calculations based on (2.12)-(2.14), we demand M in (2.5) to have the

[2]For a more elementary, but more tedious, approach, one can work out the piecewise (degree 7) polynomial representation of the box-spline B_Ξ based on (2.1) and use it to work out how to reproduce any polynomial of total degree $\leqslant 5$.

following three eigenvectors associated with eigenvalue 1/16:

$$\begin{aligned} w_1 &= \frac{1}{20}\Big[12,\ 2,\ -13,\ -13,\ 212,\ -33,\ -28,\ 102,\ -28,\ -33\Big]^T, \\ w_2 &= \frac{\sqrt{3}}{4}\Big[0,\ 0,\ -1,\ 1,\ 0,\ 9,\ -16,\ 0,\ 16,\ -9\Big]^T, \\ w_3 &= \frac{1}{20}\Big[12,\ -18,\ -3,\ -3,\ -108,\ 57,\ 132,\ -78,\ 132,\ 57\Big]^T. \end{aligned} \tag{2.17}$$

The overall conditions imposed on M are, after all, linear:

$$M[u_1, u_2, w_1, w_2, w_3] = [u_1, u_2, w_1, w_2, w_3]\ \mathrm{diag}([1/4, 1/4, 1/16, 1/16, 1/16]).$$

In terms of the parameters this can be written as the following conditions:

$$\begin{aligned} b &= 11/32 - 4e, \\ c &= 9/64 + 3e, \\ d &= 1/64 + e, \\ s &= 3/16 + 2t \end{aligned} \tag{2.18}$$

We must still verify that the remaining three parameters (e, t, u) can be chosen such that all the remaining eigenvalues are strictly less than 1/16 in modulus. This was done by eigenvalue optimization.

2.3 Eigenvalue Optimization

We have a 10×10 matrix M given by (2.5) that depends on the three parameters (e, t, u) using (2.3) and (2.18) and we know that 6 eigenvalues are

given by $(1, 1/4, 1/4, 1/16, 1/16, 1/16)$. We now want the remaining eigenvalues to be less than $1/16$ in modulus. As was done in [18], this problem can be solved by a numerical search based on minimizing the largest of the remaining eigenvalues in modulus: the so-called reduced spectral radius. The reduced spectral radius is nonconvex, nonsmooth and in fact not even Lipschitz continuous at matrices with multiple eigenvalues, although it is Hölder continuous. We used the HANSO (Hybrid Algorithm for Non-Smooth Optimization) software package [4] (see Chapter 4 for more details). After some experimentation we found a solution to our problem given by the following parameters: $(e, t, u) = (1/64, 1/128, 1/24)$ with

$$\begin{aligned}(z, s, t, u) &= (31/128,\ 26/128,\ 1/128,\ 1/24)\\ (a, b, c, d, e) &= (17/64, 9/32, 3/16, 1/32, 1/64).\end{aligned} \tag{2.19}$$

However, after more extensive numerical work we realized that it seems that all the remaining eigenvalues can be reduced to 0. Then, we realized that we can write the remaining 4 eigenvalues as $15/128 - 7e$ (repeated twice) and

$$\frac{1}{8} + e - \frac{9t}{2} - \frac{3u}{2}$$
$$\pm\tfrac{1}{32}\sqrt{13 + 16(8e - 30t - 33u) + 256(4e^2 + 81t^2 + 9u^2 - 84et + 12eu + 54ut)}.$$

To obtain these formulas, we first block-diagonalized the matrix into two 3×3 blocks and one 4×4 block. The eigenvalue computation was then done by Maple. It can then be shown analytically that these eigenvalues are

Figure 2.5: Restrictions on (e, t, u) such that all eigenvalues are smaller than $\frac{1}{16}$, shown as subsets of the $u - t$ plane for 4 values of e

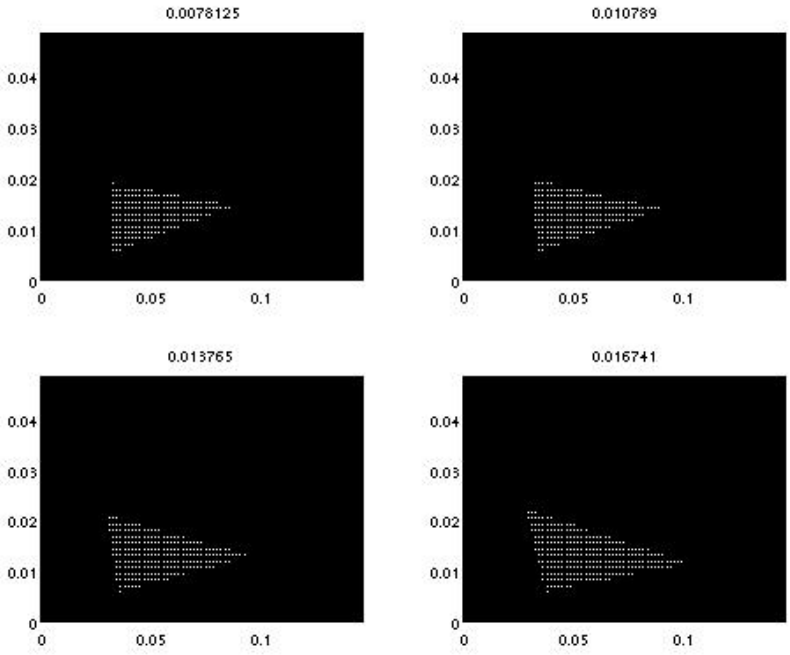

smaller than 1/16 in modulus if and only if (e, t, u) lies in a small bounded open subset of the first octant of the e-t-u space. The $u - t$ solution sets are given for several values of e in Figure 2.5. Furthermore, we can set all the eigenvalues to 0 by solving a system of equations composed of 2 linear equations and 1 quadratic equation in (e, t, u). The solution is given by:

$$(e, t, u) = (15/896, 295/19264, 1403/28896).$$

The set of all parameters reads:

$$\begin{aligned}(z, s, t, u) &= (69/448,\ 2101/9632,\ 295/19264,\ 1403/28896) \\ (a, b, c, d, e) &= (233/986, 248/896, 171/896, 29/896, 15/896).\end{aligned} \tag{2.20}$$

The following result summarizes this discussion and also shows the Jordan structure of M:

Theorem 2.3. *Using the parameter choices (2.20), the Jordan normal form of M in (2.5) is given by*

$$\begin{bmatrix} D & 0 & 0 & 0 \\ 0 & J_2(0) & 0 & 0 \\ 0 & 0 & J_1(0) & 0 \\ 0 & 0 & 0 & J_1(0) \end{bmatrix},$$

where $D = diag(1, 1/4, 1/4, 1/16, 1/16, 1/16)$ and $J_i(0)$ is a Jordan Block of size i with 0's on the diagonal.

2.4 Summary

We have obtained a subdivision scheme that is flexible C^2 smooth on meshes with only valence 3 and 6 vertices. It has better polynomial degree than the best scheme known and it is based on box splines in the regular setting. Furthermore the stencil of the scheme is small and also optimal as there is no

smaller stencil which can achieve a scheme which has the same properties ours has. We furthermore were able to reduce the resulting eigenvalues (excluding 1,1/4,1/16) to 0 which gives us favorable curvature behavior. In Figure 2.6(a) we see the curvature close to a valence 3 vertex for the set of parameters given by (2.19). Parameters of the global minimum given by (2.20) define a subdivision scheme with curvature behavior (see Figure 2.6(b)) that is much less extreme and therefore more desirable.

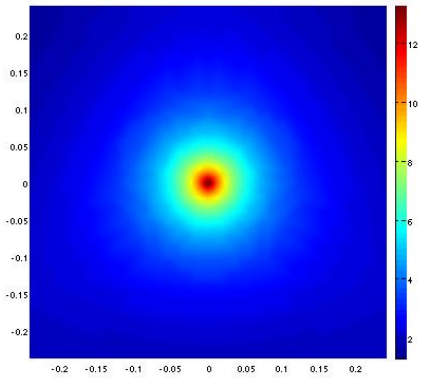

(a) parameters given by (2.19)

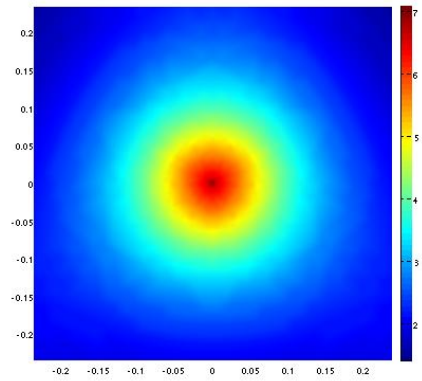

(b) parameters given by (2.20)

Figure 2.6: Plots of the Curvature in the neighborhood of a valence 3 vertex on a mesh where the original points lay on a round sphere. We would like to see curvature behavior that is close to the round sphere, which would mean constant curvature. Example (b) is much less extreme than example (a).

Chapter 3

Application of the MRA

3.1 Introduction

We will explain two algorithms we implemented using the subdivision scheme developed in Chapter 2. We implemented a finite element method to approximate the smoothing spline on an arbitrary genus 0 surface and compared it to the exact smoothing spline on the round sphere given by Wahba [41]. We furthermore implemented an algorithm that simulates the curvature flow on a subdivision surface. Since the scheme is C^2 we can compute second derivatives exactly at every point in a subdivision surface, which we will use in both these algorithms. We know that a surface converges to the round sphere under the curvature flow preserving the volume. We use this to create a mesh that approximates the sphere very well. We furthermore use our subdivision algorithm in a rational setting and explore the possibility of an

exact representation of the sphere by a relative coarse mesh.

3.2 Approximation on a genus 0 surface

Given a manifold S and observations (s_i, y_i) with $s_i \in S$ and $y_i \in \mathbb{R}$, possibly noisy, where ideally $y_i = f_{true}(s_i)$ for some unknown function f_{true}. Our goal is to estimate f_{true}. On the line this problem has a variety of algorithms. We will estimate the function by a generalization of spline smoothing [21]. The smoothing spline on the line (for a smoothing parameter λ) is the function f_λ with

$$f_\lambda = \underset{f \in W_2(\mathbb{R}}{\operatorname{argmin}} E[f] \tag{3.1}$$

$$E[f] := \frac{1}{n}\sum (y_i - f(s_i))^2 + \lambda \int f''(s)^2 ds. \tag{3.2}$$

This is a solvable problem and results in a cubic spline which can be computed.

As presented in [16] we can extend the idea of the smoothing spline to subdivision surfaces and approximate it by a finite element method. We will now assume that S is a subdivision surface corresponding to the subdivision scheme presented in Chapter 2, which means that there exists a base mesh K (a triangular mesh with only valence 3 and 6 vertices) which can be interpreted as a simplicial complex and an embedding $F : K \to \mathbb{R}^3$ such that $F(K) = S$. We furthermore have a sequence of subdivided meshes K^J with

$K^0 = K$ converging to S and functions $F_J : K^J \to S$. The smoothing spline is given by the function $f_\lambda : S \to \mathbb{R}$, for the smoothing parameter λ, that minimizes the functional

$$E[f] = \frac{1}{n}\sum (y_i - f(s_i))^2 + \lambda \int_S (\Delta_S f)^2 dA.$$

One can show that the solution is unique.

We use the finite element method presented in [16] to approximate the smoothing spline. We have a nested sequence of spaces of subdivision functions

$$V^0 \subset V^1 \subset \cdots \subset V^J \subset \cdots \subset W_2(S)$$

where V^J is given by the collection of subdivision limit functions with starting values on the J times subdivided mesh K^J interpreted on S. The union $\bigcup_{J=0}^{\infty} V^J$ is dense in $W_2(S)$. The mesh K^J has N^J mesh points in $\mathbb{R}^3$. V^J is a finite dimensional vector space and a basis is given by the subdivision limit functions $\phi_\alpha^J = \tilde{\phi}_\alpha^J \circ F_J^{-1} : S \to \mathbb{R}$, $\alpha = 1, \ldots, N^J$ where $\tilde{\phi}_\alpha^J : K^J \to \mathbb{R}$ is the function achieved by subdividing K^J to the limit with starting values 0 everywhere except 1 on the meshpoint α. We are going to find the minimizer of the functional E in the space V^J which is given by

$$E[f] = \frac{1}{n}\sum_i (y_i - \sum_\alpha f^\alpha \phi_\alpha^J(s_i))^2 + \lambda \sum_{\alpha,\beta} f^\alpha f^\beta B_{\alpha\beta} \tag{3.3}$$

$$B_{\alpha\beta}^J = \int_S \Delta_S \phi_\alpha^J \Delta_S \phi_\beta^J dA \tag{3.4}$$

for a function $f \in V^J$ given by $f = \sum f^\alpha \phi_\alpha^J$ with $f^\alpha \in \mathbb{R}$. Δ_S is the Laplace-Beltrami operator of the surface S.

Once we compute $\phi_\alpha^J(s_i)$ and $B_{\alpha\beta}^J$ finding f^α reduces to a Linear Algebra problem. For $\lambda = 0$ we find the solution such that $\sum_{\alpha\beta} f^\alpha f^\beta B_{\alpha\beta}$ is minimal and $\sum_\alpha f^\alpha \phi_\alpha^J(s_i) = y_i$.

Computing $\phi_\alpha^J(s_i)$ and $B_{\alpha\beta}^J$

The subdivision scheme from Chapter 2 is based on a box spline in the regular setting and the functions $F_J, \tilde{\phi}_\alpha^J$ are therefore given by piecewise polynomials away from valence 3 vertices. Given a triangle as in Figure 3.2 the limit polynomial in Bezier coordinates on the colored triangle is given by

$$p(u, v, w) = bQP$$

where

$$\begin{aligned} b = [&w^7, vw^6, v^2w^5, v^3w^4, v^4w^3, v^5w^2, v^6w, v^7, uw^6, uvw^5, uv^2w^4, \\ &uv^3w^3, uv^4w^2, uv^5w, uv^6, u^2w^5, u^2vw^4, u^2v^2w^3, u^2v^3w^2, \\ &u^2v^4w, u^2v^5, u^3w^4, u^3vw^3, u^3v^2w^2, u^3v^3w, u^3v^4, u^4w^3, \\ &u^4vw^2, u^4v^2w^1, u^4v^3, u^5w^2, u^5vw, u^5v^2, u^6w, u^6v, u^7] \end{aligned}$$

and $Q = [Q_1 Q_2]$ with

$$Q_1 = \frac{1}{5040} \begin{pmatrix}
0 & 0 & 0 & 0 & 6 & 30 & 6 & 0 & 30 & 516 & 516 & 30 & 0 & 6 \\
0 & 0 & 0 & 0 & 9 & 30 & 3 & 0 & 51 & 609 & 423 & 9 & 0 & 12 \\
0 & 0 & 0 & 0 & 13 & 28 & 1 & 0 & 85 & 689 & 317 & 1 & 0 & 24 \\
0 & 0 & 0 & 0 & 18 & 24 & 0 & 0 & 138 & 738 & 216 & 0 & 0 & 48 \\
0 & 0 & 0 & 0 & 24 & 18 & 0 & 0 & 216 & 738 & 138 & 0 & 0 & 96 \\
0 & 0 & 0 & 1 & 28 & 13 & 0 & 1 & 317 & 689 & 85 & 0 & 0 & 186 \\
0 & 0 & 0 & 3 & 30 & 9 & 0 & 9 & 423 & 609 & 51 & 0 & 0 & 330 \\
0 & 0 & 0 & 6 & 30 & 6 & 0 & 30 & 516 & 516 & 30 & 0 & 6 & 516 \\
0 & 0 & 0 & 0 & 12 & 51 & 9 & 0 & 51 & 702 & 609 & 30 & 0 & 9 \\
0 & 0 & 0 & 0 & 18 & 50 & 4 & 0 & 86 & 816 & 482 & 8 & 0 & 18 \\
0 & 0 & 0 & 0 & 26 & 45 & 1 & 0 & 142 & 903 & 346 & 1 & 0 & 36 \\
0 & 0 & 0 & 0 & 36 & 36 & 0 & 0 & 228 & 936 & 228 & 0 & 0 & 72 \\
0 & 0 & 0 & 1 & 45 & 26 & 0 & 1 & 346 & 903 & 142 & 0 & 0 & 141 \\
0 & 0 & 0 & 4 & 50 & 18 & 0 & 8 & 482 & 816 & 86 & 0 & 0 & 258 \\
0 & 0 & 0 & 9 & 51 & 12 & 0 & 30 & 609 & 702 & 51 & 0 & 3 & 423 \\
0 & 0 & 0 & 0 & 24 & 85 & 13 & 0 & 85 & 930 & 689 & 28 & 0 & 13 \\
0 & 0 & 0 & 0 & 36 & 81 & 5 & 0 & 142 & 1059 & 524 & 7 & 0 & 26 \\
0 & 0 & 0 & 0 & 52 & 69 & 1 & 0 & 232 & 1137 & 362 & 1 & 0 & 52 \\
0 & 0 & 0 & 1 & 69 & 52 & 0 & 1 & 362 & 1137 & 232 & 0 & 0 & 101 \\
0 & 0 & 0 & 5 & 81 & 36 & 0 & 7 & 524 & 1059 & 142 & 0 & 0 & 187 \\
0 & 0 & 0 & 13 & 85 & 24 & 0 & 28 & 689 & 930 & 85 & 0 & 1 & 317 \\
0 & 0 & 0 & 0 & 48 & 138 & 18 & 0 & 138 & 1188 & 738 & 24 & 0 & 18 \\
0 & 0 & 0 & 0 & 72 & 126 & 6 & 0 & 228 & 1314 & 540 & 6 & 0 & 36 \\
0 & 0 & 0 & 1 & 101 & 101 & 1 & 1 & 362 & 1362 & 362 & 1 & 0 & 69 \\
0 & 0 & 0 & 6 & 126 & 72 & 0 & 6 & 540 & 1314 & 228 & 0 & 0 & 126 \\
0 & 0 & 0 & 18 & 138 & 48 & 0 & 24 & 738 & 1188 & 138 & 0 & 0 & 216 \\
0 & 0 & 0 & 0 & 96 & 216 & 24 & 0 & 216 & 1440 & 738 & 18 & 0 & 24 \\
0 & 0 & 0 & 1 & 141 & 187 & 7 & 1 & 346 & 1536 & 524 & 5 & 0 & 45 \\
0 & 0 & 0 & 7 & 187 & 141 & 1 & 5 & 524 & 1536 & 346 & 1 & 0 & 81 \\
0 & 0 & 0 & 24 & 216 & 96 & 0 & 18 & 738 & 1440 & 216 & 0 & 0 & 138 \\
0 & 1 & 1 & 1 & 186 & 317 & 28 & 1 & 317 & 1632 & 689 & 13 & 0 & 28 \\
0 & 2 & 0 & 8 & 258 & 258 & 8 & 4 & 482 & 1680 & 482 & 4 & 0 & 50 \\
1 & 1 & 0 & 28 & 317 & 186 & 1 & 13 & 689 & 1632 & 317 & 1 & 0 & 85 \\
0 & 9 & 3 & 9 & 330 & 423 & 30 & 3 & 423 & 1728 & 609 & 9 & 0 & 30 \\
3 & 9 & 0 & 30 & 423 & 330 & 9 & 9 & 609 & 1728 & 423 & 3 & 0 & 51 \\
6 & 30 & 6 & 30 & 516 & 516 & 30 & 6 & 516 & 1728 & 516 & 6 & 0 & 30
\end{pmatrix}$$

and

$$Q_2 = \frac{1}{5040}\begin{pmatrix}
516 & 1728 & 516 & 6 & 0 & 30 & 516 & 516 & 30 & 0 & 6 & 30 & 6 \\
702 & 1728 & 330 & 0 & 0 & 51 & 609 & 423 & 9 & 0 & 9 & 30 & 3 \\
930 & 1632 & 186 & 0 & 0 & 85 & 689 & 317 & 1 & 0 & 13 & 28 & 1 \\
1188 & 1440 & 96 & 0 & 0 & 138 & 738 & 216 & 0 & 0 & 18 & 24 & 0 \\
1440 & 1188 & 48 & 0 & 0 & 216 & 738 & 138 & 0 & 0 & 24 & 18 & 0 \\
1632 & 930 & 24 & 0 & 1 & 317 & 689 & 85 & 0 & 1 & 28 & 13 & 0 \\
1728 & 702 & 12 & 0 & 9 & 423 & 609 & 51 & 0 & 3 & 30 & 9 & 0 \\
1728 & 516 & 6 & 0 & 30 & 516 & 516 & 30 & 0 & 6 & 30 & 6 & 0 \\
609 & 1728 & 423 & 3 & 0 & 30 & 423 & 330 & 9 & 0 & 3 & 9 & 0 \\
816 & 1680 & 258 & 0 & 0 & 50 & 482 & 258 & 2 & 0 & 4 & 8 & 0 \\
1059 & 1536 & 141 & 0 & 0 & 81 & 524 & 187 & 0 & 0 & 5 & 7 & 0 \\
1314 & 1314 & 72 & 0 & 0 & 126 & 540 & 126 & 0 & 0 & 6 & 6 & 0 \\
1536 & 1059 & 36 & 0 & 0 & 187 & 524 & 81 & 0 & 0 & 7 & 5 & 0 \\
1680 & 816 & 18 & 0 & 2 & 258 & 482 & 50 & 0 & 0 & 8 & 4 & 0 \\
1728 & 609 & 9 & 0 & 9 & 330 & 423 & 30 & 0 & 0 & 9 & 3 & 0 \\
689 & 1632 & 317 & 1 & 0 & 28 & 317 & 186 & 1 & 0 & 1 & 1 & 0 \\
903 & 1536 & 187 & 0 & 0 & 45 & 346 & 141 & 0 & 0 & 1 & 1 & 0 \\
1137 & 1362 & 101 & 0 & 0 & 69 & 362 & 101 & 0 & 0 & 1 & 1 & 0 \\
1362 & 1137 & 52 & 0 & 0 & 101 & 362 & 69 & 0 & 0 & 1 & 1 & 0 \\
1536 & 903 & 26 & 0 & 0 & 141 & 346 & 45 & 0 & 0 & 1 & 1 & 0 \\
1632 & 689 & 13 & 0 & 1 & 186 & 317 & 28 & 0 & 0 & 1 & 1 & 0 \\
738 & 1440 & 216 & 0 & 0 & 24 & 216 & 96 & 0 & 0 & 0 & 0 & 0 \\
936 & 1314 & 126 & 0 & 0 & 36 & 228 & 72 & 0 & 0 & 0 & 0 & 0 \\
1137 & 1137 & 69 & 0 & 0 & 52 & 232 & 52 & 0 & 0 & 0 & 0 & 0 \\
1314 & 936 & 36 & 0 & 0 & 72 & 228 & 36 & 0 & 0 & 0 & 0 & 0 \\
1440 & 738 & 18 & 0 & 0 & 96 & 216 & 24 & 0 & 0 & 0 & 0 & 0 \\
738 & 1188 & 138 & 0 & 0 & 18 & 138 & 48 & 0 & 0 & 0 & 0 & 0 \\
903 & 1059 & 81 & 0 & 0 & 26 & 142 & 36 & 0 & 0 & 0 & 0 & 0 \\
1059 & 903 & 45 & 0 & 0 & 36 & 142 & 26 & 0 & 0 & 0 & 0 & 0 \\
1188 & 738 & 24 & 0 & 0 & 48 & 138 & 18 & 0 & 0 & 0 & 0 & 0 \\
689 & 930 & 85 & 0 & 0 & 13 & 85 & 24 & 0 & 0 & 0 & 0 & 0 \\
816 & 816 & 50 & 0 & 0 & 18 & 86 & 18 & 0 & 0 & 0 & 0 & 0 \\
930 & 689 & 28 & 0 & 0 & 24 & 85 & 13 & 0 & 0 & 0 & 0 & 0 \\
609 & 702 & 51 & 0 & 0 & 9 & 51 & 12 & 0 & 0 & 0 & 0 & 0 \\
702 & 609 & 30 & 0 & 0 & 12 & 51 & 9 & 0 & 0 & 0 & 0 & 0 \\
516 & 516 & 30 & 0 & 0 & 6 & 30 & 6 & 0 & 0 & 0 & 0 & 0
\end{pmatrix}$$

and P is the vector containing the control data on the 27 sourrounding points seen in Figure 3.2. A point x in the triangle (P_{10}, P_{15}, P_{16}) can be expressed as a (u, v, w) tuple with $u+v+w = 1$ where $x = uP_{10} + vP_{15} + wP_{16}$. Therefore we can evaluate the functions F_J and $\tilde{\phi}_\alpha^J$ and their first 2 derivatives (as the scheme is C^2) at any point in K^J. If a point is close to a valence 3 vertex

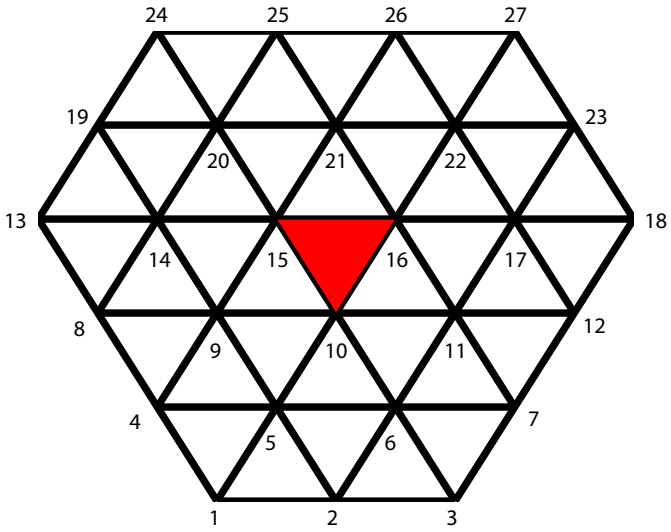

Figure 3.1: Control Data for a Triangle

we have to subdivide enough times such that the point is surrounded by a regular mesh and then evaluating the polynomial given by the box spline and by an eigenvalue analysis of the subdivision matrix for the valence 3 vertex we can compute the exact values and derivatives at the valence 3 vertex as

well. Let's look at $B^J_{\alpha\beta}$:

$$B^J_{\alpha\beta} = \int_S \Delta_S \phi^J_\alpha \Delta_S \phi^J_\beta dA \tag{3.5}$$

$$= \int_{K^J} \left((\Delta_S \phi^J_\alpha) \circ F_J\right) \left((\Delta_S \phi^J_\beta) \circ F_J\right) |dF_J| dA \tag{3.6}$$

$$= \sum_i \int_{T^J_i} \left((\Delta_S \phi^J_\alpha) \circ F_J\right) \left((\Delta_S \phi^J_\beta) \circ F_J\right) |dF_J| dA \tag{3.7}$$

$$= \sum_i \int_{\blacktriangle} \left((\Delta_S \phi^J_\alpha) \circ F_J \circ t^J_i\right) \left((\Delta_S \phi^J_\beta) \circ F_J \circ t^J_i\right) |dt^J_i| |dF_J \circ t^J_i| dA \tag{3.8}$$

$$\text{where } t^J_j : \blacktriangle \to T^J_i (i\text{the triangle in } K^J) \tag{3.9}$$

$$\text{and } \blacktriangle \text{ is the triangle with corners } (0,0)\ (1,0)\ (0,1) \tag{3.10}$$

Let's try to understand how to compute the Laplace-Beltrami operator Δ_S: Given a chart $\rho : \Omega \in \mathbb{R}^2 \to U \in S$ and a function $f : S \to \mathbb{R}$ then

$$\Delta_S f(s) = \sum_{ab} g^{ab} \left((f \circ \rho)_{x_a x_b} - \sum_c \Gamma^c_{ab} (f \circ \rho)_{x_c} \right)$$

where the right hand side is evaluated at the point x such that $\rho(x) = s$. The metric g is given by the entries g_{ab} (3.11), g^{ab} are the entries of its inverse matrix and Γ^c_{ab} are the so called Christoffel symbols (3.12). The quantities g^{ab} and Γ^c_{ab} are evaluated at x. We have

$$g_{ab} = \langle \frac{\partial \rho}{\partial x_a}, \frac{\partial \rho}{\partial x_b} \rangle \tag{3.11}$$

$$\Gamma^c_{ab} = \frac{1}{2} \sum_d g^{cd} \left(\frac{\partial g_{da}}{\partial x_b} + \frac{\partial g_{db}}{\partial x_a} - \frac{\partial g_{ab}}{\partial x_d} \right). \tag{3.12}$$

We can pick the chart ρ to be $F_J \circ t_i^J$ for each of the triangles. We are then able to compute the metric and the Christoffel symbols at given points in the triangle. Let's look at the first part of the integrand again:

$$\left((\Delta_S \phi_\alpha^J) \circ F_J \circ t_i^J\right)|_{x \in \blacktriangle} \tag{3.13}$$

$$= \sum_{ab} g^{ab} \left((\phi_\alpha^J \circ \rho)_{x_a x_b} - \sum_c \Gamma_{ab}^c (\phi_\alpha^J \circ \rho)_{x_c} \right)|_{x \in \blacktriangle} \tag{3.14}$$

$$\text{since } \rho = F_J \circ t_i^J \tag{3.15}$$

This means we need to compute the first and second derivative of $\phi_\alpha^J \circ \rho$ and ρ at $x \in \blacktriangle$. Furthermore we need to evaluate

$$|dF_J \circ t_i^J||dt_i^J| = d|(F_J \circ t_i^J)| = |d\rho| = \|\rho_{x_1} \times \rho_{x_2}\|,$$

where ρ_{x_1} and ρ_{x_2} are the first derivatives of ρ. We have that

$$\rho(x) = F_J \circ t_j^J(x) = F_J(u, v, w) \tag{3.16}$$

$$\phi_\alpha^J \circ \rho(x) = \tilde{\phi}_\alpha^J(u, v, w) \tag{3.17}$$

where $x = u(0,0) + v(1,0) + w(0,1)$. We can then compute the first derivatives

$$\frac{\partial \rho}{\partial x_1} = \frac{\partial F_J}{\partial v} - \frac{\partial F_J}{\partial u} \qquad \frac{\partial (\phi_\alpha^J \circ \rho)}{\partial x_1} = \frac{\partial \tilde{\phi}_\alpha^J}{\partial v} - \frac{\partial \tilde{\phi}_\alpha^J}{\partial u} \tag{3.18}$$

$$\frac{\partial \rho}{\partial x_2} = \frac{\partial F_J}{\partial w} - \frac{\partial F_J}{\partial u} \qquad \frac{\partial \phi_{(\alpha}^J \circ \rho)}{\partial x_2} = \frac{\partial \tilde{\phi}_\alpha^J}{\partial w} - \frac{\partial \tilde{\phi}_\alpha^J}{\partial u} \tag{3.19}$$

$$\tag{3.20}$$

and similarly the second derivatives. We evaluate the integral over ▲ with the simple quadrature rule

$$\int_{\blacktriangle} f dA = \frac{f(0,0) + f(1,0) + f(0,1)}{6}$$

Experimental Results

We start with a mesh that has 130 meshpoints and 200 observations (s_i, y_i) and compute the minimizer in the space of basis functions coming from this mesh. We then subdivide the mesh and compute a more accurate smoothing spline and repeat. The solution will not converge to the true solution but to the smoothing spline. We cannot compute the true smoothing spline except on the round sphere. This fact is due to Wahba [41]. We implemented Wahba's algorithm and found an experimental rate of convergence of h^4 where h is the reciprocal of the number of meshpoints. Using the function $f = x^T A x$ we plotted the true function, the true smoothing spline due to Wahba and the finite element solution for a mesh of size 514: see Figure 3.2

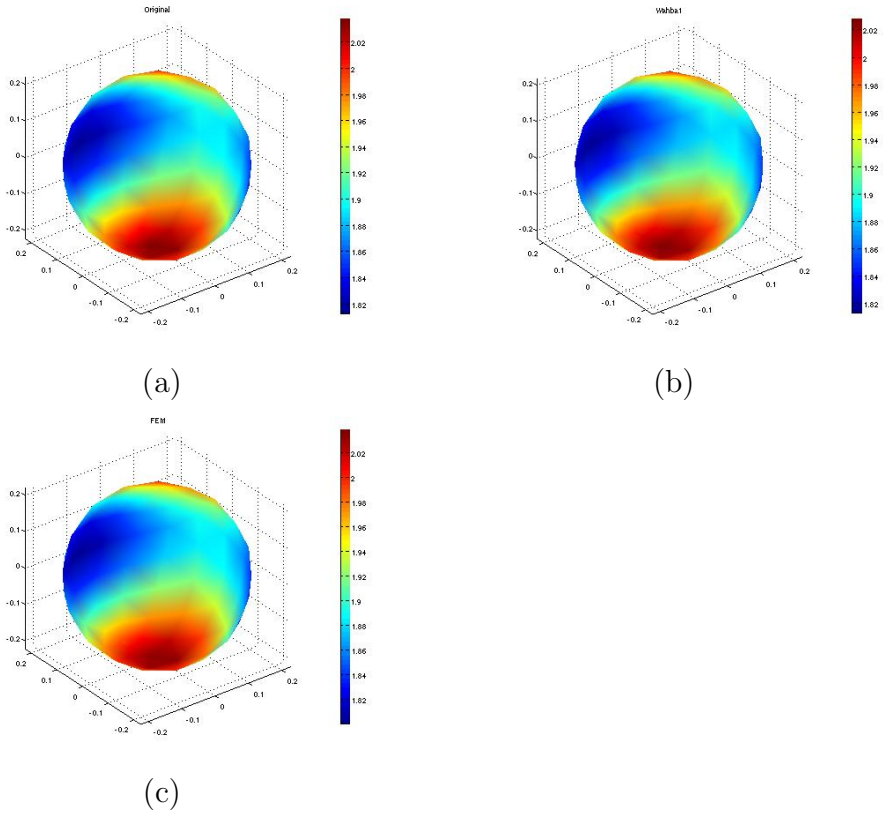

(a) (b)

(c)

Figure 3.2: Comparison of true solution (a) with Wahbas smoothing spline (b) and the finite element solution (c).

3.3 Willmore Energy, Curvature Flow and the rational sphere

We approximated the sphere above by a subdivision surface. Since the subdivision surface for our scheme is a piecewise polynomial we know that we are not able to find a mesh such that the limit surface is exactly the round sphere. We will explain how we found the best approximation to the sphere using subdivision surfaces of our scheme and extend our subdivision scheme

to a rational one. The R in NURBS stands for rational and it is a well known fact in mathematics that rational functions have better approximation properties than polynomials. We can for example represent an arch or a circle by a rational but not by a polynomial. The idea of using rational subdivision is not new but it is not used or explored widely. Since our scheme has high approximation order in the regular setting we are hoping that we can exactly parametrize the round sphere by a rational subdivision using our scheme. We are able to get a very good approximation of the sphere and hope that in the future we can prove that our subdivision scheme interpreted as a rational one can exactly represent the round sphere.

Problem 1

Given a twice subdivided tetrahedron we would like to find the mesh such that the limit surface is closest to the sphere. We assume that the mesh has the symmetry of the tetrahedral group. This leaves us 5 degrees of freedom. We know that the Willmore Energy of a genus 0 surface is 0 if and only if the surface is a sphere. Therefore we find a solution to this problem by minimizing the Willmore Energy. The Willmore Energy W is given by

$$W(S) = \int_S \kappa_m^2 dA - \int_S \kappa_G dA = \int_S \kappa_m^2 dA - 2\pi\chi(S)$$

where κ_m is the mean curvature and κ_G is the Gauss curvature. The optimal value we found is $W = 0.038$. The mesh and limit surface are given by Figure

3.3

(a) Base Mesh (B) Subdivision Limit Surface

Figure 3.3: Mesh and Subdivision Limit of the optimal approximation of the sphere

For optimizing we used a starting mesh which we created by evolving a twice subdivided tetrahedron by the curvature flow explained below to a surface close to a sphere. The flow doesn't keep the symmetry so the mesh we got from the curvature flow needed to be symmetrized before using it in our optimization. We then used a fminsearch, a function built into Matlab to find the presented solution. It is possible to optimize this result further. Since we know however that we cannot exactly describe the sphere we stopped our experiments here for now.

Problem 2

We know that a sphere can be exactly parametrized by rational patches [12]. It is however not known if there is a way to do that such that the parametrization is globally smooth. If we could find a mesh whose rational

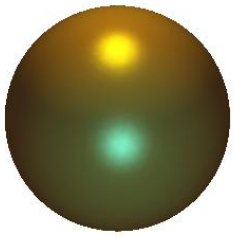

Figure 3.4: Limit surface of the rational sphere

limit is equal to the round sphere it would be a globally C^2 parametrization. We therefore consider a mesh in $\mathbb{R}^4$ and its subdivision limit. The subdivision limit in $\mathbb{R}^3$ is given by the image of the projection

$$P : \mathbb{R}^4 \to \mathbb{R}^3 \quad P(x_0, x_1, x_2, x_3) = (\frac{x_1}{x_0}, \frac{x_3}{x_0}, \frac{x_3}{x_0}).$$

We do the same optimization as in Problem 1 using the tetrahedral symmetry again gives us 8 degress of freedom. So far we are able to get the optimal value for the Willmore Energy down to 0.0001 and the limit surface is shown in Figure 3.3. Our numerical method to evaluate the Willmore Energy on such a mesh is not more accurate than 4 digits and we are therefore not able to say how close we can get to 0. We however know how to implement a better method by using exact evaluation due to J. Stam [39]. We hope that after the numerics give us hopeful results we are able to solve the following

questions:

Question 3.1. *Does a mesh with values in* $\mathbb{R}^4$ *exist such that its subdivision limit surface under the subdivision of Chapter 2 projected into* $\mathbb{R}^3$ *is the round sphere?*

Curvature Flow Simulation

The curvature flow is given by

$$\mathbf{v} = (\kappa_m - \frac{\int_S \kappa_m ds}{\int_S ds})\mathbf{n}$$

where $\mathbf{v}$ is the velocity vector on the surface. We will assume that the subdivision limit S of the mesh K is the approximation of the starting surface. We want to compute the evolution of this surface under the curvature flow over time. The subdivision surface is a smooth surface that is uniquely described by the mesh and the subdivision rules. Since our scheme is perfectly C^2 we can compute the exact curvature at every point in the mesh.

We will now compute

- κ_m^i the curvature at every mesh point
- $\mathbf{n}_i$ the normal at every mesh point
- $\int_S \kappa_m ds$ and $\int_S ds$ by a quadrature rule

We will evolve the surface by evolving the mesh points x_i only:

$$x_i^{new} = x_i^{old} + \delta t(\kappa_m^i - \frac{\int_S \kappa_m ds}{\int_S ds})\mathbf{n_i}$$

We know that in theory any given surface flows to the round sphere under the curvature flow. Our algorithm produces limit meshes which are close to the sphere. An example is given in Figure 3.5.

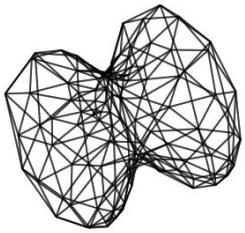

(a) Starting Mesh

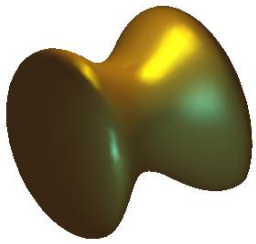

(B) Starting Surface

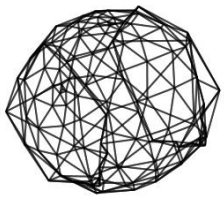

(a) Limit Mesh

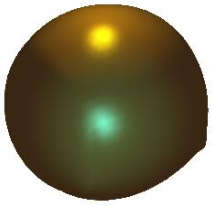

(B) Limit Surface

Figure 3.5: Example of a Curvature Flow: Start and Limit Surface.

3.4 Conclusions

The numerical method used to compute the curvature flow simulation is basically forward Euler. It is well-known that forward Euler requires very small time steps in order to produce accurate solutions. We do see that phenomenon here. The main point we are trying to make here is however that even such a crude numerical method works on as a simulation tool based on our subdivision scheme. That means that better methods will work even better. Since we approximate a surface by a C^2 smooth surface we hope to be able to model complex phenomena with this method. We furthermore see that we can approximate the sphere very well with a very simple mesh which will also be a useful tool in modeling and simulation of phenomena on spheres. We can use the refinement for finite element type analysis as seen in the approximation of functions and we are able to only locally refine as well.

Chapter 4

Quadrilateral Meshes and an Eigenvalue Optimization Problem

4.1 Quad Subdivision

In Chapter 2 we develop a Subdivision Scheme on a triangular mesh. A similar idea works on the quadrilateral mesh and one solution was proposed in [20].

We use the subdivision scheme that comes from the bi-quartic tensor product B-spline in the regular setting. This is a dual scheme and the rules are given by Figure 4.1. It does reproduce all degree 4 polynomials and therefore has the necessary approximation order. The subdivision matrix

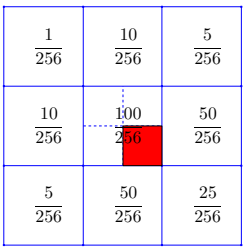

Figure 4.1: Subdivision rules for the regular setting

for the extraordinary vertex of valence 2 can be constructed depending on a number of parameters given by Figure 4.2. The matrix is then given by S:

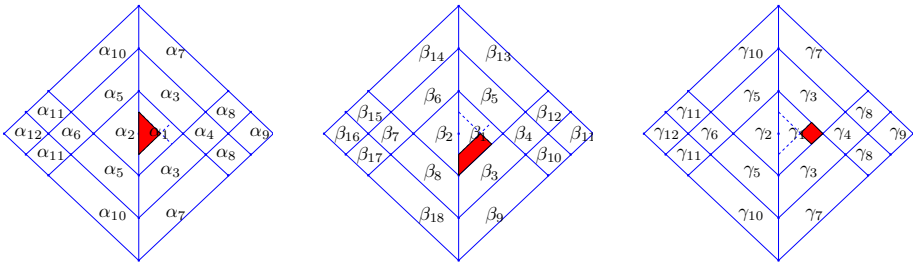

$\Sigma\alpha_i = 1$ $\Sigma\beta_i = 1$ $\Sigma\gamma_i = 1$

Figure 4.2: Valence 2 extraordinary vertex rules

$$S = \begin{bmatrix} M_1 & M_2 \\ A & B \end{bmatrix} \tag{4.1}$$

where

$$M_1 = \begin{bmatrix} \alpha_1 & \alpha_2 & \alpha_3 & \alpha_4 & \alpha_3 & \alpha_5 & \alpha_6 & \alpha_5 \\ \alpha_2 & \alpha_1 & \alpha_5 & \alpha_6 & \alpha_5 & \alpha_3 & \alpha_4 & \alpha_3 \\ \beta_1 & \beta_2 & \beta_3 & \beta_4 & \beta_5 & \beta_6 & \beta_7 & \beta_8 \\ \gamma_1 & \gamma_2 & \gamma_3 & \gamma_4 & \gamma_3 & \gamma_5 & \gamma_6 & \gamma_5 \\ \beta_1 & \beta_2 & \beta_5 & \beta_4 & \beta_3 & \beta_8 & \beta_7 & \beta_6 \\ \beta_2 & \beta_1 & \beta_6 & \beta_7 & \beta_8 & \beta_3 & \beta_4 & \beta_5 \\ \gamma_2 & \gamma_1 & \gamma_5 & \gamma_6 & \gamma_5 & \gamma_3 & \gamma_4 & \gamma_3 \\ \beta_2 & \beta_1 & \beta_8 & \beta_7 & \beta_6 & \beta_5 & \beta_4 & \beta_3 \end{bmatrix}, \tag{4.2}$$

$$M_2 = \begin{bmatrix} \alpha_7 & \alpha_8 & \alpha_9 & \alpha_8 & \alpha_7 & \alpha_{10} & \alpha_{11} & \alpha_{12} & \alpha_{11} & \alpha_{10} \\ \alpha_{10} & \alpha_{11} & \alpha_{12} & \alpha_{11} & \alpha_{10} & \alpha_7 & \alpha_8 & \alpha_9 & \alpha_8 & \alpha_7 \\ \beta_9 & \beta_{10} & \beta_{11} & \beta_{12} & \beta_{13} & \beta_{14} & \beta_{15} & \beta_{16} & \beta_{17} & \beta_{18} \\ \gamma_7 & \gamma_8 & \gamma_9 & \gamma_8 & \gamma_7 & \gamma_{10} & \gamma_{11} & \gamma_{12} & \gamma_{11} & \gamma_{10} \\ \beta_{13} & \beta_{12} & \beta_{11} & \beta_{10} & \beta_9 & \beta_{18} & \beta_{17} & \beta_{16} & \beta_{15} & \beta_{14} \\ \beta_{14} & \beta_{15} & \beta_{16} & \beta_{17} & \beta_{18} & \beta_9 & \beta_{10} & \beta_{11} & \beta_{12} & \beta_{13} \\ \gamma_{10} & \gamma_{11} & \gamma_{12} & \gamma_{11} & \gamma_{10} & \gamma_7 & \gamma_8 & \gamma_9 & \gamma_8 & \gamma_7 \\ \beta_{18} & \beta_{17} & \beta_{16} & \beta_{15} & \beta_{14} & \beta_{13} & \beta_{12} & \beta_{11} & \beta_{10} & \beta_9 \end{bmatrix}, \tag{4.3}$$

$$A = \frac{1}{256}\begin{bmatrix} 50 & 25 & 100 & 10 & 5 & 0 & 0 & 50 \\ 50 & 5 & 100 & 50 & 25 & 0 & 0 & 10 \\ 25 & 0 & 50 & 100 & 50 & 0 & 0 & 0 \\ 50 & 5 & 25 & 50 & 100 & 10 & 0 & 0 \\ 50 & 25 & 5 & 10 & 100 & 50 & 0 & 0 \\ 25 & 50 & 0 & 0 & 50 & 100 & 10 & 5 \\ 5 & 50 & 0 & 0 & 10 & 100 & 50 & 25 \\ 0 & 25 & 0 & 0 & 0 & 50 & 100 & 50 \\ 5 & 50 & 10 & 0 & 0 & 25 & 50 & 100 \\ 25 & 50 & 50 & 0 & 0 & 5 & 10 & 100 \end{bmatrix},$$

$$B = \frac{1}{256}\begin{bmatrix} 10 & 1 & 0 & 0 & 0 & 0 & 0 & 0 & 0 & 5 \\ 10 & 5 & 0 & 0 & 0 & 0 & 0 & 0 & 0 & 1 \\ 5 & 10 & 1 & 10 & 5 & 0 & 0 & 0 & 0 & 0 \\ 0 & 0 & 0 & 5 & 10 & 1 & 0 & 0 & 0 & 0 \\ 0 & 0 & 0 & 1 & 10 & 5 & 0 & 0 & 0 & 0 \\ 0 & 0 & 0 & 0 & 5 & 10 & 1 & 0 & 0 & 0 \\ 0 & 0 & 0 & 0 & 1 & 10 & 5 & 0 & 0 & 0 \\ 0 & 0 & 0 & 0 & 0 & 5 & 10 & 1 & 10 & 5 \\ 1 & 0 & 0 & 0 & 0 & 0 & 0 & 0 & 5 & 10 \\ 5 & 0 & 0 & 0 & 0 & 0 & 0 & 0 & 1 & 10 \end{bmatrix}.$$

Exactly as in the triangular case we find the eigenvectors u_1, u_2, w_1, w_2, w_3

such that

$$Su_i = \frac{1}{4}u_i \text{ and } Sw_i = \frac{1}{16}w_i. \tag{4.4}$$

Those vectors are given by

$$\begin{aligned}
u_1 &= \left[0,\ 0,\ 2,\ 0,\ -2,\ -2,\ 0,\ 2,\ 6,\ 4,\ 0,\ -4,\ -6,\ -6,\ -4,\ 0,\ 4,\ 6\right]^T,\\
u_2 &= \frac{1}{2}\left[1,\ -1,\ 3,\ 9,\ 3,\ -3,\ -9,\ -3,\ 5,\ 15,\ 25,\ 15,\ 5,\ -5,\ -15,\ -25,\ -15,\ -5\right]^T,\\
w_1 &= \frac{1}{18}\left[-1,\ -1,\ 11,\ -121,\ 11,\ 11,\ -121,\ 11,\ 467,\ 47,\ -361,\ 47,\ 467,\ 467,\ 47,\ -361,\ 47,\ 467\right]^T,\\
w_2 &= \left[0,\ 0,\ 3,\ 0,\ -3,\ 3,\ 0,\ -3,\ 15,\ 30,\ 0,\ -30,\ -15,\ 15,\ 30,\ 0,\ -30,\ -15\right]^T,\\
w_3 &= \frac{1}{9}\left[1,\ 1,\ -11,\ 121,\ -11,\ -11,\ 121,\ -11,\ -35,\ 385,\ 1225,\ 385,\ -35,\ -35,\ 385,\ 1225,\ 385,\ -35\right]^T.
\end{aligned} \tag{4.5}$$

The linear systems 4.4 give us 11 independent linear conditions. This means we can reduce the original $42 - 3 = 39$ parameters to $42 - 3 - 11 = 28$ parameters. So now we have an 18x18 matrix with 28 parameters which we know has the following 6 eigenvalues:

$$1, 1/4, 1/4, 1/16, 1/16, 1/16.$$

As in the triangular case the corresponding scheme is C^2 if we can find parameters such that all the other eigenvalues are smaller than 1/16. This leads to an optimization problem.

4.2 Eigenvalue Optimization

We look for the best choice of parameters $x \in \mathbb{R}^{28}$ by formulating an optimization problem:

$$\min f(x) \equiv \rho_R(S(x))$$

where ρ_R is the reduced spectral radius, by which we mean the spectral radius after removing the eigenvalues

$$1, 1/4, 1/4, 1/16, 1/16, 1/16.$$

The objective function f is non-smooth, nonconvex and not even Lipschitz continuous. However we are able to compute its gradient almost everywhere. The partial derivative is given by

$$\frac{\partial \rho_R(S(x))}{\partial x_i} = \mathrm{Re}(\frac{\mu}{|\mu|} u \frac{\partial S(x)}{\partial x_i} v)$$

where v is the right eigenvector and u is the left eigenvector for the eigenvalue μ for which $\rho_R(S(x)) = |\mu|$. Although at an optimal solution, μ may well be a multiple eigenvalue (as discussed below), for almost any other choice of x, including nearly optimal x, μ is a simple eigenvalue, and hence the gradient is well defined.

This is enough to use the optimization code HANSO [4]. It is based on BFGS [23] and gradient sampling [6], but in most of our computations we used only BFGS, which, as explained in [23], is surprisingly effective even on nonsmooth objective functions. We started the algorithm with multiple randomly selected points in $\mathbb{R}^{28}$ with small norm. After a few attempts BFGS

gave us a point x with $f(x) \approx 0.02$. This result was satisfying in the sense that $0.02 < \frac{1}{16}$. Furthermore, the largest eigenvalue in the scheme presented in [20] is also around 0.02. Subsequently we ran BFGS repeatedly, each time starting at a point which was a slight perturbation of the previous best point, eventually reducing f to about 2×10^{-4}.

Let us discuss the distribution of eigenvalues (excluding $1, 1/4, 1/16$) of the various matrices $S(x)$ corresponding to the parameter choices found by BFGS. In Figure 4.3 we plot the relevant eigenvalues of $S(x)$ in the complex plane and draw a circle with radius equal to the reduced spectral radius. Note the different scales in the four panels of the figure.

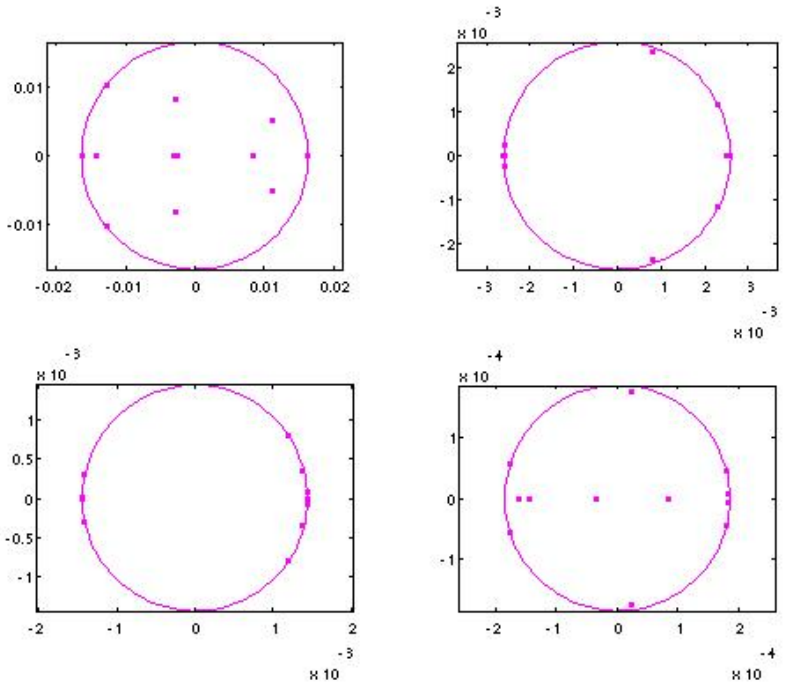

Figure 4.3: Plots of eigenvalues for various choices of x

We can see that the eigenvalue distribution in the top left panel is very arbitrary as x is not yet close to an optimizer. The second and third picture show a spectral radius of about 10^{-3}. There, all eigenvalues are very close in modulus giving us the impression that x is close to a minimizer. In other words, one can think of the sequence of approximate optimizers as steadily shrinking a circle which contains the relevant eigenvalues; from this viewpoint, it is natural that the eigenvalues lie nearly on the relevant circle. In the final panel, however, we no longer have the nice distribution. This is probably caused by the fact that x is so close to the optimum that rounding errors are scattering the eigenvalues. Indeed, we conjecture that it is possible to reduce all the eigenvalues to zero:

Conjecture 4.1. *There exists an* $\widehat{x} \in \mathbb{R}^{28}$ *such that* $f(\widehat{x}) = 0$ *meaning the 18 eigenvalues of* $S(\widehat{x})$ *are given by* $1, 1/4, 1/4, 1/16, 1/16, 1/16, 0, \ldots, 0$.

We are interested in the Jordan structure of the minimizer. We therefore computed the eigenvectors corresponding to the relevant eigenvalues (the ones that are nearly zero), normalizing them to have unit length. It turns out that if we take the Singular Value Decomposition of the matrix composed of those 12 eigenvectors we get 12 numbers that are close to

$$\sqrt{5}, \sqrt{3}, \sqrt{2}, \sqrt{2}, 0, \ldots, 0$$

This leads to our next Conjecture:

Conjecture 4.2. *The Jordan Normal Form of* $S(\widehat{x})$ *is given by*

$$\begin{bmatrix} D & 0 & 0 & 0 & 0 \\ 0 & J_5(0) & 0 & 0 & 0 \\ 0 & 0 & J_3(0) & 0 & 0 \\ 0 & 0 & 0 & J_2(0) & 0 \\ 0 & 0 & 0 & 0 & J_2(0) \end{bmatrix},$$

where $D = diag(1, 1/4, 1/4, 1/16, 1/16, 1/16)$ *and* $J_i(0)$ *is a Jordan Block of size* i *with 0's on the diagonal.*

As explained in Chapter 2 we can analytically determine the global minimum of a similar problem that comes from the triangular case: see Theorem 2.3. In that case, the singular values of the corresponding matrix of eigenvectors of the relevant eigenvalues (excluding D) is given by

$$\sqrt{2}, 1, 1, 0,$$

the zero indicating that there is only one eigenvector for $J_2(0)$ and hence it is repeated. In our view, this makes Conjectures 4.1 and 4.2 quite convincing.

Furthermore, it is well known from eigenvalue perturbation theory that a random perturbation of norm ε to a Jordan block $J_k(0)$ induces perturbed eigenvalues with approximate magnitude $\varepsilon^{1/k}$ [24]. Hence, assuming that Conjectures 4.1 and 4.2 are true, it is quite remarkable that BFGS was able to reduce f to about 2×10^{-4}, since a random perturbation of order machine

precision (about 10^{-16}) to $S(\widehat{x})$ should result in eigenvalues with magnitude about $(10^{-16})^{1/5} \approx 10^{-3}$.

Chapter 5

Boundary Analysis of subdivision schemes

5.1 Introduction

Two features of subdivision algorithms are particularly important for applications. The first is the ability to handle a large variety of input meshes, including meshes with boundary. The second is the ease of modification of subdivision rules, which makes it possible to generate different surfaces (e.g. surfaces with sharp or soft creases) out of the same input mesh.

Importance of special boundary and crease rules was recognized for some time [26, 27, 19, 38]. However, most of the theoretical analysis of subdivision [35, 29, 46, 45] focused on the case of surfaces without boundaries and schemes invariant with respect to rotations. The goal is to develop the

necessary theoretical foundations for analysis of subdivision rules for meshes with boundary, and present analysis for boundary rules extending several well-known subdivision schemes, described in [3].

The starting point for our theory is a precise description of the class of surfaces that we would like to be able to model using subdivision. We introduce the definition of surfaces with piecewise-smooth boundary. This class readily extends to a broader class of piecewise-smooth surfaces, which is sufficiently broad for many practical applications. We demonstrate how the standard constructions of subdivision theory (subdivision matrices, characteristic maps etc.) generalize to the case of surfaces with piecewise-smooth boundary. Remarkably, even at this abstract stage we make a simple, yet important observation, with substantial practical implications: convex and concave corner singularities of the boundary require separate subdivision rules.

We proceed to extend the techniques for analysis of C^1-continuity developed in [45] to the case of piecewise-smooth surfaces with boundary.

The result allowing one to analyze C^1-continuity of most subdivision schemes for surfaces without boundaries is the sufficient condition of Reif [35]. This condition reduces the analysis of stationary subdivision to the analysis of a single map, called the *characteristic map*, uniquely defined for each valence of vertices in the mesh. The analysis of C^1-continuity is performed in three steps for each valence:

1. compute the control net of the characteristic map;

2. prove that the characteristic map is regular;

3. prove that the characteristic map is injective.

We show that similar conditions hold for surfaces with boundary, and under commonly satisfied assumptions injectivity of the characteristic map for surfaces with boundary can be inferred from regularity. To avoid the need to evaluate the characteristic map in closed form, we obtain convergence estimates for subdivision schemes acting on regular grids with boundary. These estimates allow us to use sufficiently close linear approximations to draw conclusions about regularity of the characteristic map. We describe the elements of the theory of schemes acting on regular grids with boundary which we need to perform C^1-continuity analysis.

Subdivision schemes acting on grids with boundary were introduced in [44] where they were referred to as *crease subdivision schemes*. A generalization of this class of schemes was studied in [22] where they are referred to as *quasi-uniform* subdivision schemes.

Finally, we use the theory that we have developed to derive and analyze several specific boundary subdivision rules, initially proposed in [3].

Previous work The theory presented here is based on the theory developed for closed surfaces in [35, 46, 45]. As far as we know, analysis of C^1-continuity of subdivision rules for surfaces with boundary was performed only in [38], where a particular choice of rules extending Loop subdivision was analyzed.

At the same time, substantial number of papers proposed various boundary rules starting with the first papers on subdivision by Doo and Sabin, and Catmull and Clark [7, 13, 26, 28, 19]. Most recently, a method for generating soft creases was proposed in [11].

In our C^1-continuity verification method we use estimates of the convergence rate of quasi-uniform subdivision schemes, considered briefly in [44] and in greater generality and detail in [22].

Our estimates of the errors of linear approximations rely on the work of Cavaretta, Dahmen and Micchelli [8], and on the work of Cohen, Dyn and Levin [9] on matrix subdivision.

5.2 Surfaces with Piecewise-smooth Boundary

5.2.1 Definitions

In this section we define surfaces with piecewise-smooth boundaries. Unlike the case of open surfaces, there is no single commonly accepted definition that would be suitable for our purposes. We consider several definitions of surfaces with boundaries and motivate the choice that we make (Definition 5.4).

The least restrictive definition of a closed surface with boundary is a closed part of an open surface. This definition is too general for our purposes but provides a useful starting point. More formally, we define a closed surface

with boundary as follows. Recall that an open C^k-continuous surface in $\mathbf{R}^p$ can be defined as a topological space M with a map $f : M \to \mathbf{R}^p$ such that for any point $x \in M$ there is a neighborhood U_x such that $f(U_x)$ can be reparametrized over the open unit disk D using a C^k nondegenerate map $g : D \to f(U_x)$.

Definition 5.1. *Let M be a closed topological space with boundary, and f a map from M to $\mathbf{R}^p$. We say that (M, f) is a* **closed C^k surface with boundary***, if there is an open C^k-continuous surface (M', f') and an injective inclusion map $\iota : M \to M'$, such that $f' \circ \iota = f$.*

Note that this definition places very few restrictions on the boundary: for example, any subset of the plane from this point of view is a C^k-continuous surface for any k. Typically, additional restrictions are added. Most commonly the boundary is required to be a union of nonintersecting C^k-continuous curves (see [25],[14]). Assuming that the domains of these curves are separated in M', this type of surfaces can be defined using two local charts, the open unit disk D and the half-disk $Q_2 = H \cap D$, where H is the closed halfplane defined by $H = \{(x, y) | y \geqslant 0\}$.

Definition 5.2. *Consider a surface (M, f) where M is a topological space, and f is a map $f : M \to \mathbf{R}^p$. The surface (M, f) is called a* **closed C^k-continuous surface with C^k boundary** *if for any $x \in M$ there exists a neighborhood U_x and a regular C^k-continuous parametrization h of $f(U_x)$ over an open disk D (internal point) or a half-disk Q_2 (boundary point).*

This definition is too narrow for geometric modeling, as surfaces with corners (e.g. surfaces obtained by smooth deformations of a rectangle) are quite common. To include corners, we have to allow isolated singularities for the boundary curves. We consider a broader class of surfaces, which we call C^k-continuous surfaces with piecewise C^k-continuous boundary.

Definition 5.3. *Let (M, f), $f : M \to \mathbf{R}^p$ be a closed C^k-continuous surface with boundary as defined above, Let $\gamma_i : [0,1] \to M$, $i \in I$, where I is finite, be a set of curve segments, such that each endpoint is shared by exactly 2 segments, and the curve segments intersect only at endpoints. Suppose the boundary of M coincides with $\cap_i \mathrm{Im}\gamma_i$, the curves $f \circ \gamma_i$ are C^k-continuous. Then we call (M, f) a* **C^k-continuous surface with piecewise C^k-continuous boundary.**

The definition implies existence of the tangents to the boundary curves at the endpoints. However, these tangents may not coincide for two adjacent curves, and result in either a *cusp* of degree m or a C^m-continuous joint for $m \leqslant k$. In either case, k different charts are required to parametrize the surface, as two curves with a contact point of order m are clearly not C^k-diffeomorphic to two curves with a contact point of order $n \neq m$, for $n, m \leqslant k$. Moreover, the boundary of the surface is not Lipschitz if it contains cusps, which means that surfaces of this type require special treatment when we consider functions defined on such surfaces (cf. [40]).

Transversality assumption. We assume that the adjacent boundary curve segments intersect transversely, that is, their tangents are different at the shared endpoint. We call such endpoints of boundary curve segments **non-degenerate corners.** Thus, the surfaces that we consider do not contain cusps or C^m-continuous joints for $0 < m < k$, We leave analysis of surfaces with higher degree contact points as future work. There are two reasons for this.

First, mathematical description of such surfaces is more complex and best done separately, once the framework for surfaces with boundaries with non-degenerate corners is established.

Second, it appears that this type of features in most cases is best modeled using degenerate configurations of control points rather than special subdivision rules. Here, we consider only behavior of surfaces for generic configurations of control points.

It is clear however that higher-order boundary singularities are useful in applications, a simple example being a surface filling a gap between a cylinder and a tangent plane.

Once we exclude the higher-order contact cases, we can use a more constructive equivalent definition of surfaces with piecewise C^k-continuous boundary with nondegenerate corners. We use four charts, for all possible types of points of the surface (Figure 5.1). In addition to the disk D and the halfdisk Q_2, we use a quarter of the disk Q_1 and three quarters of the disk Q_3. The domains Q_i $i = 1, 3$ are defined as follows: $Q_1 = \{(x, y) | y \geqslant$

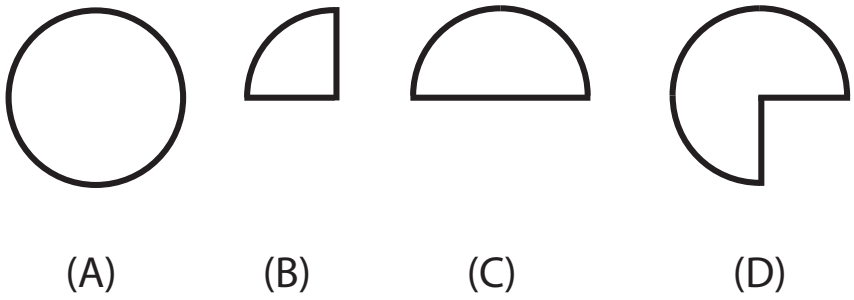

Figure 5.1: Types of local chart (A) is the disk D, (B) is he quarter disk Q_1, (C) is the half disk Q_2 and (D) is the three-quarter disk Q_3

0 and $x \geqslant 0\} \cap D$, $Q_3 = \{(x, y)|y \geqslant 0$ or $x \geqslant 0\} \cap D$.

Now we can give an alternative definition of a C^k-continuous surface with piecewise smooth boundary with nondegenerate corners:

Definition 5.4. *Consider a surface (M, f) where M is a topological space, and f is a map $f : M \to \mathbf{R}^p$. The surface (M, f) is called* **C^k-continuous with piecewise C^k-continuous boundary with non-degenerate corners** *if for any x there is a neighborhood U_x and a regular C^k-continuous parametrization of $f(U_x)$ over one of the domains Q_i, $i = 1, \ldots 3$, or over the disk D. In the first case, we call the point x a boundary point, in the second case an interior point. We distinguish two main types of boundary points: if U_x is diffeomorphic to Q_2, the boundary point is called smooth; otherwise it is called a corner. There are 2 types of corners:*

- *convex corners (U_x is diffeomorphic to Q_1);*
- *concave corners (U_x is diffeomorphic to Q_3);*

For brevity we will also use the term C^k-continuous surface with piecewise-smooth boundary.

Equivalence of definitions 5.4 and 5.3 with degenerate corners excluded is straightforward to show using the well known facts about existence of the extensions of functions defined on Lipschitz domains to the plane.

Surfaces satisfying Definition 5.4 can be used to model a large variety of features; for example, by joining the surfaces along boundary lines we can obtain surfaces with creases. However, in addition to boundary cusps, a number of useful features such as cones cannot be modeled, unless degenerate configurations of control points are used.

5.2.2 Tangent Plane Continuity and C^1-continuity

As we will see in Section 5.3, analysis of subdivision focuses on the behavior of surfaces which are known to be at least C^1-continuous in a neighborhood of a point, but nothing is known about the behavior at the point. In this case, it is convenient to split the analysis into several steps, the first being **tangent plane continuity**. In the definition below, we use $\wedge$ to denote the exterior product (vector product for $p = 3$) and $[\cdot]_+$ to denote normalization of a vector.

Definition 5.5. *Let D be the unit disk in the plane. Suppose a surface (M, f) in a neighborhood of a point $x \in M$ is parametrized by $h : U \to \mathbf{R}^p$, where U is a subset of the unit disk D containing 0, which is regular everywhere*

except 0, and $h(0) = f(x)$. *Let* $\pi(y) = [\partial_1 h \wedge \partial_2 h]_+$. *where* $\partial_1 h$ *and* $\partial_2 h$ *are derivatives with respect to the coordinates in the plane of the disk* D. *The surface is* **tangent plane continuous** *at* x *if the limit* $\lim_{y\to 0} \pi(y)$ *exists.*

For an interior point x for which the surface is known to be C^1-continuous in a neighborhood of the point x excluding x, the surface is C^1-continuous at x if and only if it is tangent plane continuous and the projection of the surface into the tangent plane is injective ([46], Proposition 1.2). The proof of this proposition does not assume that the surface is defined on an open neighborhood of x. C^1 continuity for an interior point x is inferred from existence and C^1 continuity of two independent derivatives of reparametrization of the surface over the tangent plane. This fact alone is not sufficient to guarantee that the surface has piecewise continuous boundary with nondegenerate corners: we need to impose an additional condition on the boundary curve. We can see that the boundary of (M, f) has a nondegenerate corner at x if there is a neighborhood U_x such that $f(U_x) \cap f(\partial M)$ admits a parametrization by two C^1-continuous curves $\gamma_i : \ (0, 1] \to \mathbf{R}^p$, $i = 1, 2$, such that $\gamma_1(1) = \gamma_2(1) = f(x)$, and the tangents to the curves are different at the common endpoint x.

Proposition 5.1. *Suppose a surface* (M, f) *is* C^1*-continuous with* C^1*-continuous boundary in a neighborhood* U_x *of a boundary point* x *excluding* x. *The surface is* C^1*-continuous at* x *with piecewise* C^1*-continuous boundary if and only if it is*

1. *tangent plane continuous,*

2. *the projection of the surface into the tangent plane is injective,*

3. *the boundary either has a nondegenerate corner at x or is C^1-continuous at x.*

Proof. Necessity of these conditions is straightforward. Most of the proof of sufficiency coincides with the proof of Proposition 1.2 from [46]: if we assume only that the surface is tangent plane continuous and the projection into the tangent plane is injective, we can show that the derivatives in two independent directions of π, the inverse of a projection of the surface into the tangent plane, exist and are continuous at point x.

It remains to be shown that the surface is C^1-diffeomorphic to one of the domains Q_i, $i = 1, 2, 3$.

As the boundary curves γ_i are C^1-continuous, and their tangents are in the tangent plane to the surface at all points, their projections $P\gamma_i$ into the tangent plane at x are also C^1-continuous. At the point x the tangents to the curves are in the tangent plane at x, and coincide with the tangents to the projections. By construction, the domain of π, the image of the projection of the surface into the tangent plane, is homeomorphic to a halfdisk. We have shown that the image of the boundary diameter of the halfdisk is C^1-continuous or C^1-continuous with a nondegenerate corner at x. The neighborhood U_x can be chosen in such a way that $Pf(\partial U_x \setminus \partial M)$, the image of the part of the boundary of U_x which is not the boundary of M, is a

semicircle centered at x and intersects the curves $P\gamma_i$ only at a single point each. (We omit somewhat tedious but straightforward proof of this fact.)

Thus, our surface can be parametrized in a neighborhood of x over a planar domain $Pf(U_x)$ which is a subset of an open disk $D_{Pf(x)}$ bounded by two C^1 curve segments connecting the center $Pf(x)$ to the boundary. Let l_1 and l_2 be the rays along tangent directions to γ_1 and γ_2 at x (possibly collinear). Then for sufficiently small radius of the neighborhood, we can assume that orthogonal projections of γ_i to l_i is injective. Note that $l_1 \cap l_2$ split the disk $D_{Pf(x)}$ into two parts D_1 and D_2; either both parts are half-disks, or one part is convex and the other concave. Now we can directly construct a C^1-diffeomorphism of the domain $Pf(U_x)$ to one of the domains D_1 and D_2. For example, in the simplest case of l_1 and l_2 being collinear, we can use a coordinate system (s,t) in which l_1 and l_2 form the s axis, and γ_1 and γ_2 form a graph of a function $\gamma(s)$. Assuming that the disk $D_{Pf(x)}$ has radius 1 the formula

$$(s,t) \to \left(s, \sqrt{1-s^2}\frac{t-\gamma(s)}{\sqrt{(1-s^2)-\gamma(s)}} \right)$$

defines the desired diffeomorphism.

We have shown that the surface has a parametrization g over one of the domains Q_i $i = 1,2,3$ in the neighborhood of x, which has C^1-continuous derivatives everywhere on Q_i with nowhere degenerate Jacobian. $\square$

This proposition provides a general strategy for establishing C^1-continuity

of surfaces, which is particularly convenient for subdivision surfaces. Moreover, as we shall see, in most cases of practical importance we can infer the injectivity of the projection from the other two conditions, so only local tests need to be performed.

5.3 Subdivision Schemes on Complexes with Boundary

In this section we summarize the main definitions and facts about subdivision on complexes that we use; more details for the case of surfaces without boundaries can be found in [46, 44]. The changes that have to be made to make the constructions work for the boundary case are relatively small. We restrict the presentation to the case of schemes for triangle meshes to avoid making the notation excessively complex. However, the results equally apply to quadrilateral schemes; only minor changes in notation are necessary.

5.3.1 Definitions and eigendecomposition theory

Simplicial complexes. Subdivision surfaces are naturally defined as functions on two-dimensional polygonal complexes. A simplicial complex K is a set of vertices, edges and planar simple polygons (faces) in $\mathbf{R}^N$, such that for any face its edges are in K, and for any edge its vertices are in K. We assume that there are no isolated vertices or edges. $|K|$ denotes the union of

faces of the complex regarded as a subset of $\mathbf{R}^N$ with induced metric. We say that two complexes K_1 and K_2 are *isomorphic* if there is a homeomorphism between $|K_1|$ and $|K_2|$ that maps vertices to vertices, edges to edges and faces to faces.

A *subcomplex* of a complex K is a subset of K that is a complex. A 1-neighborhood $N_1(v, K)$ of a vertex v in a complex K is the subcomplex formed by all faces that have v as a vertex. The m-neighborhood of a vertex v is defined recursively as a union of all 1-neighborhoods of vertices in the $(m-1)$-neighborhood of v. We omit K in the notation for neighborhoods when it is clear what complex we refer to.

Recall that a *link* of a vertex is the set of edges of $N_1(v, K)$ that do not contain v. We consider only complexes with all vertices having links that are connected simple polygonal lines, open or closed. If the link of a vertex is an open polygonal line, this vertex is a boundary vertex, otherwise it is an internal vertex.

In the analysis of schemes for surfaces without boundary the regular complex $\mathcal{R}$ and k-regular complexes $\mathcal{R}_k$ are are commonly used [46]. We are primarily interested in schemes that work on quadrilateral and triangle meshes, and we consider k-regular complexes with all faces being identical triangles or quads; however, similar complexes can be defined for the remaining regular tiling, with all faces being hexagons, and more generally for any Laves tiling. For schemes acting on meshes with boundary we use regular and k-regular complexes with boundary. A regular complex with boundary is isomorphic

to a regular tiling of the upper half-plane. A k-regular complex $\mathcal{R}_k^\alpha$ with apex angle α is isomorphic to the regular tiling of a sector with apex angle α, consisting of identical polygons, with all internal vertices of equal valence and all vertices on the boundary of equal valence, excluding the vertex C at the apex which has valence $k+1$. For triangle meshes the valence of regular interior vertices is six, and for boundary vertices it is three.

Note that the complex is called k-regular, because the number of faces sharing the vertex C is k, not the number of edges. In the case of closed surfaces these numbers are equal.

Tagged complexes. The vertices, edges or faces of a complex can be assigned tags, or more formally, a map can be defined from the sets of vertices, edges or faces to a finite set of tags. These tags can be used to choose a type of subdivision rules applied at a vertex. We use tags in a very limited way: specifically, a boundary vertex can be tagged as a *convex* or *concave* corner, or a smooth boundary vertex. However, as it is discussed below, the tags can be used to create creases in the interior of meshes and for other purposes. Subdivision on tagged complexes merits a separate detailed consideration.

Isomorphisms of tagged complexes with identical tag sets can be defined as isomorphisms of complexes which preserve tags, i.e. if a vertex has a tag τ its image also has a tag τ.

Subdivision of simplicial complexes. We can construct a new complex $D(K)$ from a complex K by subdivision. For a triangle scheme, $D(K)$ is

constructed by adding a new vertex for each edge of the complex and replacing each old triangular face with four new triangles. If some faces of the initial complex are not triangular, they have to be split into triangles first. For a quadrilateral scheme, $D(K)$ is constructed by adding a vertex for each edge and face, and replacing each n-gonal face with n quadrilateral faces. Note that k-regular complexes and k-regular complexes with boundary are self-similar, that is, $D(\mathcal{R}_k)$ and $\mathcal{R}_k$, as well as $D(\mathcal{R}_k^\alpha)$ and $\mathcal{R}_k^\alpha$, are isomorphic.

We use notation K^j for j times subdivided complex $D^j(K)$ and V^j for the set of vertices of K^j. Note that the sets of vertices are nested: $V^0 \subset V^1 \subset \ldots$.

If a complex is tagged, it is also necessary to define rules for assigning tags to the new edges, vertices and faces. For our vertex tags, we use a trivial rule: all newly inserted boundary vertices are tagged as smooth boundary.

Subdivision schemes. Next, we attach values to the vertices of the complex; in other words, we consider the space of functions $V \to B$, where B is a vector space over $\mathbf{R}$. The range B is typically $\mathbf{R}^l$ or $\mathbf{C}^l$ for some l. We denote this space $\mathcal{P}(V, B)$, or $\mathcal{P}(V)$, if the choice of B is not important.

A *subdivision scheme* for any function $p^j(v)$ on vertices V^j of the complex K^j computes a function $p^{j+1}(v)$ on the vertices of the subdivided complex $D(K) = K^1$. More formally, a subdivision scheme is a collection of operators $S[K]$ defined for every complex K, mapping $\mathcal{P}(K)$ to $\mathcal{P}(K^1)$. We consider only subdivision schemes that are linear, that is, the operators $S[K]$ are

linear functions on $\mathcal{P}(K)$. In this case the subdivision operators are defined by equations

$$p^1(v) = \sum_{w \in V} a_{vw} p^0(w)$$

for all $v \in V^1$. The coefficients a_{vw} may depend on K.

We restrict our attention to subdivision schemes which are finitely supported, locally invariant with respect to a set of isomorphisms of tagged complexes and affinely invariant.

A subdivision scheme is *finitely supported* if there is an integer M such that $a_{vw} \neq 0$ only if $w \in N_M(v, K)$ for any complex K (note that the neighborhood is taken in the complex K^{j+1}). We call the minimal possible M the *support size* of the scheme.

We assume our schemes to be *locally defined* and *invariant with respect to isomorphisms of tagged complexes*.

Together these two requirements can be defined as follows: there is a constant L such that if for two complexes K_1 and K_2 and two vertices $v_1 \in V_1$ and $v_2 \in V_2$ there is a tag-preserving isomorphism $\rho : N_L(v_1, K_1) \to N_L(v_2, K_2)$, such that $\rho(v_1) = v_2$, then $a_{v_1 w} = a_{v_2 \rho(w)}$. In most cases, the *localization size* $L = M$.

The final requirement that we impose on subdivision schemes is *affine invariance*: if T is a linear transformation $B \to B$, then for any v $Tp^{j+1}(v) = \sum a_{vw} Tp^j(v)$. This is equivalent to requiring that all coefficients a_{vw} for a

fixed v sum up to 1.

For each vertex $v \in \cup_{j=0}^{\infty} V^j$ there is a sequence of values $p^i(v)$, $p^{i+1}(v)$,... where i is the minimal number such that V^i contains v.

Definition 5.6. *A subdivision scheme is called convergent on a complex K, if for any function $p \in \mathcal{P}(K, B)$ there is a continuous function f defined on $|K|$ with values in B, such that*

$$\lim_{j \to \infty} \sup_{v \in V^j} \left\| p^j(v) - f(v) \right\|_2 \to 0$$

The function f is called the limit function of subdivision.

Notation: $f[p]$ is the limit function generated by subdivision from the initial values $p \in \mathcal{P}(K)$.

It is easy to show that if a limit function exists, it is unique. A *subdivision surface* is the limit function of subdivision on a complex K with values in $\mathbf{R}^3$. In this case we call the initial values $p^0(v)$ the *control points* of the surface.

Assuming the trivial rule for assigning tags to the newly inserted boundary vertices, we observe that locally any surface generated by a subdivision scheme on an arbitrary complex can be thought of as a part of a subdivision surface defined on a k-regular complex or a k-regular complex with boundary.

Note that this fact alone does not guarantee that it is sufficient to study subdivision schemes only on k-regular complexes and k-regular complexes with boundary [46]. If the number of control points of the initial complex for a k-gonal patch is less than the number of control points of the central

k-gonal patch in the k-regular complex, then only a proper subspace of all possible configurations of control points on the subdivided complexes can be realized. Although it is unlikely, it is possible that for such complexes almost all configurations of control points will lead to non-smooth surfaces, while the scheme is smooth on the k-regular complexes.

Subdivision matrices. Consider the part of a subdivision surface $f[y]$ with $y \in U_1^j = |N_1(0, \mathcal{R}_k^j)|$, defined on the domain formed by faces of the subdivided complex $\mathcal{R}_k^j$ adjacent to the central vertex. It is straightforward to show that the values at all dyadic points in $|N_1(0, \mathcal{R}_k^j)|$ can be computed given the initial values $p^j(v)$ for $v \in N_L(0, \mathcal{R}_k^j)$. In particular, the control points $p^{j+1}(v)$ for $v \in N_L(0, R_k^{j+1})$ can be computed using only control points $p^j(w)$ for $w \in N_L(0, \mathcal{R}_k^j)$. Let $\bar{p}^j$ be the vector of control points $p^j(v)$ for $v \in N_L(0, \mathcal{R}_k^j)$. Let $p+1$ be the number of vertices in $N_L(0, \mathcal{R}_k)$. As the subdivision operators are linear, $\bar{p}^{j+1}$ can be computed from $\bar{p}^j$ using a $(p+1) \times (p+1)$ matrix S^j: $\bar{p}^{j+1} = S^j \bar{p}^j$

If for some m and for all $j > m$, $S^j = S^m = S$, we say that the subdivision scheme is *stationary on the k-regular complex*, or simply stationary, and call S the *subdivision matrix* of the scheme.

Eigenbasis functions. let $\lambda_0 = 1, \lambda_i, \ldots \lambda_J$ be different eigenvalues of the subdivision matrix in nonincreasing order, the condition $\lambda_0 > \lambda_1$ is necessary for convergence.

For any λ_i let J_j^i, $j = 1 \ldots$ be the complex cyclic subspaces corresponding

to this eigenvalue.

Let n_j^i be the *orders* of these cyclic subspaces; the order of a cyclic subspace is equal to its dimension minus one.

Let b_{jr}^i, $r = 0 \ldots n_j^i$ be the complex generalized eigenvectors corresponding to the cyclic subspace J_j^i. The vectors b_{jr}^i satisfy

$$Sb_{jr}^i = \lambda_i b_{jr}^i + b_{j\,r-1}^i \quad \text{if } r > 0, \quad Sb_{j0}^i = \lambda_i b_{j0}^i \tag{5.1}$$

The complex *eigenbasis functions* are the limit functions defined by $f_{jr}^i = f[b_{jr}^i] : U_1 \to \mathbf{C}$

Any subdivision surface $f[p] : U_1 \to \mathbf{R}^3$ can be represented as

$$f[p](y) = \sum_{i,j,r} \beta_{jr}^i f_{jr}^i(y) \tag{5.2}$$

where $\beta_{jr}^i \in \mathbf{C}^3$, and if $b_{jr}^i = \overline{b_{lt}^k}$, $\beta_{jr}^i = \overline{\beta_{lt}^k}$, where the bar denotes complex conjugation.

One can show using the definition of limit functions of subdivision and (5.3) that the eigenbasis functions satisfy the following set of *scaling relations*:

$$f_{jr}^i(y/2) = \lambda_i f_{jr}^i(y) + f_{j\,r-1}^i(y) \quad \text{if } r > 0, \quad f_{j0}^i(y/2) = \lambda_i f_{j0}^i(y) \tag{5.3}$$

Real eigenbasis functions. As we consider real surfaces, it is often convenient to use real Jordan normal form of the matrix rather than the com-

plex Jordan normal form. For any pair of the complex-conjugate eigenvalues λ_i, λ_k, we can choose the complex cyclic subspaces in such a way that they can be arranged into pairs J^i_j, J^k_j, and $b^i_{jr} = \overline{b^k_{jr}}$ for all j and r. Then we can introduce a single real subspace for each pair, with the basis c^i_{jr}, c^k_{jr}, $r = 0 \dots n^i_j$, where $c^i_{jr} = \Re b^i_{jr}$, and $c^k_{jr} = \Im b^i_{jr}$. We call such subspaces *Jordan subspaces.* Then we can introduce real eigenbasis functions $g^i_{jr}(y) = f^i_{jr}(y)$ for real λ_i, and $g^i_{jr}(y) = \Re f^i_{jr}(y)$, $g^k_{jr}(y) = \Im f^i_{jr}(y)$ for a pair of complex-conjugate eigenvalues (λ_i, λ_k). For a Jordan subspace corresponding to pairs of complex eigenvalues the order is the same as the order of one of the pair of cyclic subspaces corresponding to it.

Similar to (5.2) we can write for any surface generated by subdivision on U_1:

$$f[p](y) = \sum_{i,j,r} \alpha^i_{jr} g^i_{jr}(y) \tag{5.4}$$

Now all coefficients α^i_{jr} are real. Eigenbasis functions corresponding to the eigenvalue 0 have no effect on tangent plane continuity or C^k-continuity of the surface at zero. From now on we assume that $\lambda_i \neq 0$ for all i.

We can assume that the coordinate system in $\mathbf{R}^3$ is always chosen in such a way that the single component of $f[p]$ corresponding to eigenvalue 1 is zero. This allows us to reduce the number of terms in (5.4) to p.

5.3.2 Reduction to universal surfaces

In [46] we have shown that for surfaces without boundary the analysis of smoothness of subdivision can be reduced to the analysis of *universal surfaces*. Moreover, if a subdivision scheme is C^1, almost any surface produced by subdivision is diffeomorphic to the universal surface. In this section, we introduce the universal surfaces for neighborhoods of boundary vertices, and show that a similar reduction can be performed in this case.

This fact is of considerable practical importance for design of subdivision schemes for surfaces with piecewise-smooth boundary: as we have observed in Section 5.2, convex and concave corners are not diffeomorphic; therefore, a convex and and a concave corner in $\mathbf{R}^3$ cannot be diffeomorphic to the same universal surface, and cannot be generated by the same subdivision rule.

Universal map. The decomposition (5.4) can be written in vector form. Let h^i_{jr} be an orthonormal basis of $\mathbf{R}^p$. Let ψ be $\sum_{i,j,r} g^i_{jr} h^i_{jr}$; this is a map $U_1 \to \mathbf{R}^p$. Let $\alpha^1, \alpha^2, \alpha^3 \in \mathbf{R}^p$ be the vectors composed of components of coefficients α^i_{jr} from (5.4) (each of these coefficients is a vector in $\mathbf{R}^3$). Then (5.4) can be rewritten as

$$f[p](y) = \big((\psi, \alpha^1),\, (\psi, \alpha^2),\, (\psi, \alpha^3)\big) \tag{5.5}$$

This equation indicates that all surfaces generated by a subdivision scheme on U_1 can be viewed as projections of a single surface in $\mathbf{R}^p$. We call ψ the

universal map, and the surface specified by ψ the *universal surface.* In [46], it was demonstrated that the analysis of tangent plane continuity and C^k continuity of subdivision can be reduced to analysis of the universal surface. Not surprisingly, we will see that this also holds for subdivision schemes with boundary.

In the chosen basis the matrix S is in the real Jordan normal form. Note that by definition of S for any $a \in \mathbf{R}^p$

$$(a, \psi(y/2)) = (Sa, \psi(y))$$

Using the well-known formula for inner products $(Su, v) = (u, S^T v)$, we get

$$(x, \psi(y/2)) = (x, S^T \psi(y)), \quad \text{for any } x$$

This means that the scaling relations can be jointly written as

$$\psi(y/2) = S^T \psi(y) \tag{5.6}$$

The universal map ψ is only piecewise C^k, even if we assume that subdivision produces C^k limit function on regular complexes and regular complexes with boundary: derivatives have discontinuity at the boundaries of polygons of U_1. However, one can easily construct a map κ (see [46]) such that $\phi = \psi \circ \kappa^{-1}$ is C^1-continuous away from the center.

We will impose the following condition on the subdivision schemes which

we call: **Condition A.** For any $y \in U_1$

$$\partial_1\psi(y) \wedge \partial_2\psi(y) \neq 0 \quad \text{for all } y \in U_1,\ y \neq 0$$

This condition holds for all known practical schemes.

Reduction theorem. Our goal is to relate tangent plane continuity and C^k-continuity of the universal surface in $\mathbf{R}^p$ and tangent plane continuity of the subdivision scheme. The following theorem holds under our assumptions:

Theorem 5.1. *For a subdivision scheme satisfying Condition A to be tangent plane continuous on a k-regular complex with boundary, it is necessary and sufficient that the universal surface be tangent plane continuous; for the subdivision scheme to be C^k-continuous with p.w. C^k-continuous boundary, it is necessary and sufficient that the universal surface is C^k-continuous with p.w. C^k-continuous boundary. Almost all surfaces generated by a subdivision scheme on a k-regular complex with boundary are locally diffeomorphic to the universal surface.*

Proof. Sufficiency is clear as any surface is a linear projection of the universal surface. To prove necessity, we use Proposition 5.1, and show that

- if the universal surface is not tangent plane continuous then a set of subdivision surfaces of non-zero measure is not tangent plane continuous;

- if the universal surface has non-injective projection into the tangent plane same is true for a set of subdivision surfaces of non-zero measure;
- if the projection of the universal surface into the tangent plane is not C^k, same is true for a set of subdivision surfaces of non-zero measure;
- if the boundary of the universal surface is not C^k-continuous, or is not C^k-continuous with nondegenerate corner, same is true for a set of subdivision surfaces of non-zero measure.

The proof of the first three statements coincides with the proof for the surface without boundary presented in [46].

We only need to consider the fourth statement. By assumption, the boundary of the surface is C^1-continuous away from zero. Let the two pieces of the boundary be $\gamma_i : (0, 1] \to \mathbf{R}^p$, $i = 1, 2$, with $\gamma_1(1) = \gamma_2(1)$. We can assume both pieces to be C^1-continuous away from one. Suppose γ_1 does not have a tangent at one; then there are at least two directions τ_1 and τ_2 which are limits of sequences of tangent directions to $\gamma_1(t)$ as t approaches one. There is a set of three-dimensional subspaces π of measure non-zero in the space of all three-dimensional subspaces, for which the projections of both vectors τ_1 and τ_2 to the subspace are not zero. If we project the universal surface to any of these subspaces, the boundary curve of the resulting surface will not be tangent continuous. For curves tangent continuity is equivalent to C^1-continuity. For C^k-continuity the proof for curves is identical to the proof for surfaces. We conclude that the curves γ_1 and γ_2 should be C^k-

continuous. Similarly, if the curves are joined with continuity less than k, then almost all curves obtained by projection into $\mathbf{R}^3$ will have the same property. Finally, if the tangents to the curves coincide, same is true for almost all projections of the curves, which means that almost all projections do not have a non-degenerate corner. □

The following important corollary immediately follows from Theorem 5.1:

Corollary 5.2. *Almost all surfaces generated by a given C^k-continuous subdivision scheme on a k-regular complex are diffeomorphic.*

Indeed, as any subdivision surface $f : U_k \to \mathbf{R}^3$ is obtained as a projection of the universal surface, for almost any choice of projection it defines a diffeomorphism of the universal surface and f.

This corollary implies in particular that the same subdivision rule cannot generate convex and concave corners simultaneously in a stable way, and separate rules are required for these cases. It should be noted that surfaces with convex and concave corners can be alternatively produced using standard rules and degenerate configurations of control points. We believe however, that the best approach is to use special rules and not require special constraints on control points. However, it appears to be more natural to use degenerate configurations for producing surfaces with 0 and 2π corners. Analysis of the behavior of subdivision on degenerate and constrained configurations of control points is not considered here and remains an open problem.

5.4 Criteria for tangent plane and C^1 continuity.

Tangent plane continuity criteria of [46] do not use the fact that only interior points of a surface are considered. Similarly, C^1-continuity criteria use only the fact that C^1-continuity is equivalent to tangent plane continuity and injectivity of the projection into the tangent plane. Therefore, C^1-continuity criteria also hold for boundary points. We only need to establish the conditions that guarantee that the boundary curves are C^1-continuous, possibly with corners.

We focus on a sufficient condition for C^1-continuity ([46] Theorem 3.6 and Theorem 4.1), which is most relevant for applications. More general necessary and sufficient conditions (e.g. [46] Theorem 3.5) can be extended in a similar way.

To state the sufficient condition, we need to define *characteristic maps*, which are commonly used to analyze C^1-continuity of subdivision surfaces. We use a definition somewhat different from the original definition of Reif [35].

5.4.1 Conditions on Characteristic maps

Definition 5.7. *The* **characteristic map** $\Phi : U_1 \to \mathbf{R}^2$ *is defined for a pair of cyclic subspaces* J_b^a, J_d^c *of the subdivision matrix as*

1. (f_{a0}, f_{a1}) *if* $J_b^a = J_d^c$, λ_a *is real,*

2. (f_{a0}, f_{c0}) *if* $J_b^a \neq J_d^c$, λ_a, λ_c *are real,*

3. $(\Re f_{a0}, \Im f_{a0})$ *if* $\lambda_a = \bar{\lambda_c}$, $b = d$.

Three types of characteristic maps are shown in Figure 5.2.

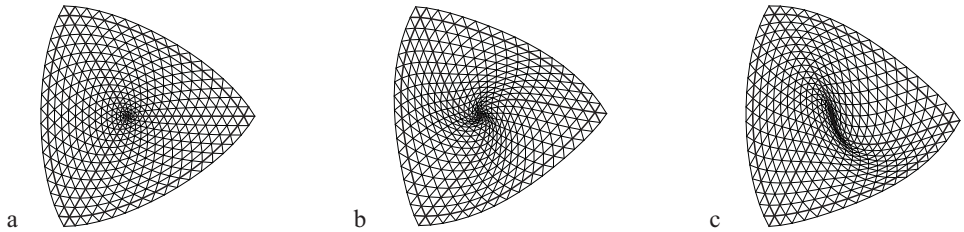

Figure 5.2: Three types of characteristic maps: control points after 4 subdivision steps are shown. a. Two real eigenvalues. b. A pair of complex-conjugate eigenvalues. c. single eigenvalue with Jordan block of size 2.

The domain of a characteristic map is the neighborhood U_1, consisting of k faces of the regular complex; we call these faces *segments*. We assume that the subdivision scheme generates C^1-continuous limit functions on regular complexes, and the characteristic map is C^1-continuous inside each segment and has continuous one-sided derivatives on the boundary.

Characteristic map satisfies the scaling relation $\Phi(t/2) = T\Phi(t)$, where T is one of the matrices

$$T_{\text{scale}} = \begin{pmatrix} \lambda_a & 0 \\ 0 & \lambda_c \end{pmatrix}, \quad T_{\text{skew}} = \begin{pmatrix} \lambda_a & 1 \\ 0 & \lambda_a \end{pmatrix}, \quad T_{\text{rot}} = |\lambda_a| \begin{pmatrix} cos\phi & -\sin\phi \\ \sin\phi & \cos\phi \end{pmatrix},$$

where ϕ is the argument of a complex λ_a.

Sufficient condition for C^1-continuity. The following sufficient condition is a special case of the condition that was proved in [46]. Although all our constructions apply in the more general case, we state only a simplified version of the criterion to simplify the presentation. This form captures the main idea of the sufficient condition. This condition generalizes Reif's condition [35].

Define for any two cyclic subspaces ord $\left(J_j^i, J_l^k\right)$ to be $n_j^i + n_l^k$, if $J_j^i \neq J_l^k$; let ord $\left(J_j^i, J_j^i\right) = 2n_j^i - 2$; note that for $n_j^i = 0$, this is a negative number, and it is less than ord for any other pair. This number allows us to determine which components of the limit surface contribute to the limit normal (see [46, 44] for details). We say that a pair of cyclic subspaces J_b^a, J_d^c is *dominant* if for any other pair J_j^i, J_l^k we have either $|\lambda_a\lambda_c| > |\lambda_i\lambda_k|$, or $|\lambda_a\lambda_c| = |\lambda_i\lambda_k|$ and ord $(J_b^a, J_d^c) >$ ord $\left(J_j^i, J_l^k\right)$. Note that the blocks of the dominant pair may coincide.

Theorem 5.3. *Let b_{jr}^i be a basis in which a subdivision matrix S has Jordan normal form. Suppose that there is a dominant pair J_b^a, J_d^c. If $\lambda_a\lambda_c$ positive real, and the Jacobian of the characteristic map of J_b^a, J_d^c has constant sign everywhere on U_1 except zero, then the subdivision scheme is tangent plane continuous on the k-regular complex. If the characteristic map is injective, the subdivision scheme is C^1-continuous.*

In the special case when all Jordan blocks have size 1, this condition reduces to an analog of Reif's condition. Theorem 5.3 doesn't make any

claim about the type of boundary however. It is therefore not enough for the analysis of the desired surfaces.

Criterion for piecewise C^1-continuity of the boundary. Assuming that the scheme at a boundary vertex satisfies the conditions of Theorem 5.3, we establish additional conditions which guarantee that the scheme for almost all control meshes generates C^1-continuous surfaces with piecewise C^1-continuous boundary with nondegenerate corners. The domain of the characteristic function is called U_1. We assume that the part of U_1 that corresponds with the boundary of the surface is a straight line. We call I_1 and I_2 the two parts of this boundary line which we get by excluding the center vertex. When we talk about ∂_1 we mean the derivative in the direction of this boundary line. ∂_2 will be the orthogonal direction. We will call the two components of the characteristic map by f_1 and f_2 in the following theorem.

Theorem 5.4. *Suppose a subdivision scheme satisfies conditions of Theorem 5.3 for boundary vertices of valence k. Then the scheme is p.w. C^1-continuous with nondegenerate corners for boundary vertices of valence k if and only if the following conditions are satisfied.*

1. *λ_a and λ_c are positive real.*

2. *Suppose $\lambda_a > \lambda_c$, (diagonal scaling matrix, asymmetric scaling). Then the scheme is boundary C^1-continuous if and only if $\partial_1 f_1 \neq 0$ and has the same sign on I_1 and I_2 or $\partial_1 f_1 \equiv 0$ on I_1 and I_2.*

The scheme is a nondegenerate corner scheme, if and only if $\partial_1 f_1 \neq 0$ *on* I_1 *and* $\partial_1 f_1 \equiv 0$ *on* I_2*. Same is true if* I_1 *and* I_2 *are exchanged.*

3. *Suppose* $J_c^a = J_d^b$ *(scaling matrix is a Jordan block of size 2), and* ∂f_1 *does not vanish on* I_1 *and* I_2*. The scheme is boundary* C^1*-continuous if* $\partial_1 f_2$ *has the same sign everywhere on* I_1 *and* I_2 *and if* $\partial_1 f_2(t_1) = 0$ *then* $\partial_1 f_1(t_1)$ *needs to have this sign as well. Nondegenerate corners cannot be generated by a scheme of this type.*

4. *Suppose* $a = c$ *(diagonal scaling matrix, symmetric scaling). The boundary is* C^1*-continuous if and only if there is a nontrivial linear combination* $\alpha_1 \partial_1 f_1 + \alpha_2 \partial_1 f_2$ *identically vanishing on* I_1 *and* I_2*, and any other independent linear combination has the same sign on* I_1 *and* I_2*. The scheme is a corner scheme if and only if there is a linear combination* $\alpha_1 \partial_1 f_1 + \alpha_2 \partial_1 f_2$ *identically vanishing on* I_1 *and a different linear combination* $\beta_1 \partial_1 f_1 + \beta_2 \partial_1 f_2$ *identically vanishing on* I_2 *with* $[\alpha_1, \alpha_2]$ *and* $[\beta_1, \beta_2]$ *linearly independent.*

Proof. For each of the boundary segments defined on I_1 and I_2 we need to show that the limit of the tangent exists at the common endpoint. If these limits coincide then the boundary curve of the universal surface is C^1-continuous; if the limits have different directions, then the universal surface has a nondegenerate corner.

First, we observe that by assumption the characteristic map has nonzero Jacobian on the boundary. This means that one of the components has

nonzero derivative along the boundary $\partial_1 f_1(t) \neq 0$ or $\partial_1 f_2(t) \neq 0$ at any point $t \in I_1 \cup I_2$. Consider the tangent to the boundary of the surface defined by the characteristic map. It is a two-dimensional vector $v(t) = (\partial_1 f_1(t), \partial_1 f_2(t))$, where t is a point of I_1 or I_2. The tangent satisfies the scaling relation of the form $v(t/2) = 2Tv(t)$, where T is the scaling matrix for the characteristic map. The direction of the tangent has a limit if and only if T is either T_{scale} or T_{skew} and its eigenvalues are positive (Lemma 3.1, [46]). As the projection of the universal surface is arbitrarily well approximated by the characteristic map, or coincides with it for simple Jordan structures of the subdivision matrix, we conclude that for the universal surface boundary to have well-defined tangents at zero, the eigenvalues of the characteristic map have to be positive and real. However, this condition is not sufficient for existence of tangents.

Diagonal scaling matrix, asymmetric case. First we consider the case of dominant cyclic subspace pair J_b^a, J_d^c with $a \neq c$ (different eigenvalues). In this case the sequences $\partial_1 f_1(t/2^m)$ and $\partial_1 f_2(t/2^m)$, for $\partial_1 f_1(t), \partial_1 f_2(t) \neq 0$, change at a different rate. This can be easily seen from the scaling relation. Moreover, the ratio $\|\partial_1 f_2(t/2^m)\|/\|\partial_1 f_1(t/2^m)\|$ approaches zero as $m \to \infty$.

Suppose at some points t_1, t_2 of I $\partial_1 f_1(t_1) \neq 0$ and $\partial_1 f_1(t_2) = 0$. Then $\partial_1 f_2(t_2) \neq 0$ and the tangents at points $t_2/2^m$ all point in the direction $\pm e_2$, where e_2 is the unit vector along the coordinate axis corresponding to f_2. $\|\partial_1 f_2(t_1/2^m)\|/\|\partial_1 f_1(t_1/2^m)\| \to 0$ as $m \to \infty$, thus, at points $t_1/2^m$

the direction of the tangent approaches $\pm e_1$. We conclude that there is no limit, unless $\partial_1 f_1$ is either nowhere or everywhere zero I_1. Same applies to I_2. Conversely, if $\partial_1 f_1$ is nowhere zero, then the limit tangent direction at the center is $\pm e_1$. If it is zero everywhere, then by assumption about the characteristic map, $\partial_1 f_2$ is nowhere zero, and the limit tangent direction is $\pm e_2$. The choice of sign in each case depends on the sign of $\partial_1 f_1$ or $\partial_1 f_2$.

If $\partial_1 f_1$ is not zero and has the same sign on both I_1 and I_2 then the tangent is continuous, and the boundary curve is C^1-continuous. If $\partial_1 f_1 \equiv 0$ on I_1 and I_2 the images of I_1 and I_2 under the characteristic map are straight lines on the e_2 axis and therefore the boundary curve is C^1 continuous. If it is zero on I_1 and nonzero on I_2, then the tangents are not parallel, and the surface defined by the characteristic map has a corner; and the same for I_1 and I_1 interchanged which proves the second part.

Scaling matrix is a Jordan block of size 2. The second condition of the theorem applies if the characteristic map components correspond to a cyclic subspace of size 2, i.e. satisfy $f_1(t/2) = \lambda_a f_1(t) + f_2(t)$. Thus, $\partial_1 f_1 \equiv 0$ implies $\partial_1 f_2 \equiv 0$ on I_1 or I_2. $v(t/2^m)$ converges to $\pm e_1$ for any t on I_1 as well as I_2. If $\partial_1 f_2(t) \neq 0$ its sign determines the sign of the limit tangent.

Diagonal scaling matrix, symmetric case. In the symmetric case where $a = b$ the sequences defined above change at the same rate, and any linear combination $\alpha_1 f_1 + \alpha_2 f_2$ is also an eigenbasis function. Suppose f_1 and f_2 come from different cyclic subspaces of the same eigenvalue which have the

same size. Suppose $\alpha_1\partial_1 f_1 + \alpha_2\partial_1 f_2$ does not vanish identically on I_1 for any nontrivial choice of α_1 and α_2. Pick two linearly independent combinations $g_1 = \alpha_1\partial_1 f_1 + \partial_1\alpha_2 f_2$ and $g_2 = \beta_1\partial_1 f_1 + \beta_2\partial_1 f_2$ which do not vanish at points t_1 and t_2 of I_1 respectively. Then the vectors $v(t_i) = [\partial_1 f_1(t_i), \partial_1 f_2(t_i)]$ are linearly independent and the sequences $v(t_1/2^m)$ and $v(t_2/2^m)$ converge to different limit directions. Therefore, for the limit tangents at zero to exist, there should be a nontrivial linear combination of $\partial_1 f_1$ and $\partial_1 f_2$ which vanishes on I_1. If $\alpha_1\partial_1 f_1 + \alpha_2\partial_1 f_2$ is such combination, it is easy to see that the limit tangent direction is, up to the sign,the direction of the vector $[-\alpha_2, \alpha_1]$. For the boundary to be C^1-continuous, the direction should be the same on two sides. Finally, the tangents on two sides exist and do not coincide if the vectors (α_1, α_2) for I_1 and I_2 are linearly independent. □

An interesting corollary of this theorem is that in the symmetric case it is necessary for p.w. C^1-continuity of the boundary that the images of I_1 and I_2 under the characteristic map are straight line segments. In this case we have that $\alpha_1\partial_1 f_1 + \alpha_2\partial_1 f_2 \equiv 0$ which means that $\alpha_1 f_1 + \alpha_2 f_2$ is constant and the image of $(f1, f2)$ is a straight line segment. Note that this is not necessary if the eigenvalues λ_a and λ_b are different.

5.4.2 Analysis of Characteristic Maps

To verify conditions of Theorem 5.3 we need to establish that the characteristic map is regular and injective, and verify that it has the expected behavior

on the boundary. Typically, analysis of the boundary behavior is relatively easy, as in most cases the boundary curve is independent from the interior. In this section we focus on regularity and injectivity of the characteristic map.

Regularity of the characteristic map. Just as in the case of interior points we use self-similarity of the characteristic map to verify the regularity condition of Theorem 5.3: for any $t \in U_1$, the Jacobian satisfies $J[\Phi](t/2) = 4\lambda_a\lambda_b J[\Phi](t)$. It is immediately clear that to prove regularity of the characteristic map it is sufficient to consider the Jacobian on a single annular portion of U_1 as shown in Figure 5.3. As all vertices of such a ring are either regular or boundary regular, we can estimate the Jacobian of the characteristic map using tools developed for analysis of subdivision on regular grids. However, there is a significant difference from the case of interior vertices: to establish regularity on a single ring, in general, we have to consider subdivision schemes not just on regular meshes but on regular meshes with boundary, which makes the estimates for the Jacobians somewhat more complex.

Injectivity of the characteristic map. Even if the Jacobian of a map is nonzero everywhere, only local injectivity is guaranteed. However, for interior vertices, self-similarity of the characteristic maps allows one to reduce the injectivity test to computing the index of a closed curve around zero [45]. This is a relatively simple and fast operation: for example, the index can be

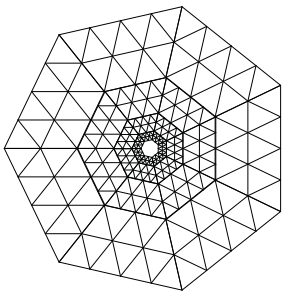

Figure 5.3: The k-gon without origin $U_1 \backslash \{0\}$ can be decomposed into similar rings, each two times smaller than the previous ring. The size of the ring is chosen in such a way that the control set of any ring does not contain the extraordinary vertex. In this figure the control set is assumed to consist out of the vertices of the triangles of the ring itself, and of a single layer of vertices outside the ring.

computed counting the number of intersections of the curve with a line. This test cannot be applied for boundary points, as there are no closed curves around zero.

For boundary points, a different simple test (Theorem 5.5) suffices, which in all cases that we have considered is even easier to apply. However, unlike the curve index test, it does not immediately yield a general computational algorithm.

The characteristic map can be extended using scaling relations to a complete k-regular complex with boundary. In the following theorem we assume that the characteristic map is defined on the whole complex $|\mathcal{R}_k^\alpha|$.

Theorem 5.5. *Suppose a characteristic map $\Phi = (f_a, f_c)$ satisfies the following conditions:*

1. *the preimage* $\Phi^{-1}(0)$ *contains only one element, 0;*

2. *the characteristic map has a Jacobian of constant sign at all points of the domain besides 0.*

3. *The image of the boundary of the characteristic map has no self-intersections;*

4. *the image of the characteristic map is not the whole plane.*

Then this characteristic map is injective.

Proof. As in [45] we can show that the characteristic map is continuous at infinity, and if P is the stereographic projection of the sphere to the plane such that the south pole gets mapped to 0, $\tilde{\Phi} = P^{-1}\Phi P$ is a continuous mapping of a subset $D = P^{-1}(|\mathcal{R}_k^\alpha|)$ of the sphere into the sphere, with the south pole mapped to the south pole; $\tilde{\Phi}$ is a local homeomorphism away from the south pole.

We observe that the points of the boundary of the image $\tilde{\Phi}(D)$ can be images only of the boundary of D due to the properties of local homeomorphisms meaning $\partial\left(\tilde{\Phi}(D)\right) \subset \tilde{\Phi}(\partial D)$. Suppose the boundary of the image is not empty; we show that the image of the boundary curve $\tilde{\Phi}(\partial D)$ coincides with the boundary of the image $\partial\left(\tilde{\Phi}(D)\right)$.

The image of the boundary has no self intersections. It is easy to see that the boundary of the domain is a simple closed Jordan curve, and so is its image $\tilde{\Phi}(\partial D)$. Suppose $\partial\left(\tilde{\Phi}(D)\right) \neq \tilde{\Phi}(\partial D)$. Then there is a point y on the image of the boundary $\tilde{\Phi}(\partial D)$ which is an interior point of $\tilde{\Phi}(D)$. As $\tilde{\Phi}(\partial D)$

separates the sphere into two linearly connected domains, we can connect each point in either domain to point y with a continuous curve which does not intersect $\partial\left(\tilde{\Phi}(D)\right)$. Thus, any two points on the sphere can be connected by a continuous curve which does not intersect $\partial\tilde{\Phi}(D)$. We conclude that the image $\tilde{\Phi}(D)$ is the whole sphere. Therefore, either $\partial\left(\tilde{\Phi}(D)\right) = \tilde{\Phi}(\partial D)$, or the image is the whole sphere. The latter option contradicts the last condition of the theorem.

Now we need to use this to prove that the map is injective. If we exclude the south pole of the sphere, the mapping is a local homeomorphism of one simply connected domain to another. We can easily prove it is a covering: consider an interior point y of the image, and the set $\tilde{\Phi}^{-1}(y)$. Suppose it is infinite. Then it has a limit point, which cannot be an interior point of D (otherwise, $\tilde{\Phi}$ is not a local homeomorphism at that point). Similarly, it cannot be a boundary point, unless it is the south pole. It cannot be the south pole x_s for which $P(x_s) = 0$, because then $\tilde{\Phi}(x_s)$ has to be y which means that $y = x_s$ which contradicts the assumption $\Phi^{-1}(0) = \{0\}$. We conclude that $\tilde{\Phi}^{-1}(y)$ is finite for each point y of the interior of the image. Similar is true for boundary points away from the poles. $\tilde{\Phi}$ is a local homeomorphism and maps the boundary exactly to the boundary. Let y be a point of the image away from poles, and let $x_1, x_2, \ldots x_n$ be points of $\tilde{\Phi}^{-1}(y)$. Then for each x_i there is a sufficiently small neighborhood U_i which maps homeomorphically to a neighborhood of $x_i \in \tilde{\Phi}(D)$. Then the inverse image of $\cap_i \tilde{\Phi}(U_i)$ is a finite union of disjoint diffeomorphic subsets of D. We conclude that $\tilde{\Phi}$ is a

covering on D with south pole excluded. However, we have observed that the image of D is simply connected. Therefore, the covering has to be injective. We conclude that the characteristic map is injective. □

5.5 Verification of C^1-continuity

5.5.1 Loop scheme

In this section we describe the structure of the boundary subdivision matrices for the Loop scheme. Some parts of our analysis are similar to the analysis performed by Jean Schweitzer [38].

The control mesh for a boundary patch surrounding an extraordinary vertex is shown in Figure 5.4. There are 3 different types of vertices in the control mesh, shown in the same figure. A different subdivision mask is used for each type. There are two masks for the vertices of types 1 and 3, one for boundary vertices and one for interior vertices. We consider these vertices to have the same type for notational convenience.

The figure also shows the masks of the rules that we consider. Our family of schemes includes all schemes satisfying the following conditions:

1. The support for each mask is the same as for the Loop scheme or for the cubic B-spline on the boundary;

2. The only masks that are modified are the masks for odd vertices adjacent to the central vertex, and for the central vertex itself (types

0,1).

3. The masks for interior edge vertices of type 1 are all identical and symmetric with respect to the edge connecting the vertex with the central vertex. The masks for two boundary vertices of type 1 are also identical.

We assume that all coefficients in the masks are positive. This choice is sufficiently general to construct a variety of schemes; on the other hand, complete eigenanalysis can be performed for all schemes from this family. We show that no scheme from this family can produce a rule for a concave corner. There are reasons to believe that this is true for any scheme with positive coefficients or small support.

For the specific schemes that we consider the boundaries do not depend on the control points in the interior. Potentially, the boundary can depend on the valence of a boundary vertex, this is the case with the scheme presented in [19]. However, we believe that this is best avoided, and present a set of schemes for which the boundary rules are simply cubic spline rules, except at vertices marked as corners, where interpolation is forced.

Subdivision matrix. We assume that $k > 1$; we will consider the case $k = 1$ separately. The subdivision matrix for a boundary vertex with k adjacent triangles has the following form:

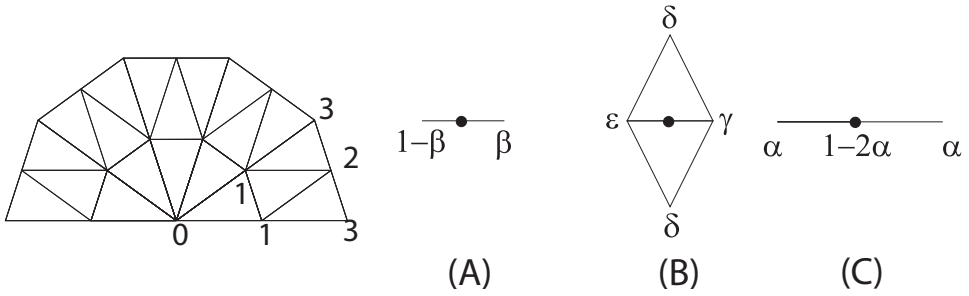

Figure 5.4: Control mesh for a boundary patch of a Loop subdivision surface and masks of the subdivision rules. (A) The rule for the odd vertices on the boundary adjacent to the central vertex (type 1). (B) The rule for the interior odd vertices adjacent to the central vertex (type 1). (C) The rule for the central vertex (type 0). The rules for vertices of type 2 and 3 (interior) are the standard Loop rules; the rule for the vertex of type 3 (boundary) is the standard one-dimensional cubic spline rule.

$$
\left(\begin{array}{|c|cc|cccccc|c|cccccc|}
\hline
1-2\alpha & \alpha & \alpha & & & & & & & & & & & & & \\
\hline
1-\beta & \beta & & & & & & & & & & & & & & \\
1-\beta & & \beta & & & & & & & & & & & & & \\
\hline
\epsilon & \delta & & \gamma & \delta & & & & & & & & & & & \\
\epsilon & & & \delta & \gamma & \delta & & & & & & & & & & \\
\cdot & & & & \cdot & \cdot & \cdot & & & & & & & & & \\
\epsilon & & & & & \delta & \gamma & \delta & & & & & & & & \\
\epsilon & & \delta & & & & \delta & \gamma & & & & & & & & \\
\hline
1/8 & 3/8 & & 3/8 & & & & & & 1/8 & & & & & & \\
1/8 & & & 3/8 & 3/8 & & & & & & 1/8 & & & & & \\
\cdot & & & & \cdot & \cdot & & & & & & \cdot & & & & \\
\cdot & & & & & \cdot & \cdot & & & & & & \cdot & & & \\
1/8 & & & & & & 3/8 & 3/8 & & & & & & 1/8 & & \\
1/8 & & 3/8 & & & & & 3/8 & & & & & & & 1/8 & \\
\hline
1/8 & 3/4 & & & & & & & & & & & & & & 1/8 \\
1/8 & & 3/4 & & & & & & & & & & & & & 1/8 \\
\hline
1/16 & 1/16 & & 5/8 & 1/16 & & & & & 1/16 & 1/16 & & & & & \\
1/16 & & & 1/16 & 5/8 & 1/16 & & & & & 1/16 & 1/16 & & & & \\
\cdot & & & & \cdot & & & & & & & \cdot & \cdot & & & \\
1/16 & & & & & 1/16 & 5/8 & 1/16 & & & & & 1/16 & 1/16 & & \\
1/16 & & 1/16 & & & & 1/16 & 5/8 & & & & & & 1/16 & 1/16 & \\
\hline
\end{array}\right)
\tag{5.7}
$$

where $\epsilon = 1 - 2\delta - \gamma$. In block form this matrix can be written as

$$\left(\begin{array}{c|cc|c|c|c|c}
1-2\alpha & \alpha & \alpha & & & & \\
\hline
1-\beta & \beta & & & & & \\
1-\beta & & \beta & & & & \\
\hline
a_1 & A_{10} & & A_{11} & & & \\
\hline
a_2 & A_{20} & & A_{21} & \frac{1}{8}I_k & & \\
\hline
1/8 & 3/4 & & & & 1/8 & \\
1/8 & & 3/4 & & & & 1/8 \\
\hline
a_3 & & & A_{31} & A_{32} & & \frac{1}{16}I_{k-1}
\end{array}\right) \tag{5.8}$$

The vectors a_1 and a_3 have length $k-1$, the vector a_2 has length k, I_k and I_{k-1} are unit matrices of sizes k and $k-1$. Note that the eigenvalues of the matrix are 1/8 1/16, the eigenvalues of the upper-left 3×3 block A_{00} and the eigenvalues of the matrix A_{11}. The matrix A_{11} is tridiagonal, of size $k-1 \times k-1$. The eigenvalues of A_{00} are $1, \beta, \beta - 2\alpha$ where the eigenvector to 1 is the vector $\mathbf{e} = [1, \ldots, 1]$. Following [38], we observe that $k-1 \times k-1$ tridiagonal symmetric matrices have the following eigenvectors, independent of the matrix, $j = 1 \ldots k-1$:

$$v^j = [\sin j\theta_k, \sin 2j\theta_k, \ldots \sin (k-1)j\theta_k] \tag{5.9}$$

where $\theta_k = \pi/k$. Multiplying the matrix A_{11} by the vectors, we see that the eigenvalues are $\lambda_j = 2\delta \cos j\theta_k + \gamma$.

If $\alpha \neq 0$, Out of two remaining eigenvectors, only the eigenvector v^β corresponding to β is typically of interest to us. It has the form

$$[0, 8C, -8C, \left(\beta I - A_{11}^{-1}\right)[C, 0 \ldots - C],$$

where C is a constant, if $\beta I - A_{11}$ is non-degenerate.

A more revealing expression for the components can be found if we regard the eigenvector as a solution to the recurrence

$$\delta\left(v_{i-1}^\beta + v_{i+1}^\beta\right) + (\gamma - \beta)v_i^\beta = 0, \quad i = 1 \ldots k-1$$

(the numbering of entries in v_β is such that $v^\beta = [0, v_0^\beta, v_k^\beta, v_1^\beta, ..., v_{k-1}^\beta]$ to make the equations uniform equations). In addition, we have an additional condition $v_0^\beta = -v_k^\beta$, to ensure that $\left[0, v_\beta^0, v_\beta^1\right]$ is the eigenvector of A_{00}.

The behavior of the solution of the recurrence depends on the ratio $r = (\gamma - \beta)/\delta$, assuming $\delta \neq 0$ (otherwise, A_{11} is diagonal with all eigenvalues equal to γ and the eigenvector with respect to β is found easily.). The additional condition $v_0^\beta = -v_k^\beta$ determines a unique solution up to a constant multiplier, even if the matrix $\beta I - A_{11}$ is degenerate. Solutions are listed in Table 5.1.

If $\alpha = 0$, the eigenvalue β has a two-dimensional eigenspace. Two eigenvectors v^β and v'^β satisfying conditions $v_0^\beta = 0$ and $v'^\beta_k = 0$ are shown in

$r > 2,\ k$ odd	$(-1)^i \cosh\left(i - \frac{k}{2}\right)\theta, \quad r = 2\cosh\theta$
$r > 2,\ k$ even	$(-1)^i \sinh\left(i - \frac{k}{2}\right)\theta, \quad r = 2\cosh\theta$
$r = 2,\ k$ odd	$(-1)^i$
$r = 2,\ k$ even	$(-1)^i\left(n - \frac{k}{2}\right),$
$-2 < r < 2$	$\sin\left(i - \frac{k}{2}\right)\theta, \quad r = -2\cos\theta$
$r = -2$	$i - \frac{k}{2}$
$r < -2$	$\sinh\left(i - \frac{k}{2}\right)\theta, \quad r = -2\cosh\theta$

Table 5.1: Solutions for v^β

$r > 2,$	$(-1)^i \sinh i\theta,\ (-1)^i \sinh (i-k)\,\theta,$	$r = 2\cosh\theta$
$r = 2,$	$(-1)^i i,\ (-1)^i (i-k)$	
$-2 < r < 2$	$\sin i\theta,\ \sin (i-k)\,\theta,$	$r = -2\cos\theta$
$r = -2$	$i,\ i-k$	
$r < -2$	$\sinh i\theta,\ \sinh (i-k)\,\theta,$	$r = -2\cosh\theta$

Table 5.2: Solutions for v^β and v'^β

Table 5.2, for the cases when the matrix $\beta I - A_{11}$ is not degenerate, i.e. when for all $1 \leqslant j \leqslant k-1$, $r \neq -2\cos j\theta_k$.

Finally, suppose $\alpha = 0$ and $r = -2\cos(j\theta_k)$ for some j. In this case $\beta = \gamma - \delta r$ is also an eigenvalue of A_{11}, and, therefore, has multiplicity 3. In this case it has a Jordan block of size 2, and only 2 eigenvectors which can be taken to be $v_i^\beta = \sin i\theta_k$ and $v'^\beta_i = \cos i\theta_k$, $i = 0 \ldots k$.

Summary of the eigenstructure. We have determined that the eigenvalues of the subdivision matrix are 1,β,$\beta - 2\alpha$, $1/8$, $1/16$, and $\lambda_j = 2\delta\cos j\theta_k + \gamma$, $j = 1 \ldots k-1$. The eigenvectors corresponding to the eigenvalues λ_j do not depend on the matrix and are given by (5.9). The eigenvectors corresponding to the eigenvalue β depends on the ratio $r = (\gamma - \beta)/\delta$; its entries are given by the formulas in Table 5.1 for $\alpha \neq 0$, in which case there is a single

eigenvector. For $\alpha = 0$, there is a pair of eigenvectors (Table 5.2) for the case when β is not an eigenvalue of A_{11}. If β is an eigenvalue of A_{11}, it has a nontrivial Jordan block of size 2.

The case $k = 1$. The matrix in this case has eigenvalues β, $\beta - 2\alpha$, and a triple eigenvalue $1/8$. The eigenvectors can be trivially computed.

Coefficients for smooth boundary vertices. One possible choice was given by Hoppe et al. [19] and examined in detail in [38]. In our notation, this choice corresponds to $\beta = 5/8$, $\alpha = 1/8$, $\gamma = 3/8$, $\delta = 1/8$. For extraordinary vertices, and $\beta = 1/2$ for other vertices. Remarkably, the ratio r is -2. The disadvantage of this choice is that the shape of the boundary curve depends on the valence of the vertices on the boundary, hence it becomes impossible to join two meshes continuously along a boundary if extraordinary vertices on two sides do not match.

If we require the boundary curve to be a cubic spline, β has to be $1/2$ and α has to be $1/8$. We have two degrees of freedom left: γ and δ. It turns out to be sufficient to use only one, and we fix δ at the value corresponding to the regular valence, i.e. $1/8$.

We consider the cases $k > 2$, $k = 2$ and $k = 1$ separately.

Case $k > 2$. Once α, β and δ are fixed, the eigenvalues of the subdivision matrix become 1, $\beta = 1/2$, $\beta - 2\alpha = 1/4, 1/8, 1/16$, and $\lambda_j = (1/4)\cos j\theta_k + \gamma$.

The tangent vector on the boundary of the surface corresponds to the eigenvector of the subdivision matrix with eigenvalue $\beta = 1/2$. This vector

should be one of the subdominant eigenvectors. The second subdominant eigenvector is likely to correspond to the largest of the eigenvalues λ_j, i.e. to the eigenvalue $\lambda_1 = \gamma + (1/4)\cos\theta_k$. In order for the eigenvalue $1/2$ to be subdominant, we choose γ in such a way that $|\lambda_j| < 1/2$ for $j > 1$, i.e. $\lambda_2 < 1/2$ and $\lambda_{k-1} > -1/2$. For positive γ, the second condition is satisfied automatically. We also would like $\lambda_1 > \beta - 2\alpha = 1/4$. This leads to the following range for γ:

$$\frac{1}{4}(1 - \cos\theta_k) < \gamma < \frac{1}{2} - \frac{1}{4}\cos 2\theta_k \tag{5.10}$$

In this range we also have $|\lambda_1| > |\lambda_j|$ for $j > 1$. There are two choices of γ that we find particularly interesting: $\gamma = 1/4$ and $\gamma = 1/2 - 1/4\cos\theta_k$.

The first choice, $\gamma = 1/4$, is the maximal value of γ independent of k for which it is in the correct range for all $k > 2$. Note that in this case $r = -2$ again. The second choice, leads to equal subdominant eigenvalues $\beta = \lambda_1 = 1/2$. In this case, $r = -2\cos\theta_k$, that is, we can choose θ to be θ_k. The expressions for the subdominant eigenvectors are $v_j^1 = \sin j\theta_k$ and $v_j^\beta = \cos j\theta_k$, i.e. form a half of a regular $2k$-gon.

The choice of $\gamma = 1/2 - 1/4\cos\theta_k$, although being slightly more complex, appears to be more natural. It has the additional advantage of coinciding with the regular value $\gamma = 3/8$ for $k = 3$.

Case $k = 2$. In this case, the eigenvalues are 1, 1/2, 1/4, 1/8, 1/16, and $\lambda_1 = \gamma$. Thus, we need to pick $1 > \gamma > 1/4$, to get the same eigenvectors

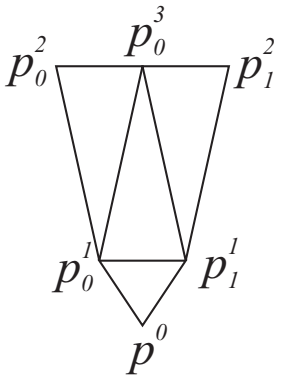

Figure 5.5: The control mesh for the characteristic map in the case $k = 1$.

as in the case $k > 2$. It is interesting to note however, that the choice of $\gamma = 1/4$ also results in a C^1 surface, although the behavior of the scheme becomes less desirable.

Case $k = 1$. The subdominant eigenvalues are $1/2$ and $1/4$. They define a configuration of eigenvectors shown in Figure 5.5.

Proposition 5.2. *Let* $\beta = 1/2, \alpha = 1/8, \delta = 1/8$ *and* $\gamma = 1/2 - 1/4\cos\theta_k$ *and* Φ *be the characteristic map which is defined by the eigenvectors to* $\beta = 1/2$ *and* $\lambda_1 = 1/4\cos(\theta_k) + \gamma = 1/2$ *. Then*

1. *the preimage* $\Phi^{-1}(0)$ *contains only one element, 0;*
2. *the characteristic map has a Jacobian of constant sign at all points of the domain besides 0;*
3. *the image of the boundary of the characteristic map has no self-intersections;*
4. *the image of the characteristic map is not the whole plane.*

Proof. We consider the boundary k-regular 2 ring mesh with data given by the 2 eigenvectors (shown for $k = 7$ in Figure 5.6(a)). We subdivide this twice by our given rules. We then have 5 accurate rings of a k-regular mesh. In the standard Loop scheme if a triangle is sourrounded by one ring of triangles and all subdivision at all those 12 points and points inserted on these edges and faces going forward are done by regular Loop subdivision the polynomial on the triangles in (u, v, w) Bezier coordinates $u + v + w = 1$ is given by (see [38]):

$$p(u, v, w) = B \cdot Q \cdot P$$

where

$$B = (u^4, 4u^3v, 4u^3w, 6u^2v^2, 12u^2vw, 6u^2w^2, 4uv^3,$$
$$12uv^2w, 12uvw^2, 4uw^3, v^4, 4v^3w, 6v^2w^2, 4vw^3, w^4)$$

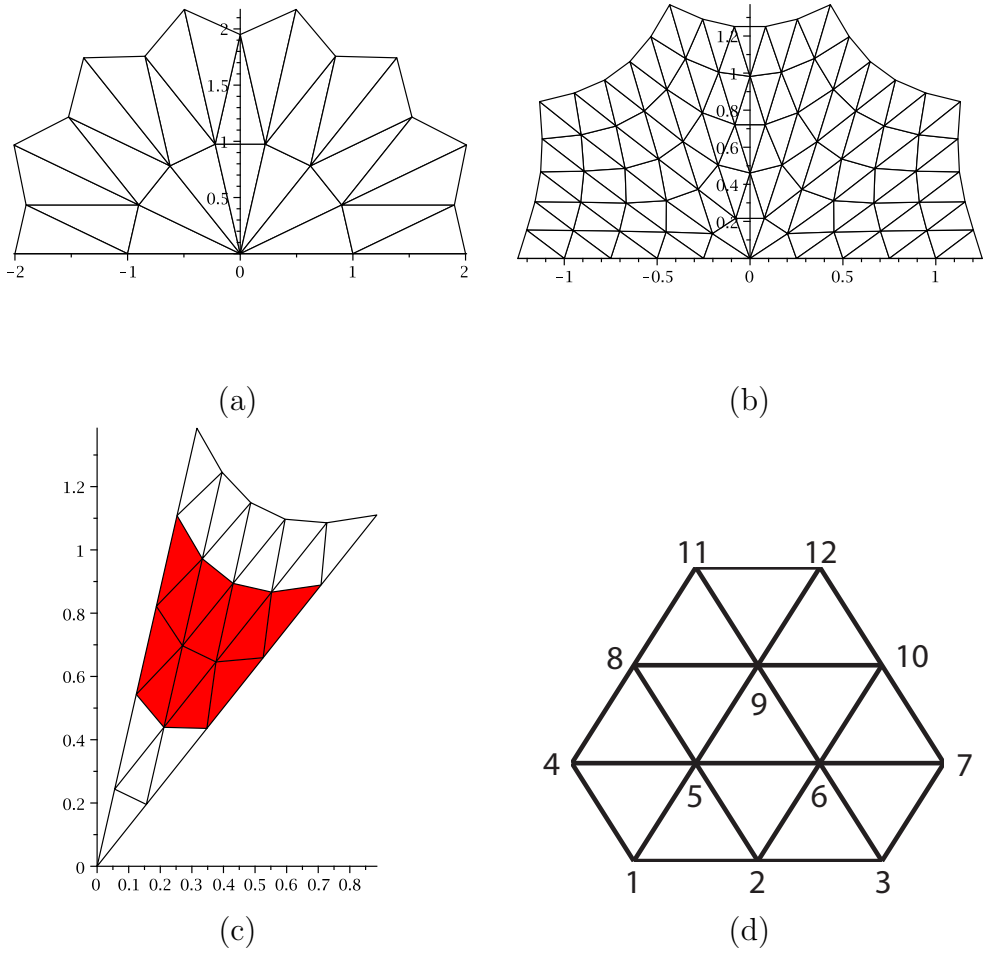

Figure 5.6: Fig (a) show the 2 ring control data for a mesh with 5 sectors which we subdivide twice. We get 5 rings show in Fig (b) for a mesh with 5 sectors. In Fig (c) we see one sector in which the relevant triangles are marked and Fig (d) shows a control net for a given triangle.

and

$$Q = \frac{1}{24}\begin{pmatrix} 2 & 2 & 0 & 2 & 12 & 2 & 0 & 2 & 2 & 0 & 0 & 0 \\ 0 & 1 & 0 & 1 & 12 & 3 & 0 & 3 & 4 & 0 & 0 & 0 \\ 1 & 3 & 0 & 0 & 12 & 4 & 0 & 1 & 3 & 0 & 0 & 0 \\ 0 & 0 & 0 & 0 & 8 & 4 & 0 & 4 & 8 & 0 & 0 & 0 \\ 0 & 1 & 0 & 0 & 10 & 6 & 0 & 1 & 6 & 0 & 0 & 0 \\ 0 & 4 & 0 & 0 & 8 & 8 & 0 & 0 & 4 & 0 & 0 & 0 \\ 0 & 0 & 0 & 0 & 4 & 3 & 0 & 3 & 12 & 1 & 1 & 0 \\ 0 & 1 & 0 & 1 & 6 & 6 & 0 & 1 & 10 & 1 & 0 & 0 \\ 0 & 1 & 0 & 0 & 6 & 10 & 0 & 0 & 6 & 1 & 0 & 0 \\ 0 & 3 & 1 & 0 & 4 & 12 & 0 & 0 & 3 & 1 & 0 & 0 \\ 0 & 0 & 0 & 0 & 2 & 2 & 0 & 2 & 12 & 2 & 2 & 2 \\ 0 & 0 & 0 & 0 & 3 & 4 & 0 & 1 & 12 & 3 & 0 & 1 \\ 0 & 0 & 0 & 0 & 4 & 8 & 0 & 0 & 8 & 4 & 0 & 0 \\ 0 & 1 & 0 & 0 & 3 & 12 & 1 & 0 & 4 & 3 & 0 & 0 \\ 0 & 2 & 2 & 0 & 2 & 12 & 2 & 0 & 2 & 2 & 0 & 0 \end{pmatrix} \tag{5.11}$$

and $P \in \mathbf{R}^{12\times n}$ such that $P_i \in \mathbf{R}^n$ is the data on the point i numbered as shown in Figure 5.6(d). The 12 triangles in the 3rd and 4th ring of our 5 ring mesh see for Example Figure 5.6(b) for $k = 5$ which are away from the boundary satisfy this condition. We can therefore compute the 12 different polynomials which for each sector are numbered as in Figure 5.6(c). We are able to compute the polynomials depending on the number of sectors $k > 3$ and which sector $i = 3, \ldots k-2$. We have to treat the case $k \leqslant 3$ and the

case where $i = 1, 2, k-1, k$ separately. The triangles on the boundary and close to the boundary are surrounded by a control net of regular vertices but since the boundary rules are regular cubic B-spline rules subdividing with boundary rules is equivalent to subdividing with regular rules a mesh that is extended by a mirror image over the boundary. The sectors 2 and $k-1$ have to be considered separately only in creating the 5 rings as they are more influenced by the extraordinary boundary rules then the other sectors. If $k \leqslant 3$ we check all the triangles directly. For any k however the eigenvector data has a symmetry across the y-axes and therefore the characteristic map has the same symmetry. In total we construct the following polynomials

12 for the interior sector with $i = 3, \ldots, k-2$ and arbitrary k

12 for $i = 2$ or $i = k-1$ and arbitrary k

12 for $i = 1$ or $i = k$ and arbitrary k

12 for k=1;

12 for k=2 and $i = 1$ or $i = 2$

12 for k=3 and $i = 1$ or $i = 3$

12 for k=3 and $i = 2$

This means that we have $12 \times 7 = 84$ polynomials $p = (f_1, f_2)$.

We will prove the claim holds for each of those polynomials and by the scaling property

$$\Phi(t/2) = T\Phi(t) \text{ where } T = \begin{pmatrix} \beta & 0 \\ 0 & \lambda_1 \end{pmatrix} = \frac{1}{2}I \tag{5.12}$$

we can then extend it to the whole sector

1. In order to prove that there is no other element than 0 in the preimage $\Phi^{-1}(0)$ we check that $f_1^2 + f_2^2 > 0$ in each triangle of each sector. We do this by first constructing the polynomial $f_1^2 + f_2^2$ in each triangles, then extracting the coefficients and then checking its positivity. Since the polynomials are given in Bezier coordinates this means that the polynomial is positive everywhere on the domain. Then by the scaling property we know that

$$\begin{aligned} f_1(t/2)^2 + f_2(t/2)^2 &= \lambda_a^2 f_1(t)^2 + \lambda_b^2 f_2(t)^2 \\ &= (\lambda_a^2 - \lambda_b^2) f_1(t)^2 + \lambda_b (f_1(t)^2 + f_2(t)^2) > 0 \end{aligned}$$

   and therefore only 0 at 0.

2. We compute the Jacobian

$$\begin{aligned} J[\Phi] &= \partial_x f_1 \partial_y f_2 + \partial_x f_2 \partial_y f_1 \\ &= (\partial_u f_1 - \partial_w f_1)(\partial_v f_2 - \partial_w f_2) + (\partial_u f_2 - \partial_w f_2)(\partial_v f_1 - \partial_w f_1) \end{aligned}$$

   in each triangle and see that the coefficients of J (a polynomial in Bezier coordinates) are all of the same sign independent of k and i. Therefore the polynomial has the same sign everywhere. By the scaling property we can extend it from the ring to the sector. The scaling property for

the Jacobian is

$$J[\Phi](t/2) = 4\beta\lambda_1 J[\Phi](t) = J[\Phi](t)$$

3. We take the the 2 triangles in the third ring that form the boundary to the second ring and find the expression of the polynomial that describes the boundary curve in Bezier coordinates. We do this by setting the relevant coordinate to 0. We will have to function depending on to coordinates (u, v) such that $u+v = 1$ given by $f_1(u, v)$ and $f_2(u, v)$. We want to show that the angle grows monotonically in either u and since the angle is given by $\arctan(f1/f2)$ it is enough to show that $f1/f2$ grows monotonically. We compute $(\partial_u f_1 - \partial_v f_1)f_2 - (\partial_u f_2 - \partial_v f_2)f_1$, the derivative of $f1/f2$ and see that all coefficients have the same sign. This means that $f1/f2$ is monoton, and therefore the angle is monoton. Therefore in each sector the curves can not intersect. There can not be intersection between sectors as the curves limit lies strictly within their sectors.

4. Box Spline surfaces lie strictly within the convex hull of their control net and therefore the image of the characteristic map has to lie in the upper half plane.

All the explicit checks were done in Maple. □

We can now conclude by Theorem 5.5 that the characteristic map is

injective. It is also regular as the Jacobian of the characteristic map has constant sign everywhere. This means that in order for the scheme to be C^1 smooth with smooth boundary we have to check the 4th condition of Theorem 5.4. Because the limit boundary is given by the one dimensional B-spline and the eigenvector data starts with points on the x-axes the limit satisfies both those condition for the case of the smooth boundary. Therefore we checked that this scheme is as wanted in the case of a smooth boundary. Lets now consider the corner case.

Coefficients for corner vertices. Separate rules have to be defined for corners. The interpolation conditions for corners require $\alpha = 0$. Therefore, the block A_{00} has a double eigenvalue β. For a corner, the tangent plane is defined by the two tangents at the non-C^1-continuous point of the boundary. Unlike the case of the smooth boundary points, there is no need to fix all rules on the boundary – parameter β still can be used to ensure smoothness of the limit surface. Hence the rules of Hoppe et al. [19] can be used. One can see [38] that the characteristic map has a convex corner. Therefore, this scheme cannot produce concave corners. *It turns out that in fact no scheme from the class that we have defined can produce smooth concave corners.*

The explicit knowledge of eigenvectors and the convex hull property allows us to determine quickly if a scheme can possibly produce convex or concave corner. If β has multiplicity 3 with Jordan blocks of size 2 and 1 which happens when it is an eigenvalue of A_{11}, the scheme is likely to be non tangent

plane continuous; we assume that this is not the case. Then the eigenvectors of interest can be found in Table 5.2 for various values of $r = (\gamma - \beta)/\delta$.

It is easy to see that positive values of r are of little interest to us, because the components of the vectors alternate signs in these cases, and are likely to produce non-regular characteristic maps. Also, for $r \leqslant -2$ we are guaranteed to get a convex configuration of control points for the characteristic map. As the characteristic map interpolates the boundary curve, it cannot have a concave corner. We conclude that we have to use r from the range $(-2, 0)$. We have seen that in this case the eigenvectors corresponding to the eigenvalue β can be taken to be $\sin i\theta$, $\sin(i-k)\,\theta$, where θ is such that $r = -2\cos\theta$. *This means that the corner is convex if $\theta < \theta_k$, and concave otherwise.* In other words, $r = -2\cos\theta < -2\cos\theta_k$, or

$$\gamma < \beta - 2\delta\cos\theta_k \tag{5.13}$$

In addition, we need to ensure that the double eigenvalue β is actually subdominant. To achieve this, we choose δ and γ large enough so that $2\delta\cos j\theta_k + \gamma < \beta$, $j = 1 \ldots k-1$. As $2\delta\cos j\theta_k + \gamma$ decreases as a function if j, and we assume that $\gamma > 0$, it is sufficient to require that $2\delta\cos\theta_k + \gamma < \beta$, which coincides with the convexity condition. We conclude that for $r < 0$ the subdivision scheme can generate only convex smooth corners).

One can show that this is true even if we do not assume that $\alpha = 0$.

In the case $k = 1$, one can also immediately see that the corner produced

by subdivision is convex.

Concave corner vertices. We assume that $k > 1$. It is impossible to have stationary subdivision rules for a triangular mesh producing a concave corner for $k = 1$. As we have observed, concave corners cannot be produced simply by changing some of the coefficients using the same stencil. One can also show that no scheme with positive coefficients can produce interpolating smooth concave corners. It is possible to construct rules to produce C^1-continuous surfaces with concave corners, but negative coefficients and larger support have to be used.

Our approach to deriving the rules is based on the idea of reduction of the magnitudes of all eigenvalues, excluding 1 and $\beta = 1/2$. It turns out that this approach leads to a particularly simple rules for subdivision.

For the scheme to produce smooth surfaces at a corner vertex the eigenvectors x^β, x'^β of the eigenvalue $\beta = 1/2$ should be subdominant. If we choose these eigenvectors to be

$$x^\beta = [0, 0, 1, v_1^\beta / \sin k\theta, \ldots], \quad x'^\beta = [0, 1, 0, v'^\beta_1 / \sin k\theta \ldots]$$

(cf. Table 5.2), corresponding left eigenvectors are very simple:

$$l = [-1, 0, 1, 0, \ldots], \quad l' = [-1, 1, 0, 0, \ldots 0].$$

The left eigenvector l^0 for the the eigenvalue 1 is $[1, 0, \ldots 0]$. Consider the

following modification of the vector of control points

$$\tilde{p} = (1-s)p + s\left((l^0, p)x^0 + (l, p)x^\beta + (l', p)x'^\beta\right)$$

where x_0 is the eigenvector $[1, \ldots 1]$ of the eigenvalue 1. Substituting expressions for the left eigenvectors we get

$$\tilde{p} = (1-s)p + s\left(p^0 x^0 + \left(p_0^1 - p^0\right)x^\beta + \left(p_k^1 - p^0\right)x'^\beta\right) \tag{5.14}$$

The effect of this transformation is to scale all components of p in the eigenbasis of the subdivision matrix by $(1-s)$ except those corresponding to the eigenvalues 1 and β. If repeated at each subdivision step, it is equivalent to scaling all eigenvalues except 1 and β by $(1-s)$.

To simplify the rules, we observe that it is unnecessary to scale multiple eigenvalues 1/16 and 1/8 of the lower-right blocks of the subdivision matrix. If we apply the rules (5.14), not to the whole vectors of control points p, but to a truncated part, modifying only control points of type 1, as a result, the eigenvalues 1/8 and 1/16 will not change. This observation leads us to the following choice of rules:

$$\tilde{p}_i^1 = (1-s)p_i^b + s\left(p^0 + \left(p_0^1 - p^0\right)\frac{\sin(k-i)\theta}{\sin k\theta} + \left(p_k^1 - p^0\right)\frac{\sin i\theta}{\sin k\theta}\right) \tag{5.15}$$

In the matrix form, this transformation can be written as

$$T = \left(\begin{array}{c|c} M & 0 \\ \hline 0 & I \end{array}\right)$$

Multiplying this matrix by the subdivision matrix on the left, we see that the eigenvalues of the product ST are eigenvalues of the blocks $B_{00}M$ and B_{11}. By construction. eigenvalues of $B_{00}M$ are 1, 1/2, $(1-s)(2\delta\cos j\theta_k + \gamma)$, $j = 1 \ldots k-1$. As we have seen before, the eigenvalues of B_{11} are 1/8 and 1/16.

By choosing the value of s so that $(1-s)(2\delta\cos\theta_k + \gamma) < 1/2$, we can ensure that the $\beta = 1/2$ is the subdominant eigenvalue. The parameter s can be viewed as a tension parameter for the corner, which determines how flat the surface is near the corner.

We can therefore consider the case of convex and concave corners together

Proposition 5.3. *Let $\beta = 1/2, \alpha = 0, \delta = 1/8$ and $\gamma = 1/2 - 1/4\cos(\theta)$ where $0 < \theta < \pi$ for convex corners and $\pi < \theta < 2\pi$ for concave corners. Then Φ, the characteristic map is defined by the eigenvectors corresponding to $\beta = 1/2$. Then*

1. *the preimage $\Phi^{-1}(0)$ contains only one element, 0;*
2. *the characteristic map has a Jacobian of constant sign at all points of the domain besides 0;*
3. *the image of the boundary of the characteristic map has no self-intersections;*

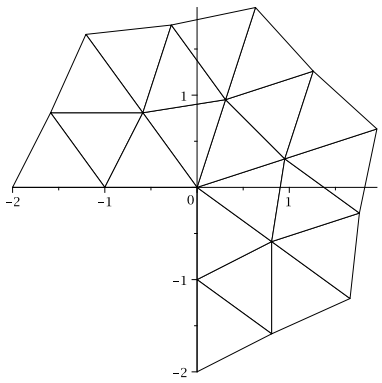

Figure 5.7: Control mesh for a boundary patch of a Loop subdivision surface with concave corner

4. the image of the characteristic map is not the whole plane.

Proof. The proof is done exactly the same way as in the non-corner case. The characteristic map we need to check has a parameter θ. Also in the case of the concave corner the convex hull of the control points (see Figure 5.7) no longer lies in the upper half plane. However we can look at the sectors individually and see that the limit function does not span the whole complex plane. □

With this we have established that the characteristic map is injective and regular. Now we need to check condition 4 in Theorem 5.4. Since the boundary of the control mesh away form 0 is a straight line for $k > 1$ the limit curve which is a B-spline is also a straight line. This means it satisfies the condition.

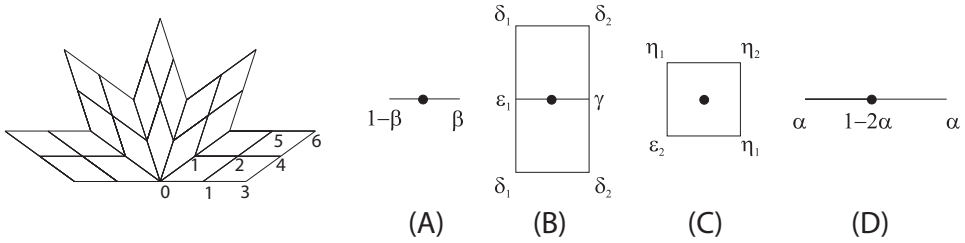

Figure 5.8: Control mesh for a boundary patch of a Catmull-Clark subdivision surface and masks of the subdivision rules. (A) The rule for the boundary vertices adjacent to the central vertex (type 1). (B) The rule for the interior edge vertices adjacent to the central vertex (type 1). (C) The rule for the face vertices adjacent to the central vertex (type 2). (D) The rule for the central vertex (type 0). The rules for vertices of type 4, 5 and 6 are the standard Catmull-Clark rules; the rule for the vertex of type 3 is the standard one-dimensional cubic spline rule.

5.5.2 Catmull-Clark scheme

The analysis of the eigenstructure of the boundary subdivision matrices becomes more complex in the case of the Catmull-Clark scheme. Using the Catmull-Clark scheme as an example, we describe a technique that can be used to analyze schemes with larger support.

The control mesh for a boundary patch surrounding an extraordinary vertex is shown in Figure 5.8.

There are 6 different types of vertices in the control mesh, shown in the same figure. For two types (1 and 3) there are two different masks that are used for boundary and interior vertices respectively. As we did in the case of the Loop scheme, we introduce a number of undefined coefficients into the masks and find eigenvalues and eigenvectors of the subdivision matrix as

functions of coefficients. The choice of the parameters is guided by the same considerations as for the Loop scheme.

Various types of boundary behavior (smooth convex corner, smooth boundary) can be obtained by choosing appropriate values of the parameters. Again, we can show that no scheme from this class can generate surfaces with smooth concave corners.

Subdivision matrix. The subdivision matrix has somewhat more complex structure for the Catmull-Clark scheme. The general form is shown in Figure 5.9. Note that a few of the blocks of the matrix are not symmetric, or even square, and it is not immediately clear how to diagonalize the matrix.

In the block form, the matrix can be written as

$$\left(\begin{array}{c|c|c|c} A_{00} & & & \\ \hline A_{10} & \frac{1}{8}I_2 & & \\ \hline A_{20} & A_{21} & A_{22} & \\ \hline A_{30} & A_{31} & A_{32} & \frac{1}{64}I_k \end{array}\right)$$

where the diagonal blocks are

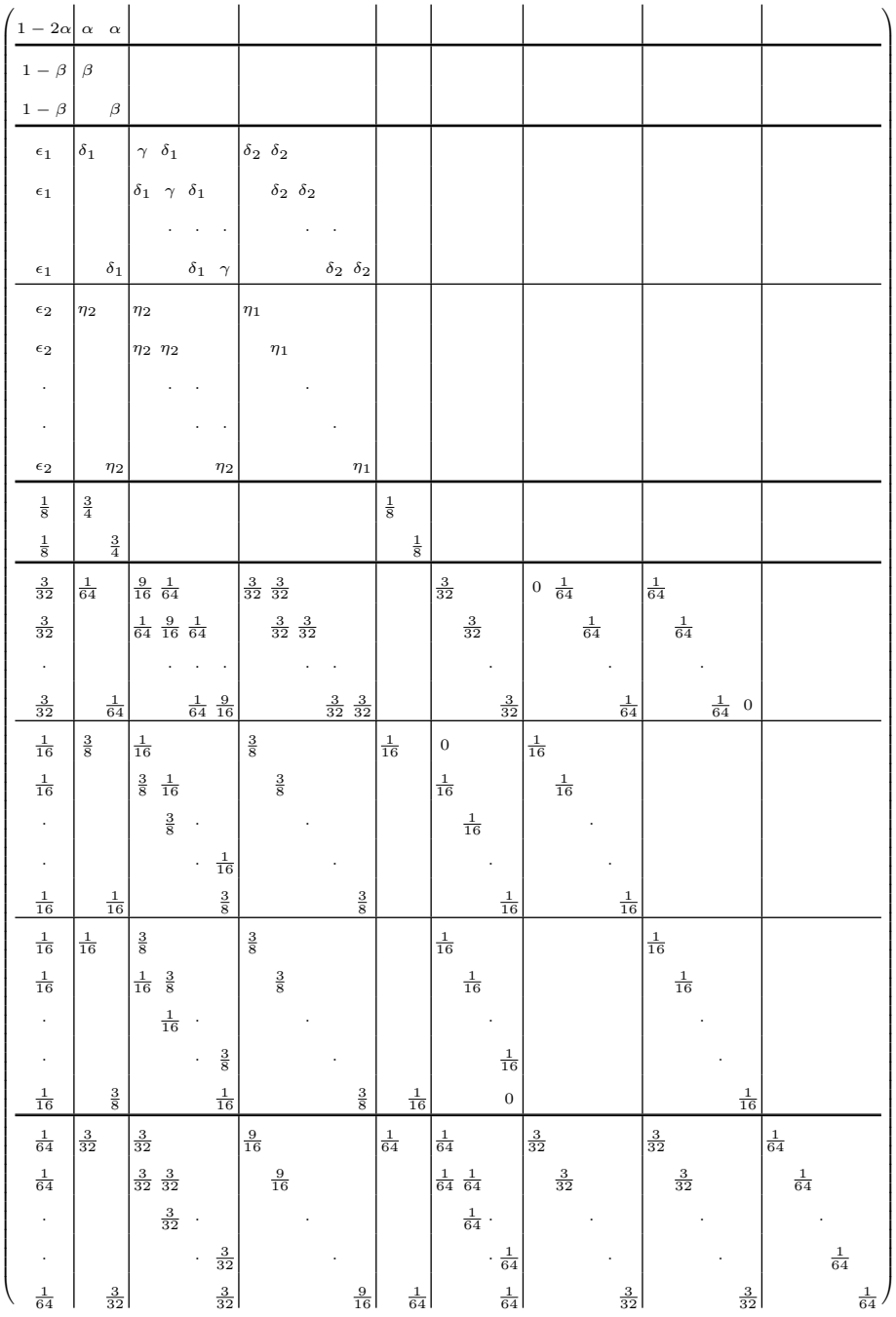

Figure 5.9: The subdivision matrix for the Catmull-Clark scheme.

$$A_{00} = \left(\begin{array}{c|cc|ccc|cccc} 1-2\alpha & \alpha & \alpha & & & & & & & \\ 1-\beta & \beta & & & & & & & & \\ 1-\beta & & \beta & & & & & & & \\ \hline \epsilon_1 & \delta_1 & & \gamma & \delta_1 & & \delta_2 & \delta_2 & & \\ \epsilon_1 & & & \delta_1 & \gamma & \delta_1 & & \delta_2 & \delta_2 & \\ & & & & \cdot & \cdot & & & \cdot & \cdot \\ \epsilon_1 & & \delta_1 & & & \delta_1 & \gamma & & & \delta_2 & \delta_2 \\ \hline \epsilon_2 & \eta_2 & & \eta_2 & & & \eta_1 & & & \\ \epsilon_2 & & & \eta_2 & \eta_2 & & & \eta_1 & & \\ \cdot & & & & \cdot & \cdot & & & \cdot & \\ \cdot & & & & & \cdot & \cdot & & & \cdot \\ \epsilon_2 & & \eta_2 & & & \eta_2 & & & & \eta_1 \end{array}\right) \tag{5.16}$$

$$A_{22} = \left(\begin{array}{ccc|ccc|ccc}
\frac{3}{32} & & & 0 & \frac{1}{64} & & \frac{1}{64} & & \\
 & \frac{3}{32} & & & \frac{1}{64} & & & \frac{1}{64} & \\
 & . & & & . & & & . & \\
 & & \frac{3}{32} & & & \frac{1}{64} & & \frac{1}{64} & 0 \\
\hline
0 & & & \frac{1}{16} & & & & & \\
\frac{1}{16} & & & & \frac{1}{16} & & & & \\
 & \frac{1}{16} & & & & . & & & \\
 & . & & & & . & & & \\
 & & \frac{1}{16} & & & \frac{1}{16} & & & \\
\hline
\frac{1}{16} & & & & & & \frac{1}{16} & & \\
 & \frac{1}{16} & & & & & & \frac{1}{16} & \\
 & . & & & & & & . & \\
 & & \frac{1}{16} & & & & & . & \\
 & & 0 & & & & & & \frac{1}{16}
\end{array}\right) \tag{5.17}$$

Note that all eigenvalues of A_{22} are guaranteed to be less than 1/8 (the sum of the magnitudes of the entries on any row does not exceed 1/8). Thus, only the eigenvalues of A_{00} are of interest to us. Next, we observe that the matrix A_{00} itself has two blocks on the diagonal; the first 3×3 block is identical to the block that we have considered for the Loop scheme; it has eigenvalues 1, β and $\beta - 2\alpha$. The only remaining block that we have to consider is

$$\bar{A}_{00} = \left(\begin{array}{ccccc|ccccc}
\gamma & \delta_1 & & & & \delta_2 & \delta_2 & & & \\
\delta_1 & \gamma & \delta_1 & & & & \delta_2 & \delta_2 & & \\
 & \cdot & \cdot & \cdot & & & & \cdot & \cdot & \\
 & & \delta_1 & \gamma & & & & & \delta_2 & \delta_2 \\
\hline
\eta_2 & & & & & \eta_1 & & & & \\
\eta_2 & \eta_2 & & & & & \eta_1 & & & \\
 & \cdot & \cdot & & & & & \cdot & & \\
 & & \cdot & \cdot & & & & & \cdot & \\
 & & & \eta_2 & & & & & & \eta_1
\end{array}\right)$$

This matrix acts on control points of types 1 and 2, excluding boundary control points of type 1.

Transformation of the subdivision matrix. Assume $k > 1$ (we will consider the case $k = 1$ separately). The eigenvalues and eigenvectors of $\bar{A}_{00}$ can be found directly from the recurrences derived from the subdivision rules. We take a somewhat different approach, similar to the DFT analysis used for interior extraordinary vertices. This approach has somewhat greater generality and can potentially be applied to analyze subdivision schemes with larger supports. To find the eigenvalues of $\bar{A}_{00}$, we introduce a new set of control points. We replace control points of type 2 p_i^2, $i = 0 \ldots k-1$, with $k+1$ control points $\tilde{p}_i^2$ satisfying

$$p_i^2 = \frac{1}{2}\left(\tilde{p}_i^2 + \tilde{p}_{i+1}^2\right) \tag{5.18}$$

for $i = 0 \ldots k-1$. Also, let $\tilde{p}_i^1 = p_i^1$ for control points of type 1. Note that we increase the number of control points. These equations clearly do not define the new control points uniquely. However, it is not relevant for our purposes. In the matrix form, the relation between the original vector of control points of types 1 and 2 and the transformed vector $\tilde{p}$ can be written as $p = T\tilde{p}$, where T is a $2k+1 \times 2k+2$ matrix.

In addition, we define the subdivision rules for the new control points. We choose the rules for $\tilde{p}$ in such a way that the relations 5.18 also hold after the subdivision rules are applied to p and $\tilde{p}$. Let $\tilde{S}$ be the subdivision matrix for $\tilde{p}$. Then our choice of rules means that

$$ST\tilde{p} = T\tilde{S}\tilde{p}$$

If λ is an eigenvalue of $\tilde{S}$, then $\tilde{S}\tilde{p}^\lambda = \lambda\tilde{p}^\lambda$ where $\tilde{p}^\lambda$ is the corresponding eigenvector, and

$$ST\tilde{p}^\lambda = T\tilde{S}\tilde{p}^\lambda = \lambda T\tilde{p}^\lambda$$

Therefore, λ is also an eigenvalue of S, unless $T\tilde{p}^\lambda = 0$. Note that the nullspace of T has dimension 1 and contains the vector $p_i^1 = 0$, $\tilde{p}_i^2 = (-1)^i$. Hence a complete set of eigenvalues and eigenvectors of S can be obtained from eigenvalues and eigenvectors of $\tilde{S}$ once we exclude the eigenvalue corre-

sponding to this vector, if it happens to be an eigenvector.

We choose the subdivision rule for $\tilde{p}_i^2$ as follows:

$$[\tilde{S}\tilde{p}]_i^2 = \epsilon_2 p^0 + 2\eta_2 p_i^1 + \eta_1 \tilde{p}_i^2 \tag{5.19}$$

In terms of new control points, the rule for control points of type 1 becomes

$$[Sp]_i^1 = \epsilon_1 p^0 + \delta_1 \left(p_{i-1}^1 + p_{i+1}^1\right) + \gamma p_i^1 + \frac{\delta_2}{2}\left(\tilde{p}_{i-1}^2 + 2\tilde{p}_i^2 + \tilde{p}_{i+1}^2\right)$$

The matrix $\bar{A}_{00}$ is transformed into

$$\tilde{A}_{00} = \left(\begin{array}{ccccc|ccccccc}
\gamma & \delta_1 & & & & \frac{\delta_2}{2} & \delta_2 & \frac{\delta_2}{2} & & & \\
\delta_1 & \gamma & \delta_1 & & & & \frac{\delta_2}{2} & \delta_2 & \frac{\delta_2}{2} & & \\
 & \cdot & \cdot & \cdot & & & & \cdot & \cdot & \cdot & \\
 & & \delta_1 & \gamma & & & & & \frac{\delta_2}{2} & \delta_2 & \frac{\delta_2}{2} \\
\hline
 & & & & & \eta_1 & & & & & \\
2\eta_2 & & & & & & \eta_1 & & & & \\
 & 2\eta_2 & & & & & & \eta_1 & & & \\
 & & \cdot & & & & & & \eta_1 & & \\
 & & & 2\eta_2 & & & & & & \eta_1 & \\
 & & & & & & & & & & \eta_1
\end{array}\right) \tag{5.20}$$

Note that $\tilde{p}_0^2$ and $\tilde{p}_k^1$ depend on p_0^1 and p_k^1 which are outside this matrix. Rearranging the entries, we get the matrix

$$\tilde{(A)}'_{00} \begin{pmatrix}
\eta_1 & & & & & & & & & \\
 & \eta_1 & & & & & & & & \\
\hline
\frac{\delta_2}{2} & & \gamma & \delta_1 & & & \delta_2 & \frac{\delta_2}{2} & & \\
 & & \delta_1 & \gamma & \delta_1 & & \frac{\delta_2}{2} & \delta_2 & \frac{\delta_2}{2} & \\
 & & & \cdot & \cdot & \cdot & & \cdot & \cdot & \cdot \\
 & \delta_2 & & & \delta_1 & \gamma & & & \frac{\delta_2}{2} & \delta_2 \\
\hline
 & & 2\eta_2 & & & & \eta_1 & & & \\
 & & & 2\eta_2 & & & & \eta_1 & & \\
 & & & & \cdot & & & & \eta_1 & \\
 & & & & & 2\eta_2 & & & & \eta_1
\end{pmatrix}$$

which has 4 diagonal or tridiagonal subblocks of size $k-1 \times k-1$. This matrix has a double eigenvalue η_1. The rest of the eigenvalues are eigenvalues of the matrix $\tilde{A}'_{00}$ consisting only of the 4 tridiagonal subblocks. We have already observed that tridiagonal matrices have eigenvectors independent from the entries of the matrix. Denote H the matrix with entries $\sin ij\theta_k$, with $\theta_k = \pi/k$ as before, $i, j = 1 \ldots k-1$. This matrix to some extent has the same role in the analysis of subdivision matrices of boundary vertices as the DFT matrix has in the analysis of subdivision matrices of interior vertices. The transform $\mathcal{H}$ is defined as $\mathrm{diag}\,(H, H)$. The inverse of this matrix is $\mathcal{H}^{-1} = \mathrm{diag}\,((2/k)H, (2/k)H)$.

We have

$$\mathcal{H}A\mathcal{H}^{-1} = \frac{2}{k}\begin{pmatrix} H & 0 \\ 0 & H \end{pmatrix}\begin{pmatrix} B_{00} & B_{01} \\ B_{10} & B_{11} \end{pmatrix}\begin{pmatrix} H & 0 \\ 0 & H \end{pmatrix} \tag{5.21}$$

$$= \frac{2}{k}\begin{pmatrix} HB_{00}H & HB_{01}H \\ HB_{10}H & HB_{11}H \end{pmatrix} \tag{5.22}$$

where each block $HB_{ij}H$ is a diagonal matrix. Finally, we apply the following permutation to the components of the vector: $\left[p_1^1, p_2^1, \ldots p_{k-1}^1, \tilde{p}_1^2, \tilde{p}_2^2, \ldots \tilde{p}_{k-1}^2\right] \rightarrow \left[p_1^1, \tilde{p}_1^2, p_2^1, \tilde{p}_2^2 \ldots p_{k-1}^1, \tilde{p}_{k-1}^2\right]$. Let P be the corresponding permutation matrix. The matrix A is reduced to the block diagonal form

$$P\mathcal{H}A\mathcal{H}^{-1}P^{-1} = \begin{pmatrix} B(1) & & & \\ & B(2) & & \\ & & \ddots & \\ & & & B(k-1) \end{pmatrix} \tag{5.23}$$

where the blocks $B(i)$, $i = 1 \ldots k-1$, are 2×2 matrices

$$B(i) = \begin{pmatrix} \gamma + 2\delta_1 \cos\dfrac{i\pi}{k} & \delta_2\left(1 + \cos\dfrac{i\pi}{k}\right) \\ 2\eta_2 & \eta_1 \end{pmatrix}. \tag{5.24}$$

The explicit expressions for the eigenvalues are not particularly enlightening in the general case and we omit them here.

Case $k = 1$. In this case, the eigenvalues and eigenvectors can be computed

directly. The eigenvalues are β, $\beta - 2\alpha$, η_2, 1/8, 1/16 and 1/64.

Eigenvectors. We start with eigenvectors of the matrix A_{00}. We assume that $\eta_1 \neq 0$ and $\delta_1 \neq 0$ and none of the eigenvalues of the blocks $B(i)$ coincide with η_1. In this case, the eigenvectors corresponding to each block $B(i)$ can be taken to be $[0, \ldots 0, 1, r, 0, \ldots 0]^T$, where the only two nonzero entries are in positions $2i - 1$ and $2i$, $r = -2\eta_2/(\eta_1 - \lambda)$, and λ is the eigenvalue. Applying the inverse permutation and transform H, we get eigenvectors of the form $[v^i, rv^i]$, with v^i being a vector of length $k-1$ with entries $\sin(j\theta_k)$, $j = 1 \ldots k-1$. The entries of the eigenvector of A_{00} corresponding to $\tilde{p}_0^2$ and $\tilde{p}_k^2$ are zero. The remaining possible eigenvalues of A_{00} are 1, β, $\beta - 2\alpha$ and η_1. Once the eigenvalue is known, the expressions for the eigenvectors can be found directly from the subdivision rules. Keeping in mind that for all eigenvectors except the eigenvectors of the eigenvalue 1 and $\beta - 2\alpha$ for $\alpha \neq 0$ $p^0 = 0$, an interior control point of type 1, p_i^1, and a control point of type 2, p_i^2, from an eigenvector p with eigenvalue λ should satisfy

$$\begin{aligned}
\lambda p_i^1 &= \delta_1 \left(p_{i-1}^1 + p_{i+1}^1\right) + \delta_2 \left(p_i^2 + p_{i-1}^2\right) + \gamma p_i^1 \quad i = 1 \ldots k-1 \\
\lambda p_i^2 &= \eta_2 \left(p_i^1 + p_{i+1}^1\right) + \eta_1 p_i^2 \quad i = 0 \ldots k-1 \\
\lambda p_0^1 &= \beta p_0^1 \\
\lambda p_k^1 &= \beta p_k^1
\end{aligned} \tag{5.25}$$

For $\lambda \neq \eta_1$, this leads to the following system of equations for p_i^1, $i =$

$1 \dots k-1$,

$$\left(\delta_1 + \delta_2 \frac{\eta_2}{\lambda - \eta_1}\right)\left(p^1_{i-1} + p^1_{i+1}\right) + \left(\gamma - \lambda + \frac{2\delta_2\eta_2}{\lambda - \eta_1}\right) p^1_i \tag{5.26}$$

Denote $\tilde{\eta}_1 = \delta_2\eta_2/\delta_1$. Then, if $\lambda = \eta_1 - \tilde{\eta}_1$, the equation is reduced to $p^1_i(\gamma - \eta_1 + \tilde{\eta}_1 - 2\delta_2) = 0$, which has nontrivial solutions only if $\gamma - \eta_1 + \tilde{\eta}_1 - 2\delta_2 = 0$.

Now we can find expressions for the eigenvectors. We start with the eigenvector of the eigenvalue η_1. Two cases are possible:

1. $\beta = \eta_1$. Then there are two eigenvectors which both have $p^1_i = (-1)^i$, and for the first one $p^2_i = (\lambda - \gamma + 2\delta_2)(-1)^i i/\delta_1$, and for the second one $p^2_i = (\lambda - \gamma + 2\delta_2)(-1)^i(i+1)/\delta_1$.

2. $\beta \neq \eta_1$. In this case, $p^1_i = 0$, and $p^2_i = (-1)^i$.

If one of the eigenvalues β or $\beta - 2\alpha$ coincides with η_1, its eigenvectors are described by the same formulas. Suppose $\beta \neq \eta_1$. Then three cases are possible for the eigenvector of β.

1. $\beta = \eta_1 - \tilde{\eta}_1$, $\gamma + \beta - 2\delta_2 = 0$. In this case, the eigenvalue β has multiplicity $k+1$, and the components p^1_i, $i = 0 \dots k$ can be chosen arbitrarily.

2. $\beta = \eta_1 - \tilde{\eta}_1$, $\gamma + \beta - 2\delta_2 \neq 0$. In this case, the eigenvalue β has multiplicity 2, the components p^1_i, $i = 1 \dots k-1$ are zero, and p^1_0, p^1_k can be chosen arbitrarily.

3. $\beta \neq \eta_1 - \tilde{\eta}_1$, $\gamma + \beta - 2\delta_2 \neq 0$. This is the most useful case. Let

$$r(\lambda) = \frac{\gamma - \lambda + \frac{2\delta_2\eta_2}{\lambda - \eta_1}}{\delta_1 + \delta_2 \frac{\eta_2}{\lambda - \eta_1}} \tag{5.27}$$

so (5.26) reduces to $p^1_{i-1} + p^1_{i+1} + r(\beta)p^1_i = 0$. We have already explored the possible solutions of these equations in Section 5.5.1. The most useful range of $r(\beta)$ is $(-2, 0)$, in which case the eigenvector can be chosen to be $\sin((i - k/2)\theta)$, with $r(\beta) = -2\cos\theta$.

Finally, for $\beta - 2\alpha$ there are two possibilities.

1. $\beta - 2\alpha = \eta_1 - \tilde{\eta}_1$, $\gamma + \beta - 2\alpha - 2\delta_2 \neq 0$. In this case, the eigenvalue β has multiplicity $k - 1$, the components p^1_i, $i = 1 \ldots k - 1$ can be chosen arbitrarily, $p^1_0 = p^1_k = 0$.

2. $\beta - 2\alpha \neq \eta_1 - \tilde{\eta}_1$, $\gamma + \beta - 2\alpha - 2\delta_2 \neq 0$. This case is similar to the third case for the eigenvalue β, with $r(\beta)$ replaced with $r(\beta - 2\alpha)$.

If $\alpha = 0$, then in the case $\beta \neq \eta_1 - \tilde{\eta}_1$, $\gamma + \beta - 2\delta_2 \neq 0$, the eigenvalue β has two eigenvectors that can be chosen to be $\sin i\theta$ and $\sin(i - k)\theta$ (see Table 5.1).

Coefficients for smooth boundary vertices. As was discussed in Section 5.5.1, it is desirable to use $\beta = 1/2$ and $\alpha = 1/8$ for smooth boundary vertices. This choice of coefficients leads to a cubic spline boundary curve. It is easy to see that we need only a single parameter in this case to ensure

C^1-continuity. We choose the parameter γ, using the standard values for all other parameters: $\eta_1 = \eta_2 = 1/4$, $\delta_1 = \delta_2 = 1/16$. In this case, the expression for the eigenvalues λ_j, λ'_j simplifies to

$$\lambda_j, \lambda'_j = \frac{1}{2}\tilde{\eta} + \frac{1}{8} \pm \frac{1}{8}\sqrt{16\tilde{\eta}^2 - 8\tilde{\eta} + 1 + 2\left(1 + \cos j\theta_k\right)} \quad j = 1 \ldots k-1$$

Note that for any k, j and any $0 < \gamma < 1$, $|\lambda_j| < \lambda_1$ and $|\lambda'_j| < \lambda_1$. From the formulas for the eigenvectors we can tell that it is desirable to have subdominant eigenvalues $\beta = 1/2$ and λ_1. For λ_1 to be equal to $1/2$, we can take $\gamma = 3/8 - (1/4)\cos\theta_k$. Note that for the regular case $k = 2$ we get the standard value $\gamma = 3/8$. In general, for $1/2$ to be one of the subdominant eigenvalues, it is necessary that $\gamma < 3/8 - (1/4)\cos 2\theta_k$. If one wishes to use a single value of γ for all valences, then the maximal possible choice of γ is $1/8$.

Case k = 1. For the regular choices of parameters, the subdominant eigenvalues are $1/2$ and $1/4$, where $1/4$ has a Jordan block of size 2. The resulting scheme is C^1, although the normals converge to the limit slower than in other cases due to the presence of the Jordan block. In this case the *parametric map* does not coincide with the characteristic map. The parametric map can be informally characterized as the map approximating, up to affine invariance, any subdivision surface generated near the central control point. Typically, it coincides with the characteristic map, but in the

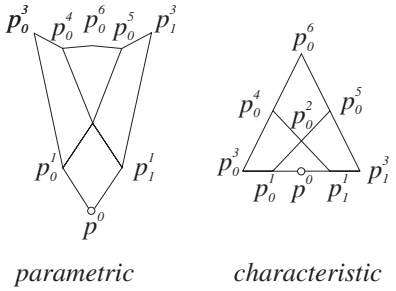

Figure 5.10: The control mesh for the parametric and characteristic maps in the case $k = 1$ for smooth boundary.

case when one of the subdominant eigenvalues has a nontrivial Jordan block, these maps can be different. The tangent vectors are actually determined by the control vectors of the parametric map. The control net of the characteristic and parametric maps for $k = 1$ and the standard choice of coefficients is shown in Figure 5.10. Assuming the ordering of components $x^1 = [p^0, p_0^1, p_1^1, p^2, p_0^3, p_1^3, p_0^4, p_0^5, p_0^6]$, the eigenvectors defining the maps are $x^1 = [0, 1, -1, 0, 2, -2, 1, -1, 0]$ (eigenvalue $1/2$),$x^2 = [0, 0, 0, 1, 0, 0, 2, 2, 4]$ (eigenvalue $1/4$ regular eigenvector) and $x'^2 = [-1, 2, 2, 5, 11, 11, 10, 10, 51/5]$ (eigenvalue $1/4$, generalized eigenvector). The characteristic map is defined by the pair (x^1, x^2) and the parametric map is defined by the pair (x^1, x'^2).

Coefficients for convex corner vertices. For the corner vertices we choose $\alpha = 0$, $\beta = 1/2$. In this case, we have to ensure that the two eigenvectors of the double eigenvalue β are the subdominant eigenvectors. The necessary condition for this is $\lambda_1 < \beta$. In addition, we have to verify that the resulting corner is indeed convex. As was the case for the Loop scheme, if

the characteristic map is regular, for convexity it is sufficient that the control mesh of the characteristic map has a convex corner at the central vertex. As the subdominant eigenvectors for the eigenvalue β can be chosen to have components p_i^1 equal to $\sin i\theta$ and $\cos i\theta$, with θ such that $-2\cos\theta = r(\beta)$ and $r(\beta)$ defined by (5.27), the condition for convexity is $r < -2\cos\theta_k$. As it was the case for the Loop scheme, this condition turns out to be exactly equivalent to the condition for the eigenvalue β to be subdominant. We arrive at the same conclusion: *no scheme from the class that we have defined can produce smooth concave corners.*

Coefficients for concave corner vertices. To obtain coefficients that would allow us to generate surfaces with smooth concave corners, we use the same approach that we used for the Loop scheme: we modify the coefficients in such a way that all eigenvalues of the matrix A_{00} except 1 and $\beta = 1/2$ are scaled by the constant $s < 1$. Recall that the idea is to use subdivision rules with γ chosen in such a way that the eigenvectors of the eigenvalue $\beta = 1/2$ produce a concave configuration, and use additional modification of control points to ensure that β are subdominant. The additional rules were derived from the expression

$$\tilde{p} = (1-s)p + s\left((l^0, p)x^0 + (l, p)x^\beta + (l', p)x'^\beta\right)$$

where x_0 is the eigenvector $[1, \ldots 1]$ of the eigenvalue 1, x^β and x'^β are eigenvectors of the eigenvalue β, and l^0, l and l' are corresponding left eigenvec-

tors. The left eigenvectors l^0, l and l' are exactly the same as for the Loop scheme: $l = [-1, 0, 1, 0, \ldots]$, $l' = [-1, 1, 0, 0, \ldots 0]$ and $l^0 = [1, 0, \ldots 0]$. The eigenvectors x^β and x'^β coincide with the eigenvectors for the Loop scheme when restricted to the vertices of type 1. To obtain the desired scaling of eigenvalues we also need to modify vertices of type 2. The components of the eigenvectors corresponding to the vertices of type 2 are easily computed using subdivision rules (cf. (5.25)):

$$p_i^2 = \frac{\eta_2}{\lambda - \eta_1}\left(p_i^1 + p_{i+1}^1\right) = \left(p_i^1 + p_{i+1}^1\right)$$

Therefore, the analog of rules (5.15) for the Catmull-Clark subdivision is

$$\begin{aligned}
[Sp]_i^1 &= (1-s)p_i^1 + s\left(p^0 + \left(p_0^1 - p^0\right)\frac{\sin(k-i)\theta}{\sin k\theta} + \left(p_k^1 - p^0\right)\frac{\sin i\theta}{\sin k\theta}\right) \\
[Sp]_i^2 &= (1-s)p_i^2 \\
&+ s\left(p^0 + \left(p_0^1 - p^0\right)\frac{\sin(k-i)\theta + \sin(k-i+1)\theta}{\sin k\theta} + \left(p_k^1 - p^0\right)\frac{\sin i\theta + \sin(i+1)\theta}{\sin k\theta}\right)
\end{aligned} \tag{5.28}$$

Proposition 5.4. *Let Φ be the characteristic map defined by the eigenvectors described as above for each of the different cases. Then*

1. *the preimage $\Phi^{-1}(0)$ contains only one element, 0;*

2. *the characteristic map has a Jacobian of constant sign at all points of the domain besides 0.*

3. *The image of the boundary of the characteristic map has no self- inter-*

sections;

4. the image of the characteristic map is not the whole plane.

Proof. We will consider the smooth boundary case and the corner case separately. For the smooth boundary case we use the coefficients $\beta = 1/2, \alpha = 1/8, \eta_1 = \eta_2 = 1/4, \delta_1 = \delta_2 = 1/16$ and $\gamma = 3/8 - 1/4\cos\theta_k$. The characteristic map is the formed by the eigenvectors to the eigenvalue $\beta = 1/2$ and $\lambda_1 = 1/2$. In the corner case we use the same coefficients besides $\alpha = 0$ and $\gamma = 3/8 - 1/4\cos\theta$ where θ is such that $r(\beta) = -2\cos\theta$. We construct the 2 ring control mesh (see Figure 5.11(a) for k=4) given by these eigenvalues and subdivide them twice. The quadrilaterals in the 3rd and 4th ring are then surrounded by one ring of regular quads. In each sector we have 12 quads. We compute the surrounding 16 control values (Figure 5.11 (c)) for the following different cases for the smooth boundary as well as for the corner case:

12 for the interior sector with $i = 3, \ldots, k-2$ and arbitrary k

12 for $i = 2$ or $i = k-1$ and arbitrary k

12 for $i = 1$ or $i = k$ and arbitrary k

12 for k=1;

12 for k=2 and $i = 1$ or $i = 2$

12 for k=3 and $i = 1$ or $i = 3$

12 for k=3 and $i = 2$

For each of those $12 \times 7 \times 2 = 168$ different cases we get the polynomial by tensor product B-spline which is given by

$$p(u,v) = \chi \cdot B \cdot P$$

where

$$\chi = (1, u, u^2, u^3, v, vu, vu^2, cu^3, v^2, v^2u, v^2u^2, v^2u^3, v^3, v^3u, v^3u^2, v^3u^3)$$

and

$$B = \frac{1}{6}\begin{pmatrix} B_1 & 4B_1 & B_1 & 0 \\ -3B_1 & 0 & 3B_1 & 0 \\ 3B_1 & -6B_1 & 3B_1 & 0 \\ -B_1 & 3B_1 & -3B_1 & B_1 \end{pmatrix} \tag{5.29}$$

with

$$B_1 = \frac{1}{6}\begin{pmatrix} 1 & 4 & 1 & 0 \\ -3 & 0 & 3 & 0 \\ 3 & -6 & 3 & 0 \\ -1 & 3 & -3 & 1 \end{pmatrix} \tag{5.30}$$

and $P \in \mathbf{R}^{16}$ given by the control data. In order to do our analysis we have to transform the polynomial into Bernstein-Bezier coordinates first. We do that by replacing the vector χ with its Bernstein-Bezier equivalent. Therefore we now have 168 polynomials $p(u, 1-u, v, 1-v) = (f_1, f_2)$ representing the characteristic map in Berstein-Bezier coordinates.

1. For each of those cases we need to check that the radius $f_1^2 + f_2^2$ is strictly bigger than 0. We do that by checking the coefficients in Berstein-

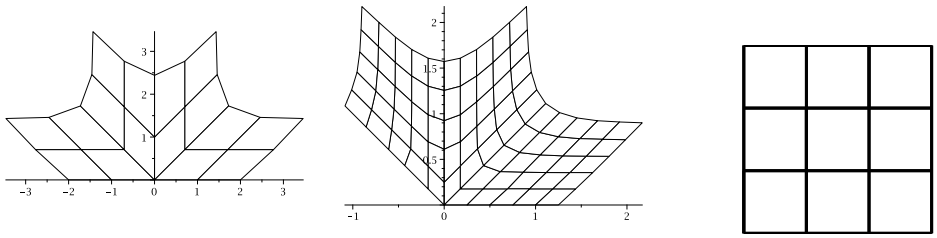

(a) (b) (c)

Figure 5.11: (a) the 2 ring control data for a mesh with 4 sectors which we subdivide twice. (b) 5 rings of 3 sectors (c) a control net for a given quadrilateral.

Bezier coordinates.

2. We compute the Jacobian on each quadrilateral and check the sign by checking the sign of the coefficients and find that they are all the same.

3. We consider the relevant boundary of the quads that from the boundary curve. The functions are given by setting $u = 0$. We then have a function depending on v and $1 - v$ only. We check the monotonicity of the quotient as in the Loop scheme.

4. This follows from the convex hull property of the regular scheme as the convex hull of the control mesh is not the whole plane. Again we have to take it sector by sector for the concave corner case.

□

We can then conclude similarly than for Loop that the scheme is C^1 by finding the cubic B-spline boundary curve and checking the condition of

Theorem 5.4

Furthermore it is not necessary to use those exact values for the parameters. We need only to ensure that β and λ_1 are subdominant as well as $r(\beta) \in [-2, 0]$ to get the similar eigenvectors and by a similar calculation the same results.

Chapter 6

Eigenvalue Variational Analysis

6.1 Introduction

In this chapter we will give a short review of the set of subgradients and regular subgradients of the spectral abscissa due to Burke and Overton [5]. In that work they found necessary and sufficient conditions for regular subgradients and necessary conditions for subgradients of the spectral abscissa. It seems hard to find a general sufficient condition. In our attempt to do so we carefully considered the simplest defective, derogatory case. It turns out that by a hands-on calculation we can fully describe the subgradients in this case.

6.2 Results on Subgradients of spectral functions

Subgradients: For functions that are not differentiable, subgradients are used instead of the derivative to analyze variational properties. The following definition may be found in [37]. Let $\phi : \mathbf{E} \to [-\infty, \infty]$, where $\mathbf{E}$ is a finite-dimensional Euclidean space, real or complex, with the real inner product $\langle \cdot, \cdot \rangle$, and let $x \in \mathbf{E}$ be such that $\phi(x) < \infty$. A vector $y \in \mathbf{E}$ is a **regular subgradient** of ϕ at x (written $y \in \widehat{\partial}\phi(x)$) if

$$\liminf_{z \to 0} \frac{\phi(x+z) - \phi(x) - \langle y, z \rangle}{\|z\|} \geqslant 0. \tag{6.1}$$

A vector $y \in \mathbf{E}$ is a **subgradient** of ϕ at x (written $y \in \partial\phi(x)$) if there exists sequences x_i and y_i in $\mathbf{E}$ satisfying

$$x_i \to x \tag{6.2}$$

$$\phi(x_i) \to \phi(x) \tag{6.3}$$

$$y_i \in \widehat{\partial}\phi(x_i) \tag{6.4}$$

$$y_i \to y. \tag{6.5}$$

The spectral abscissa: Burke and Overton [5] describe functions of the type $f \circ \lambda$, where $\lambda : \mathbb{C}^{n \times n} \to \mathbb{C}^n$ maps a matrix to its eigenvalues and the function $f : \mathbb{C}^n \to \mathbb{R}$ is invariant under permutation of its arguments. They

focus on functions $f = g \circ h_\kappa$ with $(h_\kappa(x))_i = \kappa(x_i)$ and g being the max function, especially the case where $\kappa(x) = \mathrm{Re}(x)$. Then, $f \circ \lambda$ is called the *spectral abscissa* and is denoted α. The regular subgradients of the spectral abscissa are given by [5, Thm 7.2]:

Proposition 6.1. *Let X have Jordan form*

$$P^{-1}XP = J = \begin{bmatrix} J^{(1)} & & \\ & \ddots & \\ & & J^{(p)} \end{bmatrix}, \text{ where } J^{(j)} = \begin{bmatrix} J_1^{(j)} & & \\ & \ddots & \\ & & J_{q^{(j)}}^{(j)} \end{bmatrix},$$

$$\text{with } J_k^{(j)} = \begin{bmatrix} \mu_j & 1 & & \\ & \ddots & \ddots & \\ & & \ddots & 1 \\ & & & \mu_j \end{bmatrix} \in \mathbb{C}^{m_k^{(j)} \times m_k^{(j)}}, \quad k = 1, \ldots, q^{(j)}, \quad j = 1, \ldots, p.$$

Then $\widehat{\partial}\alpha(X)$, the set of regular *subgradients of the spectral abscissa α at X,*

is the set of matrices Y satisfying

$$P^*YP^{-*} = W = \begin{bmatrix} W^{(1)} & & \\ & \ddots & \\ & & W^{(p)} \end{bmatrix}, \tag{6.6}$$

$$W^{(j)} = \begin{bmatrix} W_{11}^{(j)} & & \\ & \ddots & \\ & & W_{q^{(j)}q^{(j)}}^{(j)} \end{bmatrix}, \tag{6.7}$$

$$\text{where } W_{kk}^{(j)} = \begin{bmatrix} \theta_1^{(j)} & & & & \\ \theta_2^{(j)} & \cdot & & & \\ \cdot & \cdot & \cdot & & \\ \cdot & \cdot & \cdot & \cdot & \\ \theta_{m_k^{(j)}}^{(j)} & \cdot & \cdot & \theta_2^{(j)} & \theta_1^{(j)} \end{bmatrix}, \tag{6.8}$$

$$k = 1, \ldots, q^{(j)}, \quad j = 1, \ldots, p, \tag{6.9}$$

$$W^{(j)} = 0 \text{ if } j \notin \mathcal{A} := \{\ell : \alpha(X) = \mathrm{Re}\mu_\ell\} \tag{6.10}$$

$$\theta_1^{(j)} \in \mathbf{R}, \quad \theta_1^{(j)} \geqslant 0, \quad \sum_{j \in \mathcal{A}} m^{(j)} \theta_1(j) = 1, \tag{6.11}$$

$$\text{with } m^{(j)} = \sum_{k=1}^{q^{(j)}} m_k^{(j)} \tag{6.12}$$

$$\mathrm{Re}\theta_2^{(j)} \geqslant 0. \tag{6.13}$$

Necessary conditions for subgradients (not necessarily regular) are also

given in [5]. We shall not describe these in all generality here, but we will discuss a special case. Necessary and sufficient conditions were given in [5] for the case that all active eigenvalues of a matrix are nondefective (equivalently semisimple), that is the Jordan blocks are of size 1, or nonderogatory (there is only one Jordan block for each eigenvalue). Active eigenvalues μ of a matrix X are such that $\alpha(X) = \mathrm{Re}\mu$.

6.3 Subgradients of the spectral abscissa in the simplest defective, derogatory case

The subgradients of α at X depend on the Jordan normal form of X. When $n = 2$ the eigenvalues are either nondefective or nonderogatory, so the simplest interesting case is $n = 3$, with

$$J = \begin{pmatrix} 0 & 1 & 0 \\ 0 & 0 & 0 \\ 0 & 0 & 0 \end{pmatrix}. \tag{6.14}$$

W.l.o.g, we take $P = I$, and set the eigenvalue to 0 since subgradients do not depend on the value of the eigenvalue. Then, it follows from Proposition 6.1

that for Y to be a **regular** subgradient, it must have the form

$$\begin{pmatrix} \frac{1}{3} & 0 & 0 \\ w & \frac{1}{3} & 0 \\ 0 & 0 & \frac{1}{3} \end{pmatrix} \text{ with } \mathrm{Re}(w) \geqslant 0. \tag{6.15}$$

We know from [5, Cor 8.1] that in order for a matrix to be a subgradient (not necessarily regular) of α at J it must be of the form

$$\begin{pmatrix} a & 0 & 0 \\ b & a & c \\ d & 0 & 1-2a \end{pmatrix} \text{ with } a \in \left[0, \frac{1}{2}\right]. \tag{6.16}$$

The main result of this chapter characterizes all subgradients of α at J:

Theorem 6.1. *The set of subgradients of the spectral abscissa α at the matrix J is given by*

$$\partial\alpha(J) = \left\{ \begin{pmatrix} a & 0 & 0 \\ b & a & c \\ d & 0 & 1-2a \end{pmatrix} \textit{ with } a \in [0, \tfrac{1}{2}]. \textit{ If } a \neq \frac{1}{3} : \mathrm{Re}\left(b - \frac{cd}{1-3a}\right) \geqslant 0 \right\} \tag{6.17}$$

Proof of Theorem 6.1

The method we use to prove this result is a very direct one. We know that a subgradient Y must have the form (6.16). We also know the exact description of the regular subgradients. Since subgradients are limits of regular subgradients we study sequences $X_i \to J$ and $Y_i \to Y$ with $Y_i \in \widehat{\partial}\alpha(X_i)$.

The set of all such Y is the set of subgradients. There are only finitely many possible Jordan structures, so we assume w.l.o.g. that in each sequence all X_i have the same Jordan structure. Otherwise we can consider a subsequence. We will go through each of the possible Jordan structures and discuss what matrix limits are possible, thereby finding stronger necessary conditions. We will then prove that these conditions are sufficient.

In dimension 3 there are 9 possible Jordan structures, assuming that

$\mathrm{Re}(\alpha_i) \geqslant \mathrm{Re}(\beta_i) \geqslant \mathrm{Re}(\gamma_i)$, for $J_i = P_i^{-1} X_i P_i$, namely

$$J_i^1 = \begin{pmatrix} \alpha_i & 0 & 0 \\ 0 & \alpha_i & 0 \\ 0 & 0 & \alpha_i \end{pmatrix} \quad J_i^2 = \begin{pmatrix} \alpha_i & 1 & 0 \\ 0 & \alpha_i & 0 \\ 0 & 0 & \alpha_i \end{pmatrix}$$

$$J_i^3 = \begin{pmatrix} \alpha_i & 0 & 0 \\ 0 & \alpha_i & 1 \\ 0 & 0 & \alpha_i \end{pmatrix} \quad J_i^4 = \begin{pmatrix} \alpha_i & 1 & 0 \\ 0 & \alpha_i & 1 \\ 0 & 0 & \alpha_i \end{pmatrix}$$

$$J_i^5 = \begin{pmatrix} \alpha_i & 1 & 0 \\ 0 & \alpha_i & 0 \\ 0 & 0 & \beta_i \end{pmatrix} \quad J_i^6 = \begin{pmatrix} \alpha_i & 0 & 0 \\ 0 & \alpha_i & 0 \\ 0 & 0 & \beta_i \end{pmatrix}$$

$$J_i^7 = \begin{pmatrix} \alpha_i & 0 & 0 \\ 0 & \beta_i & 1 \\ 0 & 0 & \beta_i \end{pmatrix} \quad J_i^8 = \begin{pmatrix} \alpha_i & 0 & 0 \\ 0 & \beta_i & 0 \\ 0 & 0 & \beta_i \end{pmatrix}$$

$$J_i^9 = \begin{pmatrix} \alpha_i & 0 & 0 \\ 0 & \beta_i & 0 \\ 0 & 0 & \gamma_i \end{pmatrix}$$

Let us denote by $S_j(J)$ the set of all possible subgradients if X_i has Jordan form J_i^j. In the following we will go through each of the 9 cases and find necessary conditions for each of the $S_j(J)$. We require $X_i = P_i J_j^i P_i^{-1} \to J$. Note that, in general, P_i^{-1} and P_i are not both bounded, but the eigenvalues of X_i, namely α_i, β_i and γ_i, must converge to 0. We know that the corresponding

regular subgradient satisfies $Y_i = P_i^{-*} W_j^i P_i^*$ where W_j^i satisfies (6.6)-(6.13).

Case 1

When the Jordan type of the sequence is J_i^1 we have $X_i = P_i(\alpha_i I)P_i^{-1} = \alpha_i I$, so it cannot converge to J and hence

$$S_1(J) = \emptyset.$$

Case 2

In this case we only get regular subgradients. Let

$$X_i \to J \text{ and } Y_i \to Y$$

where

$$X_i = P_i \begin{pmatrix} \alpha_i & 1 & 0 \\ 0 & \alpha_i & 0 \\ 0 & 0 & \alpha_i \end{pmatrix} P_i^{-1} \text{ and } Y_i = P_i^{-*} \begin{pmatrix} \frac{1}{3} & 0 & 0 \\ w_i & \frac{1}{3} & 0 \\ 0 & 0 & \frac{1}{3} \end{pmatrix} P_i^*$$

with $\mathrm{Re}(w_i) \geqslant 0$. Note that the given structure for Y_i comes from Proposition 6.1 since $Y_i \in \widehat{\partial}\alpha(X_i)$. Now we do the following analysis:

$$\begin{aligned}
Y_i^* &= P_i \begin{pmatrix} \frac{1}{3} & w_i^* & 0 \\ 0 & \frac{1}{3} & 0 \\ 0 & 0 & \frac{1}{3} \end{pmatrix} P_i^{-1} \\
&= P_i \left(\frac{1}{3} I + \begin{pmatrix} 0 & w_i^* & 0 \\ 0 & 0 & 0 \\ 0 & 0 & 0 \end{pmatrix} \right) P_i^{-1} \\
&= \frac{1}{3} I + w_i^* P_i \left(\left(\begin{pmatrix} 0 & 1 & 0 \\ 0 & 0 & 0 \\ 0 & 0 & 0 \end{pmatrix} + \alpha_i I - \alpha_i I \right) \right) P_i^{-1} \\
&= \frac{1}{3} I + w_i^* (X_i - \alpha_i I).
\end{aligned}$$

Because $\alpha_i \to 0$ and $X_i \to J$ and $Y_i^* = \frac{1}{3} I + w_i^*(X_i - \alpha_i I) \to Y^*$ we see that w_i must converge, say to w. We conclude that

$$Y = \frac{1}{3} I + wJ = \begin{pmatrix} \frac{1}{3} & 0 & 0 \\ w & \frac{1}{3} & 0 \\ 0 & 0 & \frac{1}{3} \end{pmatrix} \in \widehat{\partial}\alpha(J).$$

This means Y must be a regular subgradient:

$$S_2(J) \subset \widehat{\partial}\alpha(J).$$

Case 3

In Case 3 the X_i would be given as

$$X_i = P_i \begin{pmatrix} \alpha_i & 0 & 0 \\ 0 & \alpha_i & 1 \\ 0 & 0 & \alpha_i \end{pmatrix} P_i^{-1}$$

however this can be rewritten as

$$X_i = P_i \begin{pmatrix} 0 & 0 & 1 \\ 1 & 0 & 0 \\ 0 & 1 & 0 \end{pmatrix} \begin{pmatrix} \alpha_i & 1 & 0 \\ 0 & \alpha_i & 0 \\ 0 & 0 & \alpha_i \end{pmatrix} \begin{pmatrix} 0 & 1 & 0 \\ 0 & 0 & 1 \\ 1 & 0 & 0 \end{pmatrix} P_i^{-1}$$

and therefore reduces to Case 2.

$$S_3(J) \subset \widehat{\partial}\alpha(J).$$

Case 4

In this case we require

$$X_i \to J \text{ and } Y_i \to Y$$

where

$$X_i = P_i \begin{pmatrix} \alpha_i & 1 & 0 \\ 0 & \alpha_i & 1 \\ 0 & 0 & \alpha_i \end{pmatrix} P_i^{-1} \text{ and } Y_i = P_i^{-*} \begin{pmatrix} \frac{1}{3} & 0 & 0 \\ w_i & \frac{1}{3} & 0 \\ y_i & w_i & \frac{1}{3} \end{pmatrix} P_i^{*}.$$

Again $\mathrm{Re}(w_i) \geqslant 0$ but $y_i \in \mathbb{C}$ is unrestricted. We know that Y satisfies (6.16). Since $\det(Y_i) = 1/27$ is constant it has to be stable under the limit and that means that

$$\det(Y) = a^2(1-2a) = \frac{1}{27}.$$

The only solution for $a \in [0, \frac{1}{2}]$ is then $a = 1/3$, so

$$S_4(J) \subset \left\{ Y = \begin{pmatrix} 1/3 & 0 & 0 \\ b & 1/3 & c \\ d & 0 & 1/3 \end{pmatrix} \right\}.$$

Case 5

$\underline{\mathrm{Re}(\alpha_i) > \mathrm{Re}(\beta_i)}$

Given the sequences

$$X_i \to J \text{ and } Y_i \to Y$$

where

$$X_i = P_i \begin{pmatrix} \alpha_i & 1 & 0 \\ 0 & \alpha_i & 0 \\ 0 & 0 & \beta_i \end{pmatrix} P_i^{-1} \text{ and } Y_i = P_i^{-*} \begin{pmatrix} \frac{1}{2} & 0 & 0 \\ w_i & \frac{1}{2} & 0 \\ 0 & 0 & 0 \end{pmatrix} P_i^*,$$

with $\mathrm{Re}(w_i) \geqslant 0$, we look at $X_i Y_i^*$:

$$\begin{aligned} X_i Y_i^* &= P_i \begin{pmatrix} \alpha_i & 1 & 0 \\ 0 & \alpha_i & 0 \\ 0 & 0 & \beta_i \end{pmatrix} \begin{pmatrix} \frac{1}{2} & \omega_i^* & 0 \\ 0 & \frac{1}{2} & 0 \\ 0 & 0 & 0 \end{pmatrix} P_i^{-1} && (6.18) \\ &= P_i \begin{pmatrix} \frac{\alpha_i}{2} & \alpha_i\omega_i^* + \frac{1}{2} & 0 \\ 0 & \frac{\alpha_i}{2} & 0 \\ 0 & 0 & 0 \end{pmatrix} P_i^{-1} = \alpha_i Y_i^* + H_i && (6.19) \end{aligned}$$

$$\text{where } H_i = P_i \begin{pmatrix} 0 & \frac{1}{2} & 0 \\ 0 & 0 & 0 \\ 0 & 0 & 0 \end{pmatrix} P_i^{-1}. \qquad (6.20)$$

We know that $\alpha_i \to 0$ and $X_i Y_i^* \to JY^* = aJ$ since Y satisfies (6.16). Therefore

$$H_i \to aJ.$$

We will show that this means that $a = \frac{1}{2}$. Consider

$$Y_i^* = \frac{1}{2}I + K_i \text{ where } K_i = P_i \begin{pmatrix} 0 & w_i^* & 0 \\ 0 & 0 & 0 \\ 0 & 0 & -\frac{1}{2} \end{pmatrix} P_i^{-1}.$$

Y_i converges and therefore $K_i = Y_i^* - \frac{1}{2}I$ converges and so does

$$K_i^2 = P_i \begin{pmatrix} 0 & 0 & 0 \\ 0 & 0 & 0 \\ 0 & 0 & \frac{1}{4} \end{pmatrix} P_i^{-1}.$$

$$X_i = \alpha_i I + 2H_i + 4(\beta_i - \alpha_i)K_i^2 \to 0 + 2aJ + 0$$

and we can conclude, since $X_i \to J$ that $J = 2aJ$, and therefore $a = \frac{1}{2}$.

Using $K_i = 2w_i^* H_i - 2K_i^2$ we see that w_i has to converge and we call its limit w. Since $\mathrm{Re}(w_i) \geqslant 0$ it follows that $\mathrm{Re}(w) \geqslant 0$.

We get then that

$$K_i = Y_i^* - \frac{1}{2}I \to Y^* - \frac{1}{2}I = \begin{pmatrix} 0 & b^* & c^* \\ 0 & 0 & 0 \\ 0 & d^* & -\frac{1}{2} \end{pmatrix} =: K$$

$$\text{therefore } K_i^2 \to K^2 = \begin{pmatrix} 0 & c^*d^* & -\frac{c^*}{2} \\ 0 & 0 & 0 \\ 0 & -\frac{d^*}{2} & \frac{1}{4} \end{pmatrix}$$

$$\text{therefore } K_i = 2w_i^* H_i - 2K_i^2 \to 2w^* aJ - 2K^2$$

$$= w^* J - 2K^2 = \begin{pmatrix} 0 & w^* - 2c^*d^* & c^* \\ 0 & 0 & 0 \\ 0 & d^* & -\frac{1}{2} \end{pmatrix}$$

$$\Rightarrow b^* = w^* - 2c^*d^*.$$

Thus,

$$S_5^1(J) \subset \left\{ Y = \begin{pmatrix} 1/2 & 0 & 0 \\ b & 1/2 & c \\ d & 0 & 0 \end{pmatrix} \text{ where } \mathrm{Re}(b + 2cd) \geqslant 0 \right\}.$$

We are using the superscript to denote the sub-case of Case 5. Note that the right hand side is contained in the right hand side of (6.17).

$\underline{\mathrm{Re}(\alpha_i) = \mathrm{Re}(\beta_i)}$

The sequences

$$X_i \to J \text{ and } Y_i \to Y$$

in this case are given by

$$X_i = P_i \begin{pmatrix} \alpha_i & 1 & 0 \\ 0 & \alpha_i & 0 \\ 0 & 0 & \beta_i \end{pmatrix} P_i^{-1} \text{ and } Y_i = P_i^{-*} \begin{pmatrix} p_i & 0 & 0 \\ w_i & p_i & 0 \\ 0 & 0 & 1-2p_i \end{pmatrix} P_i^*$$

where $p_i \in [0, \frac{1}{2}]$ and therefore w.l.o.g. we can assume that p_i converges.

1. The first case we consider is when $p_i \to \frac{1}{3}$. Then

$$\begin{aligned} Y_i^* - p_i I &= P_i \begin{pmatrix} 0 & w_i^* & 0 \\ 0 & 0 & 0 \\ 0 & 0 & 1-3p_i \end{pmatrix} P_i^{-1} \\ &\to \begin{pmatrix} a - \frac{1}{3} & b^* & c^* \\ 0 & a - \frac{1}{3} & 0 \\ 0 & d^* & \frac{2}{3} - 2a \end{pmatrix}. \end{aligned}$$

   Since the determinant is a continuous function we conclude that $a = \frac{1}{3}$, so

$$S_5^2(J) \subset \left\{ Y = \begin{pmatrix} 1/3 & 0 & 0 \\ b & 1/3 & c \\ d & 0 & 1/3 \end{pmatrix} \right\}.$$

2. Now assume $p_i \to p$ where $p \neq \frac{1}{3}$. Here we will consider

$$L_i = Y_i^* - p_i I =$$
$$P_i \begin{pmatrix} 0 & w_i^* & 0 \\ 0 & 0 & 0 \\ 0 & 0 & 1-3p_i \end{pmatrix} P_i^{-1} \to \begin{pmatrix} a-p & b^* & c^* \\ 0 & a-p & 0 \\ 0 & d^* & 1-2a-p \end{pmatrix}$$

and therefore

$$L_i^2 = P_i \begin{pmatrix} 0 & 0 & 0 \\ 0 & 0 & 0 \\ 0 & 0 & (1-3p_i)^2 \end{pmatrix} P_i^{-1} \text{ converges.}$$

We deduce that $M_i = 1/(1-3p_i)^2 L_i^2$ converges. Let's call the limit M:

$$M = \frac{1}{1-3p}(Y^* - pI)^2.$$

Then

$$N_i = P_i \begin{pmatrix} 0 & 1 & 0 \\ 0 & 0 & 0 \\ 0 & 0 & 0 \end{pmatrix} P_i^{-1} = X_i - \alpha_i I - (\beta_i - \alpha_i) M_i \to J.$$

Now consider

$$X_i Y_i^* = P_i \begin{pmatrix} \alpha_i p_i & \alpha_i w_i^* + p_i & 0 \\ 0 & \alpha_i p_i & 0 \\ 0 & 0 & \beta_i(1-2p_i) \end{pmatrix} P_i^{-1} \tag{6.21}$$

$$= (\alpha_i w_i^* + p_i) N_i + \alpha_i p_i I + (\beta_i(1-2p_i) - \alpha_i p_i) M_i \tag{6.22}$$

$$\to (0+p)J + 0 + 0 = pJ \tag{6.23}$$

observing that w_i converges since

$$Y_i^* = p_i I + (1-3p_i) M_i + w_i^* N_i.$$

Since $X_i Y_i^* \to JY^* = aJ$ we find that $p = a$. So,

$$Y_i^* \to aI + (1-3a)M + w^* J = \begin{pmatrix} a & w^* + \frac{c^* d^*}{1-3a} & c^* \\ 0 & a & 0 \\ 0 & d^* & 1-2a \end{pmatrix}.$$

This means $b^* = w + \frac{c^* d^*}{1-3a}$. The condition is:

$$\mathrm{Re}(b - \frac{cd}{1-3a}) \geqslant 0.$$

So

$$S_5^3(J) \subset \left\{ Y = \begin{pmatrix} a & 0 & 0 \\ b & a & c \\ d & 0 & 1-2a \end{pmatrix} \text{ where } a \neq \frac{1}{3} \text{ and } \mathrm{Re}(b - \frac{cd}{1-3a}) \geqslant 0 \right\}.$$

Case 6

$\underline{\mathrm{Re}(\alpha_i) > \mathrm{Re}(\beta_i)}$

If we assume that

$$X_i \to J \text{ and } Y_i \to Y$$

where

$$X_i = P_i \begin{pmatrix} \alpha_i & 0 & 0 \\ 0 & \alpha_i & 0 \\ 0 & 0 & \beta_i \end{pmatrix} P_i^{-1} \text{ and } Y_i = P_i^{-*} \begin{pmatrix} 1/2 & 0 & 0 \\ 0 & 1/2 & 0 \\ 0 & 0 & 0 \end{pmatrix} P_i^*$$

we easily get a contradiction which rules out this case. Assume that

$$P_i = \begin{pmatrix} p_{11}^i & p_{12}^i & p_{13}^i \\ p_{21}^i & p_{22}^i & p_{23}^i \\ p_{31}^i & p_{32}^i & p_{33}^i \end{pmatrix}$$

Then

$$X_{12}^i = \frac{p_{13}^i(\alpha_i - \beta_i)(p_{11}^i p_{32}^i - p_{12}^i p_{31}^i)}{\det(P_i)} \to 1$$

and

$$(Y_{12}^i)^* = \frac{1}{2}\frac{p_{13}^i(p_{11}^i p_{32}^i - p_{12}^i p_{31}^i)}{\det(P_i)} = \frac{1}{2}\frac{X_{12}^i}{\alpha_i - \beta_i}$$

which doesn't converge. So,

$$S_6^1(J) = \emptyset.$$

$\underline{\mathrm{Re}(\alpha_i) = \mathrm{Re}(\beta_i)}$

If we assume that there is a

$$X_i \to J \text{ and } Y_i \to Y$$

where

$$X_i = P_i \begin{pmatrix} \alpha_i & 0 & 0 \\ 0 & \alpha_i & 0 \\ 0 & 0 & \beta_i \end{pmatrix} P_i^{-1} \text{ and } Y_i = P_i^{-*} \begin{pmatrix} q_i & 0 & 0 \\ 0 & q_i & 0 \\ 0 & 0 & 1 - 2q_i \end{pmatrix} P_i^*.$$

Assume that

$$P_i = \begin{pmatrix} p_{11}^i & p_{12}^i & p_{13}^i \\ p_{21}^i & p_{22}^i & p_{23}^i \\ p_{31}^i & p_{32}^i & p_{33}^i \end{pmatrix},$$

then

$$X_{12}^i = \frac{p_{13}^i(\alpha_i - \beta_i)(p_{11}^i p_{32}^i - p_{12}^i p_{31}^i)}{\det(P_i)} \to 1$$

and

$$(Y_{12}^i)^* = \frac{1}{2}\frac{p_{13}^i(3q_i - 1)(p_{11}^i p_{32}^i - p_{12}^i p_{31}^i)}{\det(P)} = \frac{1}{2}\frac{3q_i - 1}{\alpha_i - \beta_i} X_{21}^i$$

which can only converge if $q_i \to \frac{1}{3}$. But this means that $a = \frac{1}{3}$ by a determinant argument which gives:

$$S_6^2 \subset \left\{ Y = \begin{pmatrix} 1/3 & 0 & 0 \\ b & 1/3 & c \\ d & 0 & 1/3 \end{pmatrix} \right\}.$$

Case 7

$\underline{\mathrm{Re}(\alpha_i) > \mathrm{Re}(\beta_i)}$

Let

$$X_i \to J \text{ and } Y_i \to Y$$

where

$$X_i = P_i \begin{pmatrix} \alpha_i & 0 & 0 \\ 0 & \beta_i & 1 \\ 0 & 0 & \beta_i \end{pmatrix} P_i^{-1} \text{ and } Y_i = P_i^{-*} \begin{pmatrix} 1 & 0 & 0 \\ 0 & 0 & 0 \\ 0 & 0 & 0 \end{pmatrix} P_i^*$$

Now we do the following analysis

$$X_i Y_i^* = P_i \begin{pmatrix} \alpha_i & 0 & 0 \\ 0 & 0 & 0 \\ 0 & 0 & 0 \end{pmatrix} P_i^{-1} = \alpha_i Y_i^* \to 0.$$

Since $X_i Y_i^* \to JY^* = aJ$ we deduce that $a = 0$. Considering then that, since all the Y_i are rank one, the limit also has rank one, we have

$$Y = \begin{pmatrix} 0 & 0 & 0 \\ b & 0 & c \\ d & 0 & 1 \end{pmatrix} \text{ with } b = cd.$$

So,

$$S_7^1 \subset \left\{ Y = \begin{pmatrix} 0 & 0 & 0 \\ b & 0 & c \\ d & 0 & 1 \end{pmatrix} \text{ with } b = cd \right\}.$$

$\underline{\mathrm{Re}(\alpha_i) = \mathrm{Re}(\beta_i)}$

This case is analogous to the second situation in case 5 since once the real parts are the same the ordering becomes arbitrary. So,

$$S_7^2(J) \subset \left\{ Y = \begin{pmatrix} a & 0 & 0 \\ b & a & c \\ d & 0 & 1-2a \end{pmatrix} \text{ where } a \neq \frac{1}{3} \text{ and } \mathrm{Re}(b - \frac{cd}{1-3a}) \geqslant 0 \right\}.$$

Case 8

$\underline{\mathrm{Re}(\alpha_i) > \mathrm{Re}(\beta_i)}$

The discussion of this case is analogous to the first part of Case 7:

$$S_8^1 \subset \left\{ Y = \begin{pmatrix} 0 & 0 & 0 \\ b & 0 & c \\ d & 0 & 1 \end{pmatrix} \text{ with } b = cd \right\}.$$

$\underline{\mathrm{Re}(\alpha_i) = \mathrm{Re}(\beta_i)}$

Let

$$X_i \to J \text{ and } Y_i \to Y$$

where

$$X_i = P_i \begin{pmatrix} \alpha_i & 0 & 0 \\ 0 & \beta_i & 0 \\ 0 & 0 & \beta_i \end{pmatrix} P_i^{-1} \text{ and } Y_i = P_i^{-*} \begin{pmatrix} r_i & 0 & 0 \\ 0 & \frac{1}{2} - \frac{r_i}{2} & 0 \\ 0 & 0 & \frac{1}{2} - \frac{r_i}{2} \end{pmatrix} P_i^*$$

and $r_i \in [0, \frac{1}{2}]$. We have that $X_i Y_i^* \to aJ$ and

$$X_i Y_i^* = \beta_i Y_i^* + r_i P_i \begin{pmatrix} \alpha_i - \beta_i & 0 & 0 \\ 0 & 0 & 0 \\ 0 & 0 & 0 \end{pmatrix} P_i^{-1} \tag{6.24}$$

and (6.25)

$$X_i Y_i^* = \alpha_i Y_i^* + (\frac{1}{2} - \frac{r_i}{2}) P_i \begin{pmatrix} 0 & 0 & 0 \\ 0 & \beta_i - \alpha_i & 0 \\ 0 & 0 & \beta_i - \alpha_i \end{pmatrix} P_i^{-1} \tag{6.26}$$

and since

$$P_i \begin{pmatrix} \alpha_i - \beta_i & 0 & 0 \\ 0 & 0 & 0 \\ 0 & 0 & 0 \end{pmatrix} P_i^{-1} = X_i - \beta_i I \to J \text{ and} \tag{6.27}$$

$$P_i \begin{pmatrix} 0 & 0 & 0 \\ 0 & \beta_i - \alpha_i & 0 \\ 0 & 0 & \beta_i - \alpha_i \end{pmatrix} P_i^{-1} = X_i - \alpha_i I \to J \tag{6.28}$$

we get that $r_i \to a$ and $\frac{1}{2} - \frac{r_i}{2} \to a$. This means that $a = \frac{1}{2} - \frac{a}{2}$ giving $a = \frac{1}{3}$. So,

$$S_7^2 \subset \left\{ Y = \begin{pmatrix} 1/3 & 0 & 0 \\ b & 1/3 & c \\ d & 0 & 1/3 \end{pmatrix} \right\}.$$

Case 9

$\underline{\mathrm{Re}(\alpha_i) > \mathrm{Re}(\beta_i) \geqslant \mathrm{Re}(\gamma_i)}$

We follow the same argument as in the first part of Case 7. Thus

$$S_9^1 \subset \left\{ Y = \begin{pmatrix} 0 & 0 & 0 \\ b & 0 & c \\ d & 0 & 1 \end{pmatrix} \text{ with } b = cd \right\}.$$

$\underline{\mathrm{Re}(\alpha_i) = \mathrm{Re}(\beta_i) > \mathrm{Re}(\gamma_i)}$

We have $X_i \to J$ with

$$X_i = P_i \begin{pmatrix} \alpha_i & 0 & 0 \\ 0 & \beta_i & 0 \\ 0 & 0 & \gamma_i \end{pmatrix} P_i^{-1} \text{ and } Y_i = P_i^{-*} \begin{pmatrix} r_i & 0 & 0 \\ 0 & 1-r_i & 0 \\ 0 & 0 & 0 \end{pmatrix} P_i^*$$

Since $\det(Y_i)$=0 we conclude that $\det(Y) = 0$ and therefore $a = \frac{1}{2}$ or $a = 0$. W.l.og. we assume that $r_i \to r$, since we can always consider a subsequence.

1. We will first consider the case where $a = \frac{1}{2}$. We know that $\det(Y_i - r_i I) = 0$ and $\det(Y_i - (1 - r_i)I) = 0$. By taking the limit we get that $\det(Y - rI) = \det(Y - (1-r)I) = 0$ from which we deduce that $r = 1/2$. Consider $(Y_i^* - r_i I)Y_i^*$ and $(X_i - \alpha_i I)Y_i^*$:

$$(Y_i^* - r_i I)Y_i^* = P_i \begin{pmatrix} 0 & 0 & 0 \\ 0 & (1-2r_i)(1-r_i) & 0 \\ 0 & 0 & 0 \end{pmatrix} P_i^{-1}$$

$$\rightarrow (Y^* - \frac{1}{2}I)Y^* = \begin{pmatrix} 0 & \frac{b^*}{2} + c^*d^* & 0 \\ 0 & 0 & 0 \\ 0 & 0 & 0 \end{pmatrix}$$

$$(X_i - \alpha_i I)Y_i^* = P_i \begin{pmatrix} 0 & 0 & 0 \\ 0 & (\beta_i - \alpha_i)(1-r_i) & 0 \\ 0 & 0 & 0 \end{pmatrix} P_i^{-1}$$

$$\rightarrow (J)Y^* = \begin{pmatrix} 0 & \frac{1}{2} & 0 \\ 0 & 0 & 0 \\ 0 & 0 & 0 \end{pmatrix}$$

Comparing these two we get that

$$\frac{1-2r_i}{\beta_i - \alpha_i} \rightarrow \frac{b^*/2 + c^*d^*}{1/2} = b^* + 2c^*d^*$$

and since $\mathrm{Re}(\frac{1-2r_i}{\beta_i-\alpha_i}) = 0$ we conclude that $\mathrm{Re}(b+2cd) = 0$. So,

$$S_9^2 \subset \left\{ Y = \begin{pmatrix} 1/2 & 0 & 0 \\ b & 1/2 & c \\ d & 0 & 0 \end{pmatrix} \text{ where } \mathrm{Re}(b+2cd) = 0 \right\}.$$

2. Now we consider the case where $a = 0$. Since $\det(Y_i - r_i I) = 0$ and $r_i \in [0, 1/2]$ we get that $r = 0$. Consider $(Y_i^* - (1-r_i)I)Y_i^*$ and $(Y_i^* - (1-r_i)I)(X_i - \gamma_i I)$:

$$(Y_i^* - (1-r_i)I)Y_i^* = P_i \begin{pmatrix} (2r_i-1)r_i & 0 & 0 \\ 0 & 0 & 0 \\ 0 & 0 & 0 \end{pmatrix} P_i^{-1}$$

$$\rightarrow (Y^* - I)Y^* = \begin{pmatrix} 0 & c^*d^* - b^* & 0 \\ 0 & 0 & 0 \\ 0 & 0 & 0 \end{pmatrix}$$

$$(Y_i^* - (1-r_i)I)(X_i - \gamma_i I) = P_i \begin{pmatrix} (2r_i-1)(\alpha_i-\gamma_i) & 0 & 0 \\ 0 & 0 & 0 \\ 0 & 0 & 0 \end{pmatrix} P_i^{-1}$$

$$\rightarrow (Y^* - I)J = \begin{pmatrix} 0 & -1 & 0 \\ 0 & 0 & 0 \\ 0 & 0 & 0 \end{pmatrix}$$

We get that $\frac{r_i}{\alpha_i - \gamma_i} \to b^* - c^* d^*$ and therefore $\mathrm{Re}(b - cd) \geqslant 0$. So,

$$S_9^3 \subset \left\{ Y = \begin{pmatrix} 0 & 0 & 0 \\ b & 0 & c \\ d & 0 & 1 \end{pmatrix} \text{ where } \mathrm{Re}(b - cd) \geqslant 0 \right\}$$

$\underline{\mathrm{Re}(\alpha_i) = \mathrm{Re}(\beta_i) = \mathrm{Re}(\gamma_i)}$

Let

$$X_i \to J \text{ and } Y_i \to Y$$

where

$$X_i = P_i \begin{pmatrix} \alpha_i & 0 & 0 \\ 0 & \beta_i & 0 \\ 0 & 0 & \gamma_i \end{pmatrix} P_i^{-1} \text{ and } Y_i = P_i^{-*} \begin{pmatrix} r_i & 0 & 0 \\ 0 & q_i & 0 \\ 0 & 0 & 1 - r_i - q_i \end{pmatrix} P_i^*.$$

We can assume that w.l.o.g $r_i \to r$ and $q_i \to q$. Looking at

$$0 = (Y_i - r_i I)(Y_i - q_i I)(Y_i - (1 - q_i - r_i)I)$$

we conclude

$$0 = (Y - rI)(Y - qI)(Y - (1 - q - r)I)$$

and that we have to distinguish 4 cases

1. $a \neq 1/3$ and $q = a$ and $r = a$

2. $a \neq 1/3$ and $q = a$ and $r = 1 - 2a$

3. $a \neq 1/3$ and $q = 1 - 2a$ and $r = a$

4. $a = q = r = 1/3$

1. Consider $(Y_i^* - r_i I)(Y_i^* - (1 - q_i - r_i)I)$. This gives

$$P_i \begin{pmatrix} 0 & 0 & 0 \\ 0 & (q_i - r_i)(2q_i + r_i - 1) & 0 \\ 0 & 0 & 0 \end{pmatrix} P_i^{-1} \to \begin{pmatrix} 0 & b^*(3a-1) + c^* d^* & 0 \\ 0 & 0 & 0 \\ 0 & 0 & 0 \end{pmatrix}$$

Looking at $(X_i - \alpha_i I)(Y_i^* - (1 - r_i - q_i)I)$ we get that

$$P_i \begin{pmatrix} 0 & 0 & 0 \\ 0 & (\beta_i - \alpha_i)(2q_i + r_i - 1) & 0 \\ 0 & 0 & 0 \end{pmatrix} P_i^{-1} \to \begin{pmatrix} 0 & 3a-1 & 0 \\ 0 & 0 & 0 \\ 0 & 0 & 0 \end{pmatrix}.$$

Comparing the two we can deduce that

$$\frac{q_i - r_i}{\beta_i - \alpha_i} \to b^* + \frac{c^* d^*}{3a - 1}.$$

Since q_i and r_i are real and $\beta_i - \alpha_i$ is purely imaginary we get that

$$\mathrm{Re}(b + \frac{cd}{3a-1}) = 0,$$

so

$$S_9^3 \subset \left\{ Y = \begin{pmatrix} a & 0 & 0 \\ b & a & c \\ d & 0 & 1-2a \end{pmatrix} \text{ where } \mathrm{Re}(b - \frac{cd}{1-3a}) = 0 \right\}.$$

2. Consider $(Y_i^* - r_i I)(Y_i^* - (1 - q_i - r_i)I)$. This gives

$$P_i \begin{pmatrix} 0 & 0 & 0 \\ 0 & (q_i - r_i)(2q_i + r_i - 1) & 0 \\ 0 & 0 & 0 \end{pmatrix} P_i^{-1} \to \begin{pmatrix} 0 & b^*(3a-1) + c^* d^* & 0 \\ 0 & 0 & 0 \\ 0 & 0 & 0 \end{pmatrix}.$$

Looking at $(X_i - \gamma_i I)(Y_i^* - r_i I)$ we get that

$$P_i \begin{pmatrix} 0 & 0 & 0 \\ 0 & (\beta_i - \gamma_i)(q_i - r_i) & 0 \\ 0 & 0 & 0 \end{pmatrix} P_i^{-1} \to \begin{pmatrix} 0 & 3a-1 & 0 \\ 0 & 0 & 0 \\ 0 & 0 & 0 \end{pmatrix}.$$

Comparing the two we can deduce that

$$\frac{2q_i + r_i - 1}{\beta_i - \gamma_i} \to b^* + \frac{c^* d^*}{3a-1}.$$

Since q_i and r_i are real and $\beta_i - \gamma_i$ is purely imaginary we get

$$\mathrm{Re}(b - \frac{cd}{1-3a}) = 0,$$

so

$$S_9^4 \subset \left\{ Y = \begin{pmatrix} a & 0 & 0 \\ b & a & c \\ d & 0 & 1-2a \end{pmatrix} \text{ where } \mathrm{Re}(b - \frac{cd}{1-3a}) = 0 \right\}.$$

3. Consider $(Y_i^* - q_i I)(Y_i^* - (1 - q_i - r_i)I)$. This gives

$$P_i \begin{pmatrix} (r_i - q_i)(2r_i - q_i - 1) & 0 & 0 \\ 0 & 0 & 0 \\ 0 & 0 & 0 \end{pmatrix} P_i^{-1} \to \begin{pmatrix} 0 & b^*(3a-1) + c^* d^* & 0 \\ 0 & 0 & 0 \\ 0 & 0 & 0 \end{pmatrix}.$$

Looking at $(X_i - \gamma_i I)(Y_i^* - q_i I)$ we get

$$P_i \begin{pmatrix} (\alpha_i - \gamma_i)(r_i - q_i) & 0 & 0 \\ 0 & 0 & 0 \\ 0 & 0 & 0 \end{pmatrix} P_i^{-1} \to \begin{pmatrix} 0 & 3a-1 & 0 \\ 0 & 0 & 0 \\ 0 & 0 & 0 \end{pmatrix}.$$

Comparing the two we can deduce that

$$\frac{2r_i - q_i - 1}{\alpha_i - \gamma_i} \to b^* + \frac{c^* d^*}{3a-1}.$$

Since q_i and r_i are real and $\alpha_i - \gamma_i$ is purely imaginary we get

$$\mathrm{Re}(b - \frac{cd}{1-3a}) = 0,$$

so

$$S_9^5 \subset \left\{ Y = \begin{pmatrix} a & 0 & 0 \\ b & a & c \\ d & 0 & 1-2a \end{pmatrix} \text{ where } \mathrm{Re}(b - \frac{cd}{1-3a}) = 0 \right\}.$$

4. Because $a = 1/3$ we get

$$S_9^6 \subset \left\{ Y = \begin{pmatrix} 1/3 & 0 & 0 \\ b & 1/3 & c \\ d & 0 & 1/3 \end{pmatrix} \right\}.$$

Thus we have proved that the left hand side of Theorem 6.1 is contained in the right hand side.

Sufficient Conditions

Now, we prove that the right hand side is contained in the left hand side. We will distinguish the cases $a = \frac{1}{3}$ and $a \neq \frac{1}{3}$.

$\underline{a = \frac{1}{3}}$

In this case for any b, c, d the following sequences

$$P_t = \begin{pmatrix} -c^* d^{*2} & -\frac{1}{b^* d^* t} & \frac{c^* d^{*2}}{t^3} \\ 0 & -c^* d^{*2} & 0 \\ 0 & -\frac{c^* d^*}{t} & \frac{1}{t^3} \end{pmatrix} \tag{6.29}$$

$$P_t^{-1} = \begin{pmatrix} -\frac{1}{c^* d^{*2}} & \frac{b^* - c^{*2} d^{*2}}{c^{*2} d^{*3} t} & 1 \\ 0 & -\frac{1}{c^* d^{*2}} & 0 \\ 0 & -\frac{t^2}{d^*} & t^3 \end{pmatrix} \tag{6.30}$$

$$J_t = \begin{pmatrix} t & 1 & 0 \\ 0 & t & 1 \\ 0 & 0 & t \end{pmatrix} \tag{6.31}$$

$$W_t^* = \begin{pmatrix} \frac{1}{3} & \frac{1}{t} & -\frac{1}{c^* d^* t^3} \\ 0 & \frac{1}{3} & \frac{1}{t} \\ 0 & 0 & \frac{1}{3} \end{pmatrix}. \tag{6.32}$$

are such that $X_t = P_t J_t P_t^{-1}$, $Y_t = P_t^{-*} W_t P_t^* \in \widehat{\partial}\alpha(X_t)$,

$$X_t \to J \text{ and } Y_t \to Y = \begin{pmatrix} a & 0 & 0 \\ b & a & c \\ d & 0 & a \end{pmatrix} \text{ with } a = \frac{1}{3}.$$

Here t is real and positive and decreases to zero. Since c, d, b can be arbitrary we conclude that if $a = \frac{1}{3}$ then the conditions on the right hand side of (6.17) completely characterize the subgradients, except that we have to consider the case where $c = 0$ and/or $d = 0$. This can be done by taking the sequences above and replacing c and/or d with t. Then we get a limit with c and/or d equal to 0.

$\underline{a \neq \frac{1}{3}}$

In all the cases we studied we have found the necessary condition $\mathrm{Re}(b - \frac{cd}{1-3a}) \geqslant 0$. We will show that this is sufficient by the following sequence in which $a \in [0, \frac{1}{2})$ (we will discuss the case $a = 1/2$ later) and c, d arbitrary and $\mathrm{Re}(w) \geqslant 0$:

$$P_t^{-1} = \begin{pmatrix} \frac{1}{t} & \frac{1}{t} & \frac{c^*}{(3a-1)t} \\ t & \frac{1}{t} & t \\ t & \frac{d^*}{(1-3a)t} & \frac{1}{t} \end{pmatrix}, \tag{6.33}$$

$$J_t = \begin{pmatrix} t & 1 & 0 \\ 0 & t & 0 \\ 0 & 0 & t + it \end{pmatrix}, \tag{6.34}$$

$$W_t^* = \begin{pmatrix} a + t & w^* + t & 0 \\ 0 & a + t & 0 \\ 0 & 0 & 1 - 2a - 2t \end{pmatrix} \tag{6.35}$$

are such that $X_t = P_t^{-1} J_t P_t$, $Y_t = P_t^* W_t P_t^{-*} \in \widehat{\partial}\alpha(X_t)$,

$$X_t \to J \text{ and } Y_t \to Y = \begin{pmatrix} a & 0 & 0 \\ b & a & c \\ d & 0 & a \end{pmatrix}$$

where $b = w + \frac{cd}{1-3a}$, with t positive real, converging to 0. In the case where $a = 1/2$ we can take a similar sequence with

$$W_t^* = \begin{pmatrix} \frac{1}{2} - t & w^* + t & 0 \\ 0 & \frac{1}{2} - t & 0 \\ 0 & 0 & 2t \end{pmatrix}.$$

We then get that $X_t \to J$ and $Y_t \to Y$ as above but with $a = 1/2$. This proves Theorem 6.1.

6.4 Discussion

The subdifferential analysis just performed for the spectral abscissa at the 3×3 derogatory, defective matrix J was quite complicated, suggesting that a general analysis may be difficult. In the nonderogatory case, all subgradients are regular [5, Theorem 8.2]; it is because this is not the case for active derogatory eigenvalues that the general subdifferential analysis problem is so challenging.

The purpose of deriving subgradients is so that they can be used for

analyzing *necessary* optimality conditions. In the case of the eigenvalue optimization problems studied in Chapter 4, the minimal value found for the reduced spectral radius was zero, establishing global optimality, so the Jordan structure of the zero eigenvalue was not relevant to the question of optimality. However, if the minimal value found for the eigenvalue being minimized had been a positive number, the Jordan structure would be needed for analysis of optimality conditions, and in principle it would be possible to use results along the lines of the one established in this chapter to investigate whether the minimal eigenvalue found satisfies necessary optimality conditions, making use of nonsmooth chain rules as was done in [17].

Bibliography

[1] L. Bers. *Riemann Surfaces*. Courant Institute of Mathematical Sciences, New York University, New York, 1958.

[2] H. Biermann, A. Levin, and D. Zorin. Piecewise smooth subdivision surfaces with normal control. In *SIGGRAPH 2000 Conference Proceedings*, Annual Conference Series. ACM SIGGRAPH, Addison Wesley, July 2000.

[3] H. Biermann, A. Levin, and D. Zorin. Piecewise smooth subdivision surfaces with normal control. *Proceedings of SIGGRAPH 2000*, July 2000.

[4] J. V. Burke, A.S. Lewis, and M. L. Overton. Hanso (hybrid algorithm for non-smooth optimization): a matlab package based on bfgs, bundle and gradient sampling methods. Version 1.0 released in 2006. See `www.cs.nyu.edu/faculty/overton/software/hanso/index.html`.

[5] J. V. Burke and M. L. Overton. Variational analysis of non-Lipschitz spectral functions. *Math. Program.*, 90(2, Ser. A):317–351, 2001.

[6] J.V. Burke, A.S. Lewis, and M.L. Overton. A robust gradient sampling algorithm for nonsmooth, nonconvex optimization. *SIAM J. Optim.*, 15:751–779, 2005.

[7] E. Catmull and J. Clark. Recursively generated B-spline surfaces on arbitrary topological meshes. 10(6):350–355, 1978.

[8] A. S. Cavaretta, W. Dahmen, and C. A. Micchelli. Stationary subdivision. *Memoirs Amer. Math. Soc.*, 93(453), 1991.

[9] A. Cohen, N. Dyn, and D. Levin. Matrix subdivision schemes. Technical report, Université Pierre et Marie Curie, 1997.

[10] C. de Boor, K. Höllig, and S. Riemenschneider. *Box Splines*. Springer-Verlag, 1993.

[11] T. DeRose, M. Kass, and T. Truong. Subdivision surfaces in character animation. *Proceedings of SIGGRAPH 98*, pages 85–94, July 1998. ISBN 0-89791-999-8. Held in Orlando, Florida.

[12] R. Dietz, J. Hoschek, and B. Jüttler. An algebraic approach to curves and surfaces on the sphere and on other quadrics. *Comput. Aided Geom. Design*, 10(3-4):211–229, 1993. Free-form curves and free-form surfaces (Oberwolfach, 1992).

[13] D. Doo. A subdivision algorithm for smoothing down irregularly shaped polyhedrons. In *Proceedings on Interactive Techniques in Computer Aided Design*, pages 157–165, Bologna, 1978.

[14] B. A. Dubrovin, A. T. Fomenko, and S. P. Novikov. *Modern geometry—methods and applications. Part I.* Springer-Verlag, New York, second edition, 1992. The geometry of surfaces, transformation groups, and fields, Translated from the Russian by Robert G. Burns.

[15] T. Duchamp, A. Certain, A. DeRose, and W. Stuetzle. Hierarchical computation of PL harmonic embeddings. Preprint, July 1997.

[16] T. Duchamp and W. Stuetzle. Spline smoothing on surfaces. *Journal of Computational and Graphics Statistics*, 12(3):354–381, 2003.

[17] K. K. Gade and M. L. Overton. Optimizing the asymptotic convergence rate of the Diaconis-Holmes-Neal sampler. *Adv. in Appl. Math.*, 38(3):382–403, 2007.

[18] B. Han, M. L. Overton, and T. P.-Y. Yu. Design of Hermite subdivision schemes aided by spectral radius optimization. *SIAM Journal on Scientific Computing*, 25(2):643–656, 2003.

[19] H. Hoppe, T. DeRose, T. Duchamp, M. Halstead, H. Jin, J. McDonald, J. Schweitzer, and W. Stuetzle. Piecewise smooth surface reconsruction. In *Computer Graphics Proceedings*, Annual Conference Series, pages 295–302. ACM Siggraph, 1994.

[20] K. Karčiauskas and J. Peters. Lens-shaped surfaces and C^2 subdivision. *Computing*, 86(2-3):171–183, 2009.

[21] G. S. Kimeldorf and G. Wahba. A correspondence between Bayesian estimation on stochastic processes and smoothing by splines. *Ann. Math. Statist.*, 41:495–502, 1970.

[22] A. Levin. Analysis of quasi-uniform subdivision schemes. In preparation, 1999.

[23] A.S. Lewis and M.L. Overton. Nonsmooth optimization via BFGS. 2008. http://www.cs.nyu.edu/overton/papers/pdffiles/bfgs_inexactLS.pdf.

[24] J. Moro, J. V. Burke, and M. L. Overton. On the Lidskii-Vishik-Lyusternik perturbation theory for eigenvalues of matrices with arbitrary Jordan structure. *SIAM J. Matrix Anal. Appl.*, 18(4):793–817, 1997.

[25] J. Munkres. *Elementary Differential Topology.* Princeton University Press, 1966.

[26] A. H. Nasri. Polyhedral subdivision methods for free-form surfaces. *ACM Transactions on Graphics*, 6(1):29–73, January 1987.

[27] A. H. Nasri. Boundary corner control in recursive subdivision surfaces. 23(6):405–410, 1991.

[28] A. H. Nasri. Surface interpolation on irregular networks with normal conditions. *Computer Aided Geometric Design*, 8:89–96, 1991.

[29] J. Peters and U. Reif. Analysis of generalized B-spline subdivision algorithms. *SIAM Jornal of Numerical Analysis*, 1997.

[30] J. Peters and U. Reif. Analysis of algorithms generalizing B-spline subdivision. *SIAM Journal on Numerical Analysis*, 35(2):728–748, 1998.

[31] J. Peters and U. Reif. *Subdivision Surfaces*. Springer-Verlag, Berlin, Heidelberg, 2008.

[32] H. Prautzsch and W. Boehm. Box splines. In *Handbook of computer aided geometric design*, pages 255–282. North-Holland, Amsterdam, 2002.

[33] H. Prautzsch and U. Reif. Degree estimates for C^k-piecewise polynomial subdivision surfaces. *Advances in Computational Mathematics*, 10(2):209–217, 1999.

[34] U. Reif. A unified approach to subdivision algorithms near extraordinary points. *Computer Aided Geometric Design*, 12:153–174, 1995.

[35] U. Reif. A unified approach to subdivision algorithms near extraordinary points. *Computer Aided Geometric Design*, 12:153–174, 1995.

[36] U. Reif. A degree estimate for subdivision surfaces of higher regularity. *Proceedings of the American Mathematical Society*, 124(7):153–174, 1996.

[37] R. T. Rockafellar and R. J.-B. Wets. *Variational analysis*, volume 317 of *Grundlehren der Mathematischen Wissenschaften [Fundamental Principles of Mathematical Sciences]*. Springer-Verlag, Berlin, 1998.

[38] J. E. Schweitzer. *Analysis and Application of Subdivision Surfaces*. PhD thesis, University of Washington, Seattle, 1996.

[39] J. Stam. Exact evaluation of catmull-clark subdivision surfaces at arbitrary parameter values. In *Proceedings of SIGGRAPH*, pages 395–404, 1998.

[40] E. M. Stein. *Singular integrals and differentiability properties of functions*. Princeton University Press, Princeton, N.J., 1970. Princeton Mathematical Series, No. 30.

[41] G. Wahba. Spline interpolation and smoothing on the sphere. *SIAM J. Sci. Statist. Comput.*, 2(1):5–16, 1981.

[42] Y. Xue, T. P.-Y. Yu, and T. Duchamp. Jet subdivision schemes on the k-regular complex. *Computer Aided Geometric Design*, 23(4):361–396, 2006.

[43] D. Zorin. c^k continuity of subdivision surfaces. Technical Report CS-TR-96-23, California Institute of Technology, 1996. `http://www.caltech.edu/~libraries/collections/cs.html`.

[44] D. Zorin. *Subdivision and Multiresolution Surface Representations*. PhD thesis, Caltech, Pasadena, 1997.

[45] D. Zorin. A method for analysis of c^1-continuity of subdivision surfaces. *SIAM Journal of Numerical Analysis*, 37(4), 2000.

[46] D. Zorin. Smoothness of subdivision on irregular meshes. *Constructive Approximation*, 16(3), 2000.